Title
Sunlight Inactivation of Waterborne Viruses: Mechanisms, Modeling, and Application to Surface Waters and Wastewater Treatment

Author
Silverman, Andrea Idette

Publication Date
2013

Peer reviewed|Thesis/dissertation

Sunlight Inactivation of Waterborne Viruses: Mechanisms, Modeling, and Application to Surface Waters and Wastewater Treatment

By

Andrea Idette Silverman

A dissertation submitted in partial satisfaction of the

requirements for the degree of

Doctor of Philosophy

in

Engineering – Civil and Environmental Engineering

in the

Graduate Division

of the

University of California, Berkeley

Committee in charge:

Professor Kara L. Nelson, Chair
Professor David Sedlak
Professor Lee Riley

Fall 2013

Sunlight Inactivation of Waterborne Viruses: Mechanisms, Modeling, and Application to Surface Waters and Wastewater Treatment

Abstract

Sunlight Inactivation of Waterborne Viruses: Mechanisms, Modeling, and Application to Surface Waters and Wastewater Treatment

by

Andrea Idette Silverman

Doctor of Philosophy in Engineering – Civil and Environmental Engineering

University of California, Berkeley

Professor Kara L. Nelson, Chair

Sunlight inactivation of microorganisms is a natural process that can occur in any sunlit water and has implications for microbial ecology, the fate of microbial contaminants in the environment, and natural wastewater treatment systems. This work focuses on sunlight inactivation of waterborne viruses, which present a special challenge in health-related water microbiology given that waterborne human viruses are important etiologies of disease, and are difficult to remove and inactivate in water. The research presented in this dissertation builds upon previous research by determining the mechanisms and rates of sunlight inactivation of human viruses in natural waters; these data were used to build predictive inactivation rate models that account for virus type, sunlight irradiance and water quality. Additionally, two applications of sunlight inactivation – the differential stability of indicator organisms and human viruses in the environment, and disinfection of irrigation water in wastewater-irrigated agriculture – were investigated.

There are three proposed sunlight inactivation mechanisms for viruses: the direct- and indirect-endogenous mechanisms, which require absorption of photons by virus components, and the exogenous mechanism, which involves reaction between the virus and exogenously produced reactive intermediates formed by photochemical reactions. All three mechanisms are affected by water quality. Natural organic matter, for example, is found in most aquatic environments and is capable of both attenuating sunlight – which would decrease sunlight exposure and therefore inactivation rates – and photosensitizing production of reactive intermediates – which could increase inactivation rates of viruses susceptible to the exogenous mechanism.

The first goal of this dissertation was to better understand the mechanisms of sunlight inactivation of select bacteriophage and human viruses in surface waters containing natural organic matter. Given the two main modes by which damage is delivered to viruses in sunlit surface waters – through direct absorption of photons (the direct- and indirect-endogenous mechanisms) and contact with reactive molecules formed by sensitizers in the water column (the exogenous mechanism) – a better understanding of sunlight inactivation mechanisms can help us predict how environmental conditions (e.g., sunlight irradiance, light attenuation, water quality,

depth, mixing) can affect observed inactivation rates.

Through laboratory experiments using simulated sunlight and natural organic matter-containing waters collected from the environment, we determined that the sunlight inactivation rates of human poliovirus type 3 and bacteriophage PRD1 mainly involved endogenous inactivation mechanisms, while MS2 and human adenovirus type 2 were also affected by the exogenous mechanism. Different virus types were found to have different rates of inactivation, and inactivation rates differed among water types depending on light attenuation and natural organic matter in the water source; this finding made it clear that water quality conditions and virus type must be taken into account when predicting inactivation rates. Additionally, MS2 was inactivated at the slowest rate in all waters, and PV3 the fastest, at the water depth that was studied (i.e., 5 cm).

The data obtained in the initial virus inactivation study, along with findings from other researchers, were used to develop and test models that predict the sunlight inactivation rates of viruses in surface waters containing light-attenuating photosensitizers. Models were developed for poliovirus type 3 and MS2. Inactivation rates were modeled and measured in reactors containing different, well-mixed depths of water collected from an open-water wastewater treatment system; the models performed well in predicting inactivation rates in laboratory experiments. Given the tradeoff between decreased endogenous inactivation due to light attenuation and increased exogenous inactivation due to the presence of photosensitizers in natural organic matter-containing water, we compared the measured and modeled inactivation rates of poliovirus type 3 (which is reliant on endogenous mechanisms) and MS2 (which is susceptible to the exogenous mechanism) at different well-mixed depths. The inactivation rate of poliovirus type 3 was found to be lower than that of MS2 at deeper well-mixed depths, indicating that MS2 cannot be considered a conservative indicator of poliovirus sunlight inactivation under all conditions. Some research gaps – including the development of models that take into account the solar zenith angle, annual and diurnal variation in irradiance, and water body hydraulics – must be filled to successfully translate the models to environmental waters and natural sunlight.

Many viruses are not culturable, making them difficult to study in general, let alone their inactivation rates. To better understand factors that dictate differences in sunlight inactivation rates between viruses, which could help in predicting inactivation rates of non-culturable viruses, we investigated whether sunlight inactivation of poliovirus type 3 is caused by damage to the protein capsid of the virus. More specifically, this research focused on the inhibition of viral 'life' processes that depend on an intact capsid. Comparing data from assays that quantify host cell attachment and infectivity, we found that although sunlight exposure leads to an inhibition of poliovirus type 3 attachment to host cells (which is the first step in the infection process), this damage mechanism plays a minor role in total inactivation.

The second part of this dissertation focuses on a case study of wastewater irrigation practiced in Accra, Ghana, with goals to better understand the health risks associated with wastewater irrigation in Accra, and to determine whether small, farmer-dug ponds can contribute to disinfection of irrigation water. To provide data that can be used to refine quantitative microbial risk assessment models of wastewater-fed agriculture in Accra, irrigation water samples were analyzed for concentrations of fecal indicator microorganisms (human-specific *Bacteroidales*, *E. coli*, enterococci, thermotolerant coliform, and F+ and somatic coliphages) and two human

viruses (adenovirus and norovirus genogroup II). *E. coli* concentrations in all samples exceeded recommended limits set by the World Health Organization, human viruses were detected in 75% of samples analyzed, and virus concentrations were quantified in 60% of samples. Indicator organism and virus concentrations were compared as part of an analysis of differential stability of fecal indicator organisms and pathogens in the environment, and the appropriateness of assumptions used in quantitative microbial risk assessment to relate indicator organism concentrations to those of pathogens.

After determining indicator organism and pathogen concentrations in Accra irrigation water, we investigated the ability of a farmer-developed intervention (small, on-farm ponds) to disinfect wastewater before use in vegetable irrigation. Results indicated that sunlight inactivation dominated the removal of two bacteria (*E. coli* and enterococci) and two bacteriophages (F+ and somatic coliphages) in these ponds, and that the ponds can contribute to the multi-barrier approach to reducing health risks related to wastewater irrigation. On-farm pond design and management recommendations, as well as challenges, are also discussed.

Contents

List of Figures

List of Tables

Acknowledgements

First and foremost, I want to thank Professor Kara Nelson for her guidance and constant support. I feel incredibly lucky to have Kara as a research advisor, mentor, and advocate. Kara pushed me to reach further and explore more; she always had faith in me and encouraged me to follow my interests. It was an honor to have Kara as a teacher and partner in learning.

I would like to thank Professors David Sedlak and Lee Riley for serving on my dissertation committee and providing invaluable feedback, and Professor Alexandria Boehm for her advice along the way. I also have to thank Dave Love – Dave taught me how to be a good scientist, helped me build a solid foundation in the laboratory, and passed on his passion for science. Much of my research would not have been possible with out Ann Fisher and the UC Berkeley Tissue Culture facility – thank you Ann for being a deep well of information and a cheerleader.

To all the graduate students and postdocs who made their way through O'Brien and Davis Halls: it is a privilege to have worked with you, you are impressive and taught me a lot. I especially need to thank the past and current members of the Nelson, Sedlak and Alvarez-Cohen Labs, particularly Samantha Beardsley, Ariel Grostern, Justin Jasper, Khalid Kadir, Emily Kumpel, Mi Nguyen, Andy Torkelson, and Shan Yi. I also want to thank my colleagues at Stanford University, including Mia Mattioli and Lauren Murray Sassoubre.

I owe a lot to Ashley Murray Muspratt; Ashley introduced me to Accra and the International Water Management Institute (IWMI) and continues to be an inspiration and resource. I also would not have accomplished anything in Accra without the help and support of the researchers and staff at IWMI; I especially want to thank Mark Akrong, Philip Amoah, Olufunke Cofie, and Pay Drechsel

To my amazing friends in the Bay Area, New York, London, Accra, Mumbai and everywhere in between: your friendship, support, and enthusiasm mean so much to me. Thank you!

And last but not least, I want to thank my family. I would never have reached this point without your unending love, support and belief in me. I love you, you are the greatest.

* *

This dissertation research was funded by the UC Berkeley Chancellor's Fellowship for Graduate Study, the Center for Emerging and Neglected Diseases at UC Berkeley (Science and Engineering for Global Health Fellowship), the International Water Management Institute, the Philomathia Foundation (Chang-Lin Tien Graduate Fellowship in the Environmental Sciences), an Anselmo Macchi Fellowship, and the National Science Foundation (CBET- 0853568).

Chapter 1

Introduction

Sunlight inactivation of microorganisms is a natural process that can occur in any sunlit water and has implications for microbial ecology, the fate of microbial contaminants in the environment, and natural wastewater treatment systems. This work focuses on sunlight inactivation of waterborne viruses, which present a special challenge in health-related water microbiology given that waterborne human viruses are important etiologies of disease, and are difficult to remove and inactivate in water.

Waterborne viruses that infect humans include adenoviruses, astroviruses, caliciviruses (including noroviruses), hepatitis E virus, parvoviruses, picornaviruses (including enteroviruses, polioviruses, and hepatitis A viruses) and rotaviruses. Waterborne human viruses tend to have low infectious doses and can cause diseases that include gastroenteritis, respiratory illness, hepatitis, and central nervous system diseases such as poliomyelitis and meningitis (Carter 2005). Due to their small size (between 20 and 200 nm in diameter) and resistance to inactivation, waterborne viruses often remain in wastewater effluent (Carter 2005; Sedmark et al. 2005). Viruses, for example, are generally more resistant than bacteria when subjected to chlorine (White 1999), ozone (Langlais et al. 1991) and ultraviolet (UV) light (Hijnen et al. 2006) disinfection.

Given the high concentration of viruses in wastewater, their prevalence in surface water, and the health risks they present, it is important to study sunlight inactivation of viruses, including mechanisms of inactivation, inactivation rates, and how those rates are affected by water characteristics. Two examples illustrate the usefulness of these data and the models that can be derived from them. First, whether viruses end up in surface waters from wastewater spills or leaks (Boehm et al. 2009), stormwater run-off (Jiang et al. 2001; Noble et al. 2006), or wastewater effluent (Carter 2005; Sedmark et al. 2005), a model of virus inactivation could predict the survival of viral pathogens and help inform decision making to prevent downstream water users, such as recreational users, from being exposed. A second example involves natural wastewater treatment systems, including waste stabilization ponds, which are an option for wastewater treatment and disinfection, especially in low resource settings, and for recycling of wastewater for agricultural irrigation. With an understanding of sunlight inactivation mechanisms and an ability to predict virus inactivation rates, we can better design treatment ponds to maximize disinfection.

Most waterborne viruses are non-enveloped and consist of nucleic acids (single- or double-stranded RNA or DNA) surrounded by a protective protein capsid. There are three proposed sunlight inactivation mechanisms for viruses (Figure 1.1): the direct- and indirect-endogenous mechanisms require absorption of photons by virus components, while the exogenous mechanism involves reaction between the virus and exogenously produced reactive intermediates formed by photochemical reactions. The direct- and indirect-endogenous mechanisms differ in

that the direct mechanism causes damage to the virus component that absorbed the photon, either nucleic acids (leading to formation of pyrimidine dimers and other photoproducts; Jagger 1985) or proteins (resulting in photo-oxidation of select amino acid residues; Davies and Truscott 2001), while the indirect-endogenous mechanism occurs when photons are absorbed by one part of the virus, but damage is conveyed to another (Davies 2003; Wigginton et al. 2010). The exogenous mechanism occurs when photons are absorbed by photosensitizers from the water matrix, leading to the formation of reactive intermediates, such as excited triplet states and reactive oxygen species (ROS; Blough and Zepp 1995; Cooper et al. 1989); reactive intermediates contribute to inactivation by causing oxidative damage to virion components (Curtis et al. 1992; Davies-Colley et al. 1999; Wigginton et al. 2010).

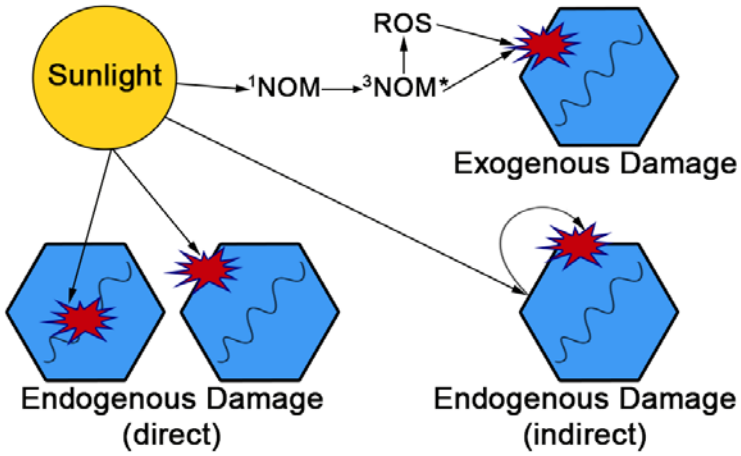

Figure 1.1. Proposed virus sunlight inactivation mechanisms.

Organic matter – including dissolved (DOM) and particulate natural organic matter (NOM), and organic matter in effluent from wastewater treatment processes (EfOM) – is capable of both sunlight attenuation and acting as a photosensitizer to produce ROS. NOM, for example, is found in most aquatic environments (Cooper et al. 1989) and, due to its high concentration of aromatic functional groups (Wershaw 2004), is one of the most important sunlight absorbing substances in natural waters (Zepp 1988). NOM varies in composition and structure depending on its source (Kördel et al. 1997), which can cause NOM from different environmental waters to possess varying propensities to absorb light, produce ROS and associate with water constituents, including viruses. Because NOM and EfOM are capable of both sunlight attenuation and ROS production, their presence in aquatic environments can increase or decrease sunlight inactivation rates depending on their structure in a particular water, and the dominant mechanism of inactivation of the target organism.

Many studies investigating sunlight inactivation of viruses have focused on MS2 and other bacteriophage (Kohn and Nelson 2007; Kohn et al. 2007; Love et al. 2010; Romero et al. 2011; Sinton et al. 1999; Sinton et al. 2002), using these organisms as models for human viruses due to their similar structure and size (Havelaar 1993). Bacteriophage, however, do not pose health threats to humans and may not accurately model human virus inactivation under all environmental conditions. Virus structures, and therefore targets of endogenous and exogenous damage, vary among organisms, which could result in different rates and dominant mechanisms of sunlight-mediated inactivation. At this point, it is not possible to predict mechanisms or rates of inactivation of viruses of public health concern based on current knowledge of bacteriophage inactivation. To better understand sunlight inactivation of human viruses, it is necessary to study the viruses themselves.

The goal of the first part of this dissertation (Chapters 2, 3 and 4) was to better understand the mechanisms of sunlight inactivation of select bacteriophage and human viruses in surface waters containing NOM and EfOM. Given the two main modes by which damage is delivered to viruses in sunlit surface waters – through (1) direct absorption of photons (the direct- and indirect-endogenous mechanisms) and (2) contact with reactive molecules formed by sensitizers in the water column (the exogenous mechanism) – a better understanding of sunlight inactivation mechanisms can help us predict how environmental conditions (e.g., sunlight irradiance, light attenuation, water quality, depth, mixing) can affect observed inactivation rates. Specific objectives were to:

- Determine the dominant sunlight inactivation mechanisms of bacteriophages (MS2 and PRD1) and human viruses (adenovirus type 2 and poliovirus type 3) in water containing NOM
- Develop and test models that predict sunlight inactivation rates of viruses (MS2 and poliovirus type 3), while taking into account light attenuation and exogenous inactivation
- Determine whether sunlight inactivates poliovirus type 3 through damage to its protein capsid

The second part of the dissertation is a case study on wastewater irrigation in Accra, Ghana, and includes an investigation into the ability of natural treatment processes, including sunlight inactivation, to disinfect wastewater before use. Wastewater irrigation in urban agriculture is prevalent around the world, and is both a product and potential alleviator of water-related challenges in rapidly growing cities. The use of wastewater for irrigation often occurs in water scarce places – where wastewater is the only source of water available for irrigation, and is collected directly from drains and treatment facilities – and in places where the development of wastewater collection and treatment infrastructure cannot keep up with wastewater production by a growing population. The latter leads to indirect wastewater use when irrigation water sources are contaminated by untreated wastewater discharged to the environment. Wastewater irrigation practiced in Accra is a combination of direct and indirect use.

In addition to the benefits of wastewater irrigation for farmers – including year-round access to irrigation water in areas where unpolluted freshwater is not available – municipalities stand to benefit if farmland can act as a sink for wastewater, reducing wastewater flows into the environment and, therefore, public exposure to sewage. Agricultural land in cities can also contribute to stormwater management and mitigate flooding (Lydecker and Drechsel 2010).

Despite the benefits of wastewater irrigation, the potential presence of human pathogens creates a health risk for farmers and consumers.

Many urban farmers in Accra store wastewater used for irrigation in small, on-farm ponds before use (volumes ranging from 0.5 to 12 m^3; Drechsel et al. 2006; Keraita et al. 2008a; Reymond et al. 2009). While not originally meant for wastewater treatment, these ponds present an opportunity for natural disinfection. The goal of the second part of this dissertation was to better understand the health risks associated with wastewater irrigation in Accra, and determine whether small, farmer-dug ponds can contribute to disinfection of irrigation water. Specific objectives were to:

- Quantify and compare the concentrations of indicator organisms and human viruses in waters used for irrigation in Accra
- Determine the extent of bacteria and bacteriophage removal in small, on-farm, wastewater storage ponds, as well as the contribution of sunlight inactivation to removal

Dissertation Overview

Chapter 2 includes a more detailed introduction to sunlight inactivation mechanisms and presents an investigation into the rates and mechanisms of sunlight inactivation of two bacteriophage (MS2 and PRD1) and two human viruses (adenovirus type 2 and poliovirus type 3) in a panel of NOM-containing waters collected from different environmental sources. The findings in this chapter – that different viruses were susceptible to inactivation mechanisms to different extents, and that sunlight inactivation rates differed among viruses and water matrices – make it clear that water quality conditions and virus type must be taken into account when predicting inactivation rates. Additionally, MS2 was inactivated at the slowest rate in all waters, and PV3 the fastest, at the water depth that was studied (i.e., 5 cm).

Data obtained in Chapter 2, along with findings from other researchers, were used in Chapter 3 to develop and test models that predict the sunlight inactivation rates of viruses in surface waters containing light attenuating photosensitizers. Models were developed for one virus whose inactivation is dominated by endogenous mechanisms (poliovirus type 3) and one dominated by the exogenous mechanism (MS2). Inactivation rates were modeled and measured in reactors containing different, well-mixed depths of water collected from an open-water wastewater treatment system. The models performed well in predicting inactivation rates in laboratory experiments. Additionally, the inactivation rate of poliovirus type 3, which depends on endogenous inactivation mechanisms, was found to be lower than that of MS2 at deeper well-mixed depths, due to the susceptibility of MS2 to the exogenous mechanism; this result indicates that MS2 cannot be considered a conservative indicator of poliovirus inactivation under all conditions. Included in the chapter is a discussion of research gaps that must be filled before translating the models to environmental waters and natural sunlight.

Chapter 4 presents an investigation into whether sunlight inactivation of poliovirus type 3 is caused by damage to the virus's protein capsid. More specifically, this research focused on the inhibition of viral 'life' processes that depend on an intact capsid. Comparing data from assays

that quantify host cell attachment and infectivity, we found that although sunlight exposure leads to an inhibition of poliovirus type 3 attachment to host cells (which is the first step in the infection process), this damage mechanism plays a minor role in total inactivation.

The second part of the dissertation focuses on a case study of wastewater irrigation in Accra, Ghana. Chapter 5 presents an investigation into the concentrations of fecal indicator organisms and two viral pathogens (human adenovirus and norovirus) in wastewater used for vegetable irrigation. *E. coli* concentrations in all samples exceeded recommended limits set by the World Health Organization, human viruses were detected in 75% of samples analyzed, and virus concentrations were quantified in 60% of samples. This research provides data that can be used in quantitative microbial risk assessment models of wastewater irrigation in Accra.

After determining indicator organism and pathogen concentrations in Chapter 5, we investigated the ability of a farmer-led intervention (small, on-farm ponds) to disinfect wastewater before use in vegetable irrigation; this work is presented in Chapter 6. Results indicated that sunlight inactivation was the dominant removal mechanism of two bacteria (*E. coli* and enterococci) and two bacteriophages (F+ and somatic coliphage) in these ponds, and that the ponds can contribute to the multi-barrier approach to reducing health risks related to wastewater irrigation. On-farm pond design and management recommendations, as well as challenges, are also discussed.

Further implications of the research presented in this dissertation are discussed in the Conclusion section.

Chapter 2

Sunlight inactivation of human viruses and bacteriophages in coastal waters containing natural photosensitizers

The following chapter is adapted from Silverman et al. (2013) Sunlight inactivation of human viruses and bacteriophages in coastal waters containing natural photosensitizers. *Environ. Sci. Technol.* 47, 1870-1878, with permission from Britt M. Peterson, Alexandria B. Boehm, Kristopher McNeill, and Kara L. Nelson.

Introduction

Surface water contamination by human enteric viruses is common and can occur through urban runoff (Jiang et al. 2001; Nobel et al. 2006) and wastewater flows into the environment (Boehm et al. 2009; Sassoubre et al. 2012). Viruses are more difficult to remove and inactivate than fecal indicator bacteria during wastewater treatment, and infectious human viruses have been found in wastewater treatment facility effluents discharged into surface waters (Sedmark et al. 2005). Sunlight – which contains UVB (λ = 280–320 nm), UVA (λ = 320–400 nm) and visible light (λ = 400–700 nm) regions – causes inactivating damage to microorganisms (Curtis et al. 1992; Davies-Colley et al. 1999; Davies-Colley et al. 2000; Kohn and Nelson 2006; Kohn et al 2007; Love et al. 2010; Romero et al. 2011) and is an important mode of disinfection in waste stabilization ponds (WSP; Curtis et al. 1992; Davies-Colley et al. 1999; Davies-Colley et al. 2005), recreational water bodies (Boehm et al. 2009), and SODIS (Fisher et al. 2008; Heaselgrave et al. 2006; Reed 2004). While viruses are a significant cause of waterborne disease, and believed to be the main etiology of disease to swimmers at recreational beaches (WHO 2003), sunlight inactivation of human viruses in the environment is understudied.

Most waterborne viruses are non-enveloped and consist of nucleic acids (single- or double-stranded RNA or DNA) surrounded by a protective protein capsid. The sunlight inactivation terminology presented below is a slight shift from that used previously (Davies-Colley et al. 1999; Davies-Colley et al. 2000; Jagger 1985; Kohn and Nelson 2006; Kohn et al 2007; Love et al. 2010; Romero et al. 2011), but is introduced to better relate mechanisms to environmental conditions; a summary is presented in Figure 1.1 and Table 2.1. There are three proposed virus inactivation mechanisms: the direct and indirect endogenous mechanisms require absorption of photons by virus components, while the exogenous mechanism involves reaction between the virus and exogenously produced reactive intermediates formed in photochemical reactions. The direct and indirect endogenous mechanisms differ in that the direct mechanism causes damage to the virus component that absorbed the photon, either nucleic acids (leading to formation of pyrimidine dimers and other photoproducts; Jagger 1985) or proteins (resulting in photo-oxidation of select amino acid residues; Boreen et al. 2008; Davies and Truscott 2001), while the indirect-endogenous mechanism occurs when photons are absorbed by one part of the virus, but

damage is conveyed to another through electron transfer or sensitized formation of and subsequent reaction with reactive intermediates, such as singlet oxygen ($^1O_2$; Davies and Truscott 2001). It is difficult to separate the two endogenous mechanisms experimentally, and they are often lumped together. The exogenous mechanism occurs when photons are absorbed by photosensitizers in the water column, leading to the formation of reactive intermediates, such as excited triplet states [e.g., triplet dissolved organic matter (^{3}DOM)] and reactive oxygen species [ROS; e.g., $^1O_2$, hydrogen peroxide (H_2O_2), superoxide (O_2^-), hydroxyl radical ($OH\cdot$), and peroxyl radicals; Blough and Zepp 1995; Cooper et al. 1989]. Reactive intermediates contribute to inactivation by causing oxidative damage to virion components (Curtis et al. 1992; Davies-Colley et al. 1999; Wigginton et al. 2010); to date, there is only evidence of $^1O_2$ involvement in photoinactivation of viruses (Kohn and Nelson 2006). While both the indirect-endogenous and exogenous mechanisms involve reaction with reactive intermediates, the indirect-endogenous mechanism depends on photons absorbed by endogenous sensitizers (e.g., amino acid residues) (Davies and Truscott 2001; Davies 2003), and the exogenous mechanism depends on photons absorbed by photosensitizers in the water (e.g., natural organic matter (NOM); Curtis et al. 1992; Sinton et al. 1999).

Many studies investigating sunlight inactivation of viruses have focused on MS2 and other F+RNA coliphage (Davies-Colley et al. 2000; Jagger 1985; Kohn and Nelson 2006; Kohn et al 2007; Love et al. 2010; Romero et al. 2011; Sinton et al. 1999; Sinton et al. 2002) – single-stranded RNA bacteriophages frequently used as model organisms for enteric viruses due to their similar structure and size (Havelaar et al. 1993) – and somatic coliphage (Love et al. 2010; Sinton et al. 2002). MS2, for example, has been found to be susceptible to endogenous (Love et al. 2010) and exogenous (Kohn and Nelson 2006; Kohn et al 2007) inactivation mechanisms when exposed to sunlight in the presence of sensitizers. Bacteriophage, however, do not pose

Table 2.1. Summary of possible viral sunlight inactivation mechanisms**.**

Mechanism	Photons absorbed by	Damage caused by	Light region responsible
Endogenous Direct	Virus components	Direct photolysis	UVB
Endogenous Indirect	Virus components (endogenous photosensitizers)	Reactive intermediates	UVB
Exogenous Indirect	Exogenous photosensitizers	Reactive intermediates	UVB, UVA and visible

human health threats and may not accurately model human virus inactivation under all environmental conditions. Variable virus structures, and therefore targets of sunlight damage, may result in different rates and dominant mechanisms of sunlight-mediated inactivation. At this point, it is not possible to predict mechanisms or rates of sunlight inactivation of viruses of public health concern based on current knowledge of bacteriophage inactivation. To better understand sunlight inactivation of mammalian viruses, it is necessary to study them directly. To date, few published studies have investigated the effect of sunlight on mammalian viruses, and no previous studies have investigated mammalian virus inactivation in environmentally sourced waters containing natural sensitizers, such as NOM.

NOM is found in most aquatic environments (Cooper et al. 1989) and, due to its high concentration of aromatic functional groups (Wershaw 2004), is one of the most important sunlight absorbing substances in natural waters (Zepp 1988). NOM varies in composition and structure depending on its source (Kördel et al. 1997), which can cause NOM from different environmental waters to possess varying propensities to absorb light, produce ROS and associate with other water constituents, including viruses. Because NOM is capable of both sunlight attenuation and ROS production, NOM can increase or decrease sunlight inactivation rates, depending on its structure and the dominant mechanism of inactivation of the target organism. To investigate the variability of virus inactivation rates in different surface waters, it is important to study sunlight inactivation of viruses in waters containing natural dissolved and particulate constituents.

In this study, we investigated sunlight inactivation of viruses in five environmentally sourced coastal waters containing NOM. The goals of this study were to: (1) determine the main mechanisms of sunlight inactivation of two human viruses (HAdV2 and PV3) and two bacteriophages (MS2 and PRD1) in environmental waters containing natural photosensitizers (see Table 2.2 for virus characteristics); (2) compare sunlight inactivation rates *among viruses*; and (3) investigate the variability in inactivation rates of each organism *among environmental matrices*. A better understanding of sunlight-mediated disinfection mechanisms and relative rates of virus inactivation in NOM-containing waters can aid in designing natural wastewater treatment schemes, predicting rates of virus inactivation in sunlit environments, and determining the best indicator organisms for tracking the fate of viruses in surface waters, such as recreational beaches and engineered treatment systems.

Methods

Target viruses were inoculated into reactors containing one of five unfiltered, environmentally sourced waters (with presumably different concentrations and sources of NOM) or a sensitizer-free control water; reactors were exposed to simulated sunlight and virus concentrations were monitored to determine rates of sunlight inactivation in each solution.

Table 2.2. Virus characteristics (Fauquet 2005; Michen and Graule 2010; Wong et al. 2012).

Virus	Poliovirus type 3 (PV3)	Adenovirus type 2 (HAdV2)	MS2	PRD1
Virus Family	Human virus; *Picornaviridae*	Human virus; *Adenoviridae*	Bacteriophage; *Leviviridae*	Bacteriophage; *Tectiviridae*
Diameter (nm)	30	70 – 90	27	62
Nucleic Acid Type	ssRNA, linear	dsDNA, linear	ssRNA, linear	dsDNA, linear
Genome Length (kb)	7 – 8.5	35.8 – 36.2	3.5	14.7
Protein Capsid Morphology	Icosahedral	Icosahedral with spikes	Icosahedral	Icosahedral with spikes
Isoelectric Point	(PV1) 6.6 – 8.3[1]	3.5 – 4	2.2 – 3.9	3.8 – 4.2

Human viruses. Detailed virus and bacteriophage methods are provided in Love et al. (2010). Briefly, PV3 (ATCC VR-300) was cultured on HeLa cells (ATCC CCL-2). HAdV2 was kindly provided by Mark Sobsey (University of North Carolina) and cultured on A549 cells (ATCC CCL-185). Viruses were propagated on 90% confluent cells in T-150 flasks; flasks were incubated at 37 ºC and 5% CO_2 for 4 d (PV3) or 7 d (HAdV2) with 1X Dulbecco's Modified Eagle Medium (DMEM; Invitrogen), 1X penicillin and streptomycin (pen/strep), and 2% (HAdV2) or 10% (PV3) fetal bovine serum (FBS). After incubation, viruses were released from cells by three freeze/thaw cycles. To remove broth constituents, crude virus stocks were chloroform extracted (1:3 vol/vol), centrifuged at 4000 ×*g* for 10 min to remove cell debris, and the supernatant was polyethylene glycol (PEG) precipitated overnight at 4 °C (9% PEG, 0.3 M NaCl), centrifuged at 20,000 ×*g* for 15 min to produce virus pellets that were resuspended in phosphate buffered saline (PBS; 10 mM NaCl, 20 mM phosphate), chloroform extracted as above and filtered through a 0.22 µm filter. Virus stocks were stored at -80 °C.

Virus plaque assays were performed in duplicate on 6-well plates of 90% confluent cells with 100 µL sample inocula and an agar overlay [1.5% wt/vol low melting point agarose (Fisher

[1] In some studies, PV1 has been observed to have two isoelectric points, with the second between 3.8 and 4.5.

Scientific), 1X DMEM, 1X pen/strep, and 2% (HAdV2) or 10% (PV3) FBS]. Plates were incubated at 37 °C and 5% CO_2 for 3 d (PV3) or 7 d (HAdV2) and plaque forming units (PFU) were counted. Samples were not filtered before analysis.

Bacteriophage. MS2 and PRD1 were kindly provided by Mark Sobsey, and were propagated and assayed using *E. coli* F_{amp} (ATCC 700891) and *Salmonella* LT2 (ATCC 19585) hosts, respectively. Bacteriophage were propagated by broth enrichment. Purified bacteriophage stocks were prepared in the same manner as human viruses except that there was no freeze/thaw step, and PRD1 was not chloroform extracted due to its 15% lipid volume by weight. Bacteriophage stocks were stored at -80 °C. Bacteriophage were assayed using the double agar layer (DAL) method with 100 µL sample inocula and modified Luria Bertani (LB) top and bottom agars. Modified LB consists of: bacto agar [0.75% (top) or 1.5% (bottom) wt/vol; BD], 10 g/L bacto tryptone (BD), 0.137 M NaCl, 1 g/L yeast extract (EMD Chemicals), 0.0055 M dextrose (EMD Chemicals), 0.002 M $CaCl_2$. DAL plates were incubated at 37 °C for 18–24 h and PFUs were counted.

Experimental waters. Viruses were inoculated into each of six different solutions: five environmental waters and a phosphate buffered saline (PBS) control. The environmental waters were collected in August 2009 as part of an associated field study (Sassoubre et al. 2012). Waters were stored at 4 °C in the dark and experiments were conducted within 8 months. The waters were as follows. MEX: mixture of seawater and partially treated wastewater collected near a coastal outfall in northern Mexico. BM: sewage-impacted seawater collected at a beach 0.5 km south of MEX. TJ: water collected from the Tijuana River estuary (Imperial Beach, California) at the end of ebb tide. ML: water collected from a section of the Malibu Lagoon coastal wetland (Malibu, CA) dominated by algae and submerged macrophytes. CT: water collected from a cattail dominated section of Malibu Lagoon. PBS consisted of 16 mM Na_2HPO_4, 4 mM NaH_2PO_4 and 10 mM NaCl. Previous research has shown that particles and colloids contribute to exogenous inactivation of MS2 (Kohn and Nelson 2007); thus, environmental waters were not filtered or sterilized before use.

The absorption spectrum of each water sample was measured before and after experiments using a UV-visible spectrophotometer (scan from 250–800 nm; Lambda 35, Perkin Elmer). Turbidity and salinity were measured in MEX, BM, TJ and ML as part of the field study, using a Hach Hydrolab Quanta. pH was measured during simulated sunlight experiments using an Accumet pH electrode.

Solar simulator experiments. Experiments were conducted using a 1000 W solar simulator with a Xe bulb (Oriel). Bulb irradiance was measured at the start of each experiment using a spectroradiometer (EPP2000C-SR-100 with CR2 cosine receptor, Stellarnet) to ensure consistent light spectrum across experiments. Reactors consisted of 200-mL glass beakers painted black on the outside. Reactors were filled with 100 mL solution and inoculated with purified virus stock: average, initial virus concentrations were $(6.3 \pm 1.3) \times 10^4$, $(6.4 \pm 3.0) \times 10^4$, $(8.3 \pm 2.5) \times 10^5$, and $(9.1 \pm 5.9) \times 10^5$ PFU/mL for PV3, HAdV2, MS2 and PRD1, respectively. Human viruses were spiked individually while bacteriophages were co-spiked; no infection of MS2 on *Salmonella* LT2 or PRD1 on *E. coli* F_{amp} was observed. During experiments, reactors were constantly mixed using a stir plate and sterile stir bars, located in a water bath cooled by a recirculating chiller to maintain a temperature of 20 °C, and exposed to simulated sunlight for

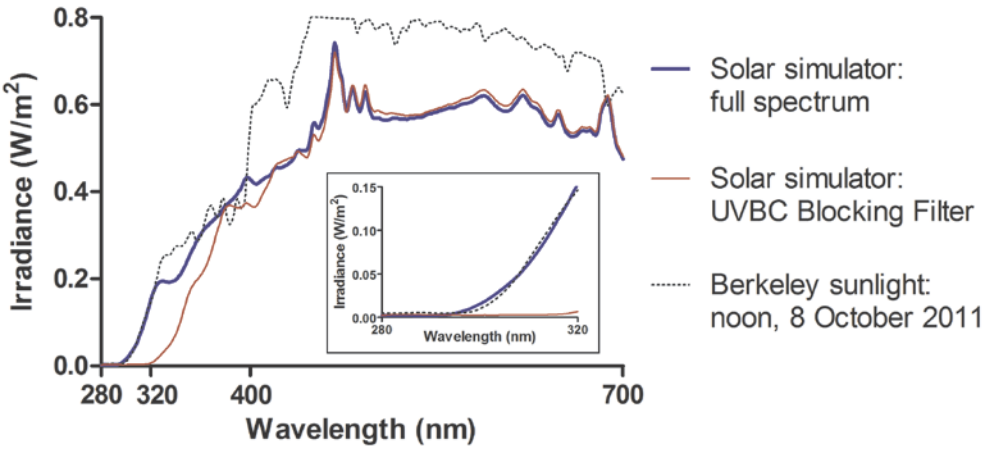

Figure 2.1. Laboratory solar simulator spectra using an atmospheric attenuation filter (thick solid blue line; $n = 7$) and a UVB blocking filter (thin solid red line; $n = 8$). A natural sunlight spectrum measured at noon in Berkeley, CA on 8 October 2011 (dotted line) is provided for comparison. The total irradiance measured from 280–700 nm was 194 W/m^2 for the atmospheric filter and 187 W/m^2 for the UVB blocking filter. The total irradiance measured in the UVB range (280–320 nm) was 1.6 W/m^2 for the atmospheric filter and 0.13 W/m^2 for the UVB blocking filter; for comparison, the total UVB irradiance of the Berkeley sunlight sample was 1.6 W/m^2. The total irradiance measured in the UVA range (320–400 nm) was 24 W/m^2 for the atmospheric filter and 17 W/m^2 for the UVB blocking filter.

10 h. One milliliter sub-samples were removed from each reactor every 2 h. Sub-samples were immediately placed on ice and assayed within 6 h of collection. Dark controls were maintained in the same way, but were covered with aluminum foil. Simulated sunlight experiments were conducted in duplicate.

Experiments were conducted using an atmospheric filter to mimic the solar spectrum or a UVB blocking filter to remove the UVB portion of the spectrum. The average total irradiance from 280–700 nm was 194 W/m^2 for the atmospheric filter and 187 W/m^2 for the UVB blocking filter. The solar simulator spectra are presented in Figure 2.1.

Steady-state singlet oxygen concentration. Bulk-phase, steady-state singlet oxygen concentrations ($[^1O_2]_{ss,bulk}$) were determined for each water through photolysis experiments using furfuryl alcohol (FFA; $k_q = 1.2 \times 10^8$ M^{-1} s^{-1}; Haag et al. 1984a) as a probe compound. Photolysis experiments were conducted in a similar manner as virus inactivation experiments described above, with FFA added to each reactor at an initial concentration of 75 µM. Reactors were irradiated with simulated sunlight for 6 h and sub-samples were collected every 1 to 2 h. Sub-samples were analyzed for FFA concentration by HPLC (Gynkotek) with a reverse-phase C18 column (Alltima C18LL, Altech) with a guard column, and eluted with 80% formic acid and

20% acetonitrile. Observed first order FFA decay constants ($k_{obs,FFA}$) were calculated as the negative slope of $\ln([FFA]_t/[FFA]_0)$ versus time, following the equation:

$$\ln \frac{[FFA]_t}{[FFA]_0} = -k_{obs,FFA} \cdot t \quad (2.1)$$

where $[FFA]_0$ is the initial FFA concentration and $[FFA]_t$ is the concentration of FFA at time t. The slope of the graph was determined by linear regression. $[^1O_2]_{ss,bulk}$ was calculated according to the equation:

$$[^1O_2]_{ss,bulk} = \frac{k_{obs,FFA}}{k_q} \quad (2.2)$$

where k_q is the second order rate constant of FFA with singlet oxygen.

Data analysis. First-order, observed inactivation rate constants for each virus in each matrix were calculated in two ways. First, the apparent first-order observed inactivation rate (k_{obs}; h^{-1}) reflects the rate of inactivation observed over time and was calculated as the negative slope of the linear regression trend line of $\ln(C_t/C_0)$ *versus time*, following the equation:

$$\ln \frac{C_t}{C_0} = -k_{obs} \cdot t \quad (2.3)$$

where C_0 is the initial virus concentration (PFU/mL) and C_t is the virus concentration (PFU/mL) at time t (h).

Second, to help elucidate inactivation mechanisms and provide a way to normalize inactivation rates across waters with different absorbance spectra, the first-order rate constant was also calculated accounting for light intensity incident on the water surface and light screening in the water column ($k_{obs,photon}$; m^2 $photon^{-1}$). $k_{obs,photon}$ was calculated as the negative slope of the linear regression trend line of $\ln(C_t/C_0)$ *versus the average photon fluence in the water column* in the spectral range of 280 to 320 nm (F_{photon}; photon m^{-2}), following the equation:

$$\ln \frac{C_t}{C_0} = -k_{obs,photon} \cdot F_{photon} \quad (2.4)$$

F_{photon} represents the number of photons available for absorption by the virus and photosensitizers, and was calculated over the range of 280–320 nm because this and previous research observed UVB light to be most important for virus inactivation (Love et al. 2010). However, a limitation of this, and similar, light screening calculations (Grandbois et al. 2008; Kohn et al. 2007; Romero et al. 2011) is that we assume all wavelengths between 280 and 320 nm have the same ability to directly damage virions or produce ROS. While photons of different wavelengths have different abilities to damage viruses directly (Fisher et al. 2011) and sensitize

production of reactive species (Haag et al. 1984b; Paul et al 2004), the complete information needed to develop weighting functions for each wavelength does not yet exist.

F_{photon} was determined by first calculating the average light irradiance at total depth z, $\langle I_\lambda \rangle_z$ (W m^{-2}), using the equation employed by Grandbois et al. (2008), Kohn et al. (2007), and Romero et al. (2011):

$$\langle I_\lambda \rangle_z = I_{\lambda,0} \frac{(1 - 10^{-\alpha_\lambda 1.2z})}{2.303\alpha_\lambda \cdot 1.2z} = I_{\lambda,0} \cdot S_\lambda \quad (2.5)$$

where $I_{\lambda,0}$ is the wavelength-specific irradiance incident on the water surface (W m^{-2}), α_λ is the decadic absorbance of the matrix water (average of absorbances at t = 0 and t = 10 h; cm^{-1}), $1.2z$ is the path length of the incident light over depth z (e.g., 5 cm; Zepp and Cline 1977; Zepp et al. 1985), and S_λ is the light screening factor. The tailing in the MEX and BM absorbance spectra indicate that there was significant light scattering; the $1.2z$ path length correction factor was used to correct for a longer path taken by photons due to scattering.

$\langle I_\lambda \rangle_z$ was translated into depth-averaged, total photon flux, ϕ_{photon} (photon m^{-2} s^{-1}), over the range 280 to 320 nm using the following equation:

$$\phi_{photon} = \sum_{\lambda=280}^{320} \frac{\langle I_\lambda \rangle_z \cdot \lambda}{h \cdot c} \quad (2.6)$$

where c is speed of light (3.0×10^8 m s^{-1}), h is Planck's constant (6.626×10^{-34} J s), λ is the wavelength (10^{-9} m). ϕ_{photon} was used in the following equation to calculate F_{photon} (photon m^{-2}):

$$F_{photon} = \phi_{photon} \cdot t \quad (2.7)$$

Simulated sunlight experiments were conducted in duplicate. k_{obs} and $k_{obs,photon}$ were computed as follows. $\ln(C_t/C_0)$ values were calculated for each time point and each replicate; these values (12 data points = six time points × two replicate experiments) were pooled and used to calculate k_{obs} (or $k_{obs,photon}$) and the standard error of the slope by linear regression. ANOVA with Dunnett's post-test were used to determine whether the slopes of the linear regression lines (i.e., k_{obs} and $k_{obs,photon}$) of the environmental waters were significantly different from that in the sensitizer-free control (PBS); inputs were k_{obs} (or $k_{obs,photon}$), standard error of the slope and the number of data points. Statistical tests were performed in Prism (v5.04, GraphPad Software).

Dark reactors were sampled at the beginning and end of 10 h experiments. Data from multiple experiments were pooled, and linear regression was used to calculate k_{dark} (n = 2 or more for all experiments except PV3 in MEX, BM and TJ, and HAdV2 in MEX, CT and PBS). An analysis of covariance (ANCOVA) was conducted in GraphPad Prism to determine if k_{dark} was significantly different from zero.

Results

Absorbance spectra, pH, and salinity. As in other NOM-containing waters (Cooper et al. 1989), the absorbance of experimental waters used in this study was highest in the UVB region, and decreased with increasing wavelength (Figure 2.2). MEX absorbance measurements were 16 to 120 times greater than the other environmental waters (total absorbance over the range 280–700 nm), followed by BM > ML = CT > TJ > PBS. Total absorbance decreased by 8, 49, 39, 4 and 13% for MEX, BM, TJ, ML, and CT, respectively, during the 10 h experiments. pH ranged from 7.4–8.2 during experiments. Salinity ranged from 11.8–30.3 psu for the five environmental waters (Table 2.3).

Singlet oxygen. Bulk-phase, steady-state singlet oxygen concentrations ($[^1O_2]_{ss,bulk}$) were between $(1.3 \pm 0.58) \times 10^{-14}$ and $(8.3 \pm 0.55) \times 10^{-14}$ M, with TJ having the lowest and MEX the highest $[^1O_2]_{ss,bulk}$ (Table 2.3). While $[^1O_2]_{ss,bulk}$ in PBS was calculated to be $(1.2 \pm 1.1) \times 10^{-14}$ M, this value was not found to be statistically different than zero.

Table 2.3. Steady-state single oxygen concentration in bulk solution ($[^1O_2]_{ss,bulk}$), turbidity and salinity of each environmental water. No turbidity or salinity data are available for CT or PBS. The ionic strength of seawater [salinity ~ 35 practical salinity units (psu)] can range between 700 and 1000 mM.

Water	$[^1O_2]_{ss,bulk}$ (x 10^{-14} M)	Turbidity (NTU)	Salinity (psu)
MEX	8.3 ± 0.55	>100	11.8
BM	2.9 ± 0.46	27.1	30.1
TJ	1.3 ± 0.57	36.4	30.3
ML	5.7 ± 0.64	15.4	12.7
CT	5.0 ± 0.28	-	-
PBS	1.2 ± 1.1	-	Ionic Strength = 62 mM

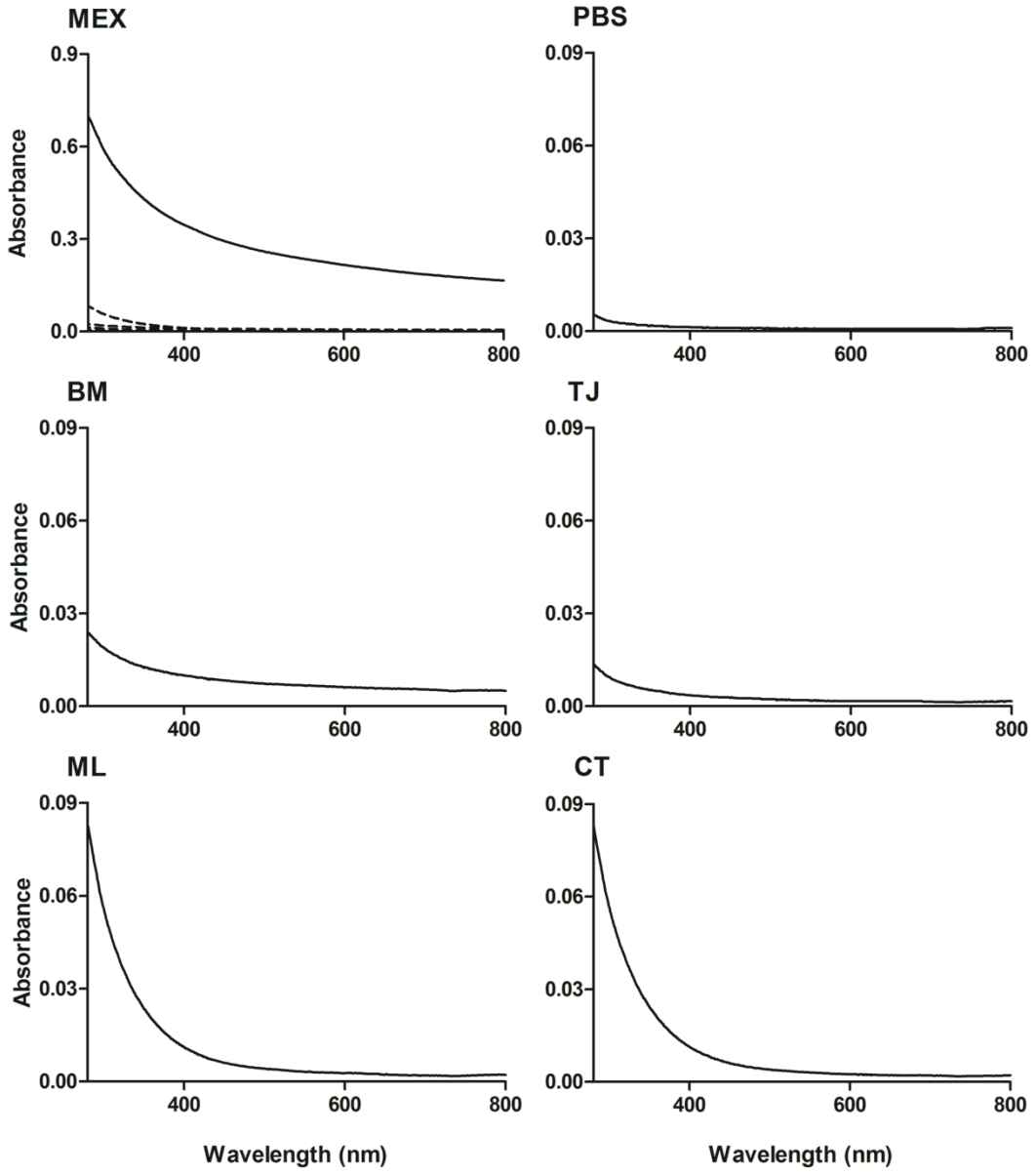

Figure 2.2. Decadic absorbance spectra of experimental matrix waters (measurement $n = 6$). Spectra are average of absorbance measured at the beginning and end of each experiment; total absorbance decreased by 8, 49, 39, 4 and 13% for MEX, BM, TJ, ML, and CT, respectively, during the 10 h experiments. The depths of 99% attenuation of 300 nm light were 186, 88, 34, 35, 3.3 cm for TJ, BM, CT, ML, and MEX, respectively; the depths of 99% attenuation of 400 nm light were greater: 445, 150, 162, 176, and 5.6 cm. Note the different y-axis scale of the MEX graph; dashed lines in MEX graph are absorbance spectra of PBS, BM, TJ, ML and CT for comparison amongst waters using the same scale.

Simulated sunlight inactivation of viruses and bacteriophage. Inactivation curves with exposure to full-spectrum simulated sunlight are presented in Figure 2.3. Inactivation rates as functions of time (k_{obs}) with exposure to full-spectrum and UVB-blocked sunlight are presented in Figures 2.4A and B, respectively, and inactivation rates as functions of photon fluence ($k_{obs,photon}$) are presented in Figure 2.4C; numerical values, standard error and R^2 of linear regressions are reported in Table 2.4. It should be noted that reported k_{obs} values are only applicable to the same exact conditions as in these experiments (e.g., same water composition, reactor depth, and sunlight spectrum and intensity). $k_{obs,photon}$ values for all four viruses in MEX are likely overestimated. The tailing in the MEX absorbance spectrum indicates significant light scattering; this likely caused artificially high absorbance measurements and an overestimation of $k_{obs,photon}$.

Dark control inactivation rates (k_{dark}) were always observed to be lower than the corresponding k_{obs} measured with exposure to simulated sunlight, except for HAdV2 exposed to UVB-blocked light in PBS, MS2 in PBS, and PV3 in CT (Table 2.4), though none of these k_{dark} values were found to be significantly different from zero.

Poliovirus. When exposed to full-spectrum simulated sunlight, PV3 was inactivated at the fastest rates in BM and the sensitizer-free control (PBS). PV3 inactivation in MEX, TJ, ML and CT occurred at significantly slower rates than in PBS ($p < 0.001$ for MEX, $p < 0.05$ for TJ, ML and CT); PV3 k_{obs} was lowest in MEX. Slower inactivation rates in chromophore-containing waters suggest that light attenuation, leading to fewer photons incident on virus nucleic acids and proteins, resulted in reduced PV3 k_{obs}. This hypothesis is supported by analysis of inactivation rates after correcting for light screening (Figure 2.4C): there was no significant difference between PV3 $k_{obs,photon}$ in the sensitizer-free control and TJ, BM, ML, or CT. $k_{obs,photon}$ was significantly larger in MEX ($p < 0.001$).

PRD1. When exposed to full-spectrum simulated sunlight, PRD1 k_{obs} in environmental waters other than MEX were faster than k_{obs} in PBS, though not significantly different statistically. PRD1 inactivation in MEX, which had the highest absorbance, was significantly slower than in PBS ($p < 0.01$). After correcting for light screening, PRD1 $k_{obs,photon}$ in MEX, ML and CT were significantly faster than that in PBS ($p < 0.01$). The finding that PRD1 inactivation was enhanced in some waters containing light-absorbing natural constituents suggests that the exogenous mechanism contributed to inactivation.

Adenovirus. Inactivation of HAdV2 in ML, BM and TJ occurred at significantly faster rates than in PBS ($p < 0.05$, $p < 0.001$, and $p < 0.001$, respectively), with the greatest k_{obs} in TJ. While not statistically significant, HAdV2 inactivation in CT was also greater than in PBS. Sunlight inactivation of HAdV2 in PBS and MEX occurred at the slowest rates. After correcting for light screening, HAdV2 $k_{obs,photon}$ in MEX was greater than that in the other waters ($p < 0.001$), while $k_{obs,photon}$ in the other environmental waters were not significantly different from that in PBS. As with PRD1, our results demonstrate the contribution of the exogenous mechanism in sunlight inactivation of HAdV2.

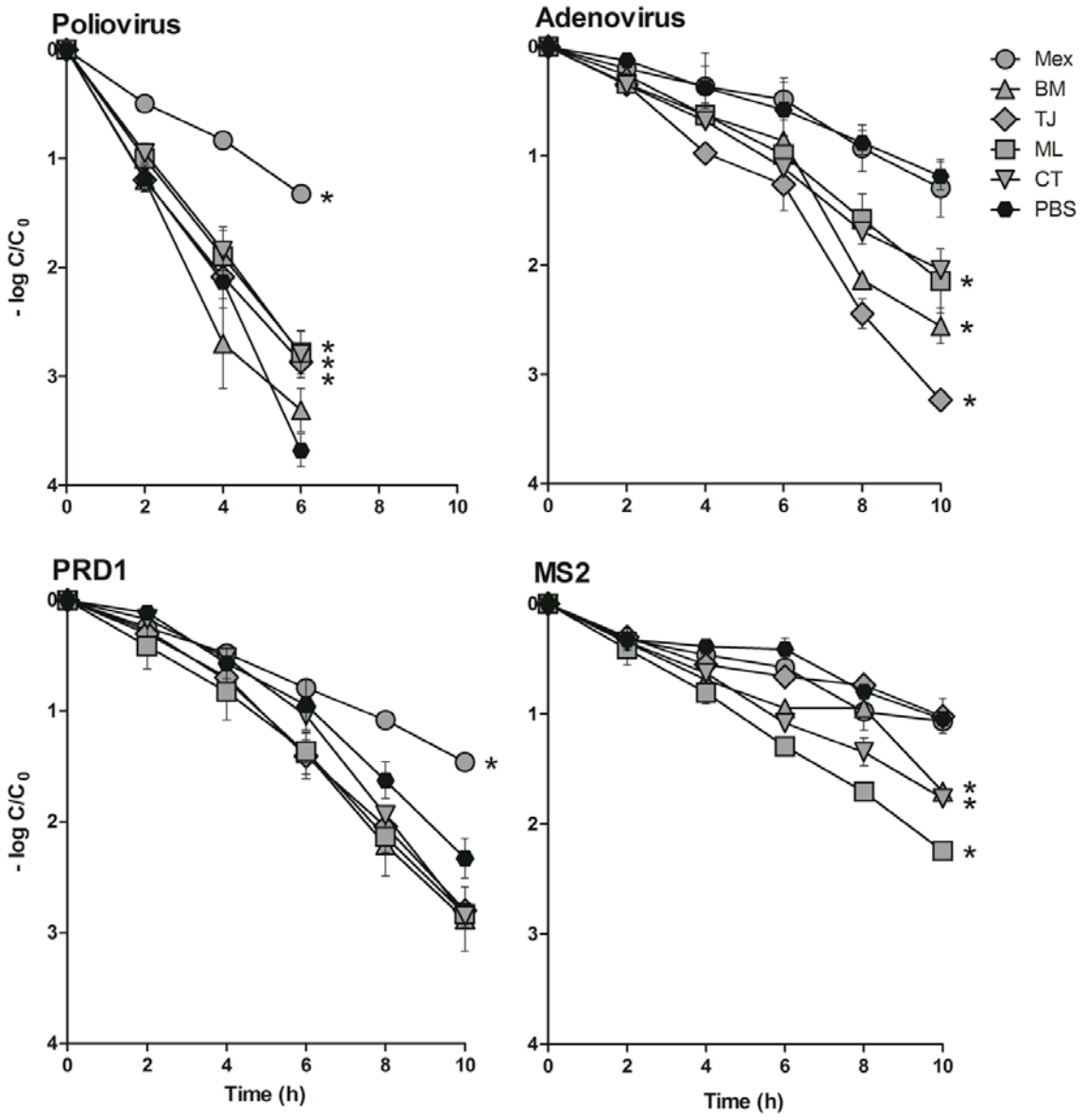

Figure 2.3. Solar simulator inactivation of PV3, HAdV2, MS2 and PRD1 inoculated into PBS or one of five environmental waters and exposed to full-spectrum simulated sunlight (experiment $n = 2$, except $n = 1$ for HAdV2 in CT). Error bars represent standard error. Asterisks indicate inactivation rates that differ significantly from PBS ($p < 0.05$; Dunnett's post test).

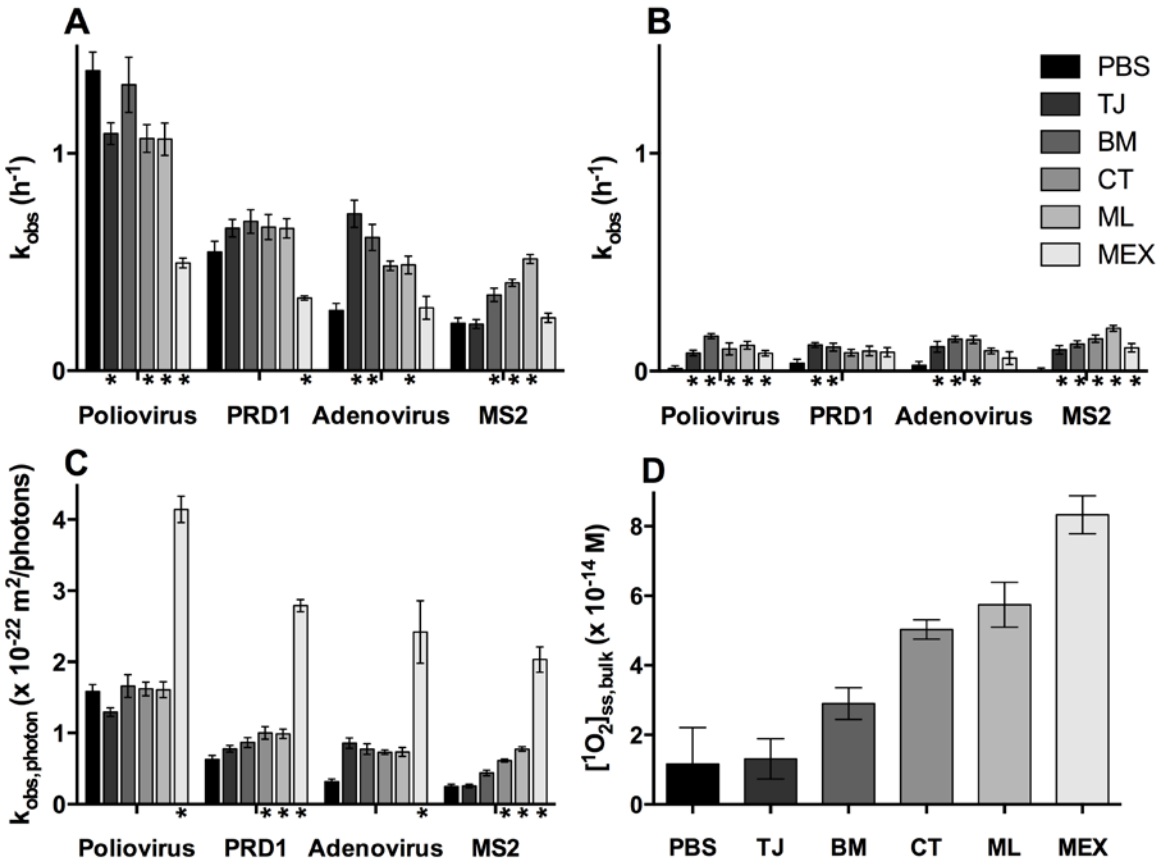

Figure 2.4. Panels A and B: First-order observed inactivation rates as functions of time (k_{obs}; h^{-1}) for viruses exposed to full-spectrum simulated sunlight (A) or simulated sunlight with the UVB region removed by an attenuation filter (B). Panel A was derived from data in Figure 2.3. Panel C: First-order observed inactivation rates as functions of photon fluence ($k_{obs,photon}$; m^2 $photon^{-1}$) with exposure to full-spectrum sunlight. Panel D: Bulk phase steady state singlet oxygen concentrations ($[^1O_2]_{ss,bulk}$) with exposure to full-spectrum simulated sunlight. Waters are listed in order of increasing $[^1O_2]_{ss,bulk}$. Experiment $n = 2$ for all, except $n = 1$ for Panel D and HAdV2 in CT in Panel A. Error bars represent standard error. Asterisks indicate inactivation rates that differ significantly from PBS ($p < 0.05$; Dunnett's post test).

Target Organism	Water	Full-spectrum Sunlight Mean k_{obs} ± Standard Error [h^{-1}] (R^2; n)	UVA and Visible Light Mean $k_{obs,UVB\text{-}block}$ ± Standard Error [h^{-1}] (R^2; n)	k_{dark} [h^{-1}]	Full-spectrum Sunlight Mean $k_{obs,photon}$ ± Standard Error [x 10^{-22} m^2 $photon^{-1}$] (R^2; n)
Poliovirus type 3	MEX	0.50 ± 0.02 (0.99; 2)	0.08 ± 0.01 (0.81; 2)	0.017*	4.14 ± 0.19 (0.99; 2)
	BM	1.32 ± 0.13 (0.95; 2)	0.16 ± 0.01 (0.95; 2)	0.041*	1.66 ± 0.16 (0.95; 2)
	TJ	1.09 ± 0.05 (0.99; 2)	0.08 ± 0.01 (0.81; 2)	0.032*	1.30 ± 0.06 (0.99; 2)
	ML	1.07 ± 0.07 (0.97; 2)	0.12 ± 0.02 (0.81; 2)	0.001 ± 0.021*	1.61 ± 0.11 (0.97; 2)
	CT	1.07 ± 0.06 (0.98; 2)	0.10 ± 0.03 (0.57; 2)	0.122 ± 0.117*	1.62 ± 0.10 (0.98; 2)
	PBS	1.38 ± 0.09 (0.98; 2)	0.01 ± 0.01 (0.08; 2)*	0.006 ± 0.002*	1.59 ± 0.10 (0.98; 2)
Adenovirus type 2	MEX	0.29 ± 0.05 (0.77; 2)	0.06 ± 0.03 (0.29; 2)*	0.047*	2.42 ± 0.44 (0.77; 2)
	BM	0.61 ± 0.06 (0.91; 2)	0.15 ± 0.01 (0.92; 2)	0.069 ± 0.086*	0.77 ± 0.08 (0.91; 2)
	TJ	0.72 ± 0.06 (0.94; 2)	0.11 ± 0.03 (0.66; 2)	0.087 ± 0.075*	0.86 ± 0.07 (0.94; 2)
	ML	0.49 ± 0.04 (0.94; 2)	0.09 ± 0.01 (0.83; 2)	0.071 ± 0.055*	0.74 ± 0.06 (0.94; 2)
	CT	0.48 ± 0.02 (0.99; 1)	0.15 ± 0.02 (0.88; 2)	0.118*	0.73 ± 0.03 (0.99; 1)
	PBS	0.28 ± 0.03 (0.88; 2)	0.03 ± 0.02 (0.17; 2)*	0.123*	0.32 ± 0.04 (0.88; 2)
PRD1	MEX	0.33 ± 0.01 (0.99; 2)	0.09 ± 0.02 (0.62; 2)	-0.036 ± 0.030*	2.79 ± 0.09 (0.99; 2)
	BM	0.68 ± 0.06 (0.94; 2)	0.11 ± 0.02 (0.79; 2)	-0.034 ± 0.045*	0.87 ± 0.07 (0.94; 2)
	TJ	0.66 ± 0.04 (0.97; 2)	0.12 ± 0.01 (0.93; 2)	-0.034 ± 0.037*	0.78 ± 0.05 (0.97; 2)
	ML	0.66 ± 0.04 (0.96; 2)	0.09 ± 0.02 (0.64; 2)	-0.020 ± 0.060*	0.99 ± 0.07 (0.96; 2)
	CT	0.66 ± 0.06 (0.93; 2)	0.08 ± 0.02 (0.77; 2)	-0.022 ± 0.080*	1.00 ± 0.09 (0.93; 2)
	PBS	0.55 ± 0.05 (0.92; 2)	0.03 ± 0.02 (0.27; 2)*	-0.043 ± 0.0394*	0.63 ± 0.06 (0.92; 2)
MS2	MEX	0.24 ± 0.02 (0.93; 2)	0.11 ± 0.02 (0.75; 2)	-0.035 ± 0.078*	2.03 ± 0.18 (0.93; 2)
	BM	0.35 ± 0.03 (0.93; 2)	0.12 ± 0.03 (0.88; 2)	0.012 ± 0.061*	0.44 ± 0.04 (0.93; 2)
	TJ	0.22 ± 0.02 (0.92; 2)	0.10 ± 0.02 (0.71; 2)	-0.015 ± 0.086*	0.26 ± 0.03 (0.92; 2)
	ML	0.51 ± 0.02 (0.99; 2)	0.20 ± 0.01 (0.96; 2)	0.040 ± 0.008	0.78 ± 0.03 (0.99; 2)
	CT	0.40 ± 0.02 (0.99; 2)	0.15 ± 0.02 (0.88; 2)	0.042 ± 0.034 *	0.61 ± 0.02 (0.99; 2)
	PBS	0.22 ± 0.03 (0.89; 2)	0.01 ± 0.02 (0.02; 2)*	0.013 ± 0.045*	0.25 ± 0.03 (0.89; 2)

Table 2.4. Summary of virus inactivation rates in different environmental waters using a solar simulator, with and without a filter to block UVB light. k_{obs} is the average, observed first-order sunlight inactivation rate and k_{dark} is the inactivation rate seen in dark controls. $k_{obs,photon}$ (m^2 $photon^{-1}$) in full-spectrum sunlight, calculated based on the photon fluence, are also presented. Asterisks indicate values *not* significantly different from zero. k_{dark} n = 1 for PV3 in MEX, BM and TJ, and HAdV2 in MEX, CT and PBS, thus, no standard error is available.

***MS2*.** MS2 inactivation rates in TJ and MEX were similar to those in PBS, while inactivation in BM, ML and CT occurred at significantly faster rates ($p < 0.001$). After correcting for light screening, simulated sunlight inactivation in TJ and PBS occurred at similar rates while inactivation in MEX, ML and CT occurred at rates significantly faster than in PBS ($p < 0.01$). As with PRD1 and HAdV2, our results demonstrate the contribution of the exogenous mechanism in sunlight inactivation of MS2.

UVB-blocking experiments. In experiments conducted with the UVB-blocking filter, k_{obs} ($k_{obs,UVB\text{-}block}$) of all viruses in PBS were not significantly different from zero. $k_{obs,UVB\text{-}block}$ of all viruses in environmental waters were found to be greater than those measured in PBS, though remained smaller than k_{obs} measured with exposure to full-spectrum sunlight (Table 2.4). $k_{obs,UVB\text{-}block}$ values were significantly different from zero (ANCOVA; $p<0.05$) for all viruses in all environmental waters, other than HAdV2 in MEX (Table 2.4).

Relative rates of virus inactivation. Despite the dependence of k_{obs} on environmental conditions, PV3 k_{obs} in every experimental water was significantly greater than k_{obs} of the other viruses in that water ($p < 0.001$ for all, except $p < 0.01$ for PV3 and PRD1 in MEX; ANOVA, Tukey's post-test; Figure 2.5). MS2 and HAdV2 were the most resistant to sunlight-mediated inactivation in all waters; MS2 and HAdV2 k_{obs} were only significantly different from each other in TJ ($p < 0.001$; ANOVA, Tukey's post-test), with MS2 inactivation slower than that of HAdV2.

Discussion

Mechanisms of sunlight-mediated inactivation. There are two ways that virus inactivation mechanisms occur in sunlit surface waters: through (1) absorption of photons by the virus itself (direct and indirect endogenous inactivation) and (2) reaction with reactive species formed by photosensitizers in the water column (exogenous inactivation). Determining which mechanisms dominate inactivation for a specific virus is important for understanding how environmental conditions (e.g., sunlight irradiance, water quality, depth, mixing) affect k_{obs}.

The presence of photosensitizing molecules decreased the rate of sunlight-mediated inactivation of PV3, signaling that inactivation was dominated by endogenous mechanisms. Conversely, the inactivation rates of HAdV2 and MS2 were enhanced in most environmental waters, indicating that the exogenous mechanism contributed; under the conditions studied, the net contribution of chromophores in the water to exogenous inactivation was greater than the decrease in endogenous inactivation due to light screening. The results for PRD1 were somewhere in between, with some evidence for exogenous inactivation.

All three inactivation mechanisms are wavelength dependent. The main components of non-enveloped viruses (proteins and nucleic acids) do not absorb light at wavelengths greater than ca. 320 nm (Davies and Truscott 2001; Jagger 1985), which results in a reliance of endogenous mechanisms on UVB light. Conversely, the exogenous mechanism can be initiated by longer wavelengths due to the ability of NOM to absorb light into the visible region (Cooper et al. 1989). In experiments utilizing the UVB-blocking filter, we assume that all virus inactivation

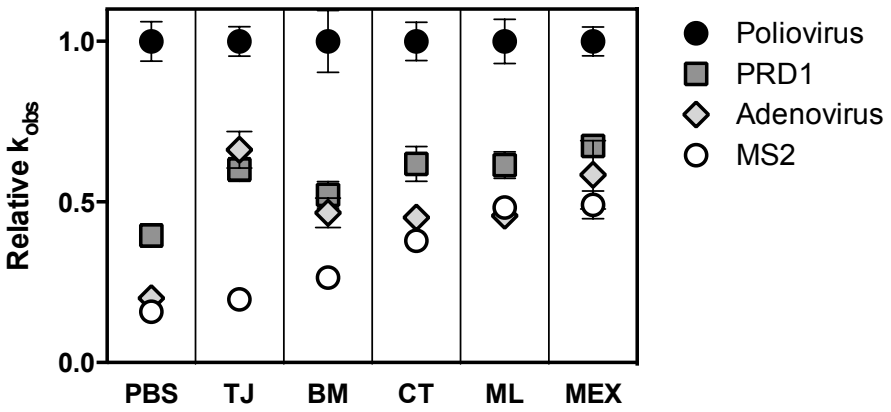

Figure 2.5. Relative k_{obs} (h^{-1}) of each virus in each matrix, as normalized by PV3 k_{obs} in the same matrix. Waters are listed in order of increasing $[^1O_2]_{ss,bulk}$. Error bars are normalized standard error.

is attributed to the exogenous mechanism only. This assumption is validated by observing $k_{obs,UVB\text{-}block}$ in PBS, where exogenous inactivation is not possible due to the absence of exogenous photosensitizers; $k_{obs,UVB\text{-}block}$ in PBS was not observed to be significantly different from zero for any of the viruses. This result agrees with previous studies by our lab that found PV3, HAdV2 and MS2 inactivation in sensitizer-free water to be due to UVB light alone (Fisher et al. 2011; Love et al. 2010). One difference is that we previously found that UVA light made a small contribution to endogenous PRD1 inactivation (Fisher et al. 2011; Love et al. 2010), possibly due to PRD1's internal lipid membrane or the modified method used for its purification, which could potentially leave photosensitizers in the virus stock solution or attached to the virus.

$k_{obs,UVB\text{-}block}$ values were significantly different from zero for all viruses in all environmental waters, other than HAdV2 in MEX, indicating that all four viruses were susceptible to exogenous inactivation sensitized by UVA and visible light. Under full-spectrum sunlight, the contribution of the exogenous mechanism to inactivation of PV3 was not observed because endogenous mechanisms were so fast they masked the contribution of exogenous inactivation.

Differences in nucleic acid type and length *and* protein capsid composition and structure could account for the variability in observed endogenous and exogenous sunlight inactivation rates. DNA and RNA are well known targets of damage caused by UV light (Jagger 1985). It has been postulated that the rate of genome damage depends on both the type of nucleic acid (i.e., single- or double-stranded DNA or RNA), and the length of the genome (Lytle and Sagripanti 2005) or the number of sites susceptible to UV-photoreaction (Kowalski et al. 2009), such as adjacent pyrimidines. Proteins are another potential target for endogenous sunlight damage: tyrosine, tryptophan and cysteine disulfide bonds absorb light in the UVB range (Davies and Truscott 2001), and dissolved tyrosine and tryptophan have been found to undergo direct photolysis with exposure to simulated sunlight (Boreen et al. 2008). For exogenous inactivation, $^1O_2$ was

previously found to be more responsible for MS2 inactivation than $OH^{\cdot}$, O_2^{-} or H_2O_2 in WSP water (Kohn and Nelson 2007). Recent work by Wigginton et al. (2012) found $^1O_2$ to cause significant MS2 genome decay, leading to inactivation of the virus. Proteins are also a potential target of exogenous sunlight damage due to their abundance in virus capsids, high reactivity with $^1O_2$ and ability to bind exogenous photosensitizers (Davies 2003). HAdV, for example, may exhibit enhanced susceptibility to sunlight inactivation in waters containing photosensitizers due to the role of proteins as targets for photooxidative damage. Due to its double-stranded genome, HAdV is able to infect host cells despite DNA damage and then use host cell machinery to repair DNA and retain viability (Eischeid et al. 2009). Damage to HAdV proteins, on the other hand, cannot be repaired and could therefore render the virus irreversibly inactivated (Eischeid and Linden 2011).

The role of NOM. Variability in NOM structure can play a role in the variability in inactivation rates observed for each virus in different environmentally sourced waters. NOM has a complex structure that varies depending on its source, and affects its ability to absorb light, produce ROS, and interact with viruses (Blough and Zepp 1995; Cooper et al. 1989; Lytle and Sagripanti 2005; Templeton et al. 2008). While NOM in the water column can enhance sunlight inactivation of viruses susceptible to exogenously produced ROS, it can also inhibit all three sunlight inactivation mechanisms by attenuating light or shielding viruses from radiation (Templeton et al. 2008). PV3 and PRD1 k_{obs} in MEX, for example, were lower than k_{obs} in PBS (Figure 2.4A) due to the importance of endogenous mechanisms for these viruses.

For MS2 and HAdV2 inactivation in environmental waters, light attenuation was compensated for by increased damage through the exogenous mechanism, resulting in higher k_{obs} in some environmental waters compared to PBS. In full-spectrum simulated sunlight, Kohn and Nelson (2007) had a similar finding for MS2 in WSP water, whereas Romero et al. (2011) observed the opposite: the addition of 20 mg C/L of Suwannee River NOM (SRNOM) resulted in slower MS2 inactivation kinetics. The discrepancy between the Romero et al. finding and ours could be due to a higher fraction of UVB light emitted by their light source (6.24%, as compared to 0.81% in the present study), which would result in greater relative k_{obs} in clear water (i.e., endogenous k_{obs}) as compared to k_{obs} in waters containing light-absorbing photosensitizers.

Given the importance of $^1O_2$ in exogenous MS2 inactivation, (Kohn and Nelson 2006) we investigated $[^1O_2]_{ss,bulk}$ in the environmental waters. Natural waters have microheterogeneous $[^1O_2]_{ss}$, with higher concentrations closer to the source of production (Wershaw 2006; Latch and McNeill 2006). Thus, the effective $[^1O_2]_{ss}$ that viruses are exposed to could be higher than $[^1O_2]_{ss,bulk}$ if viruses are associated with photosensitizers. If virus-NOM association differs between environmental waters we could observe a non-linear relationship between $k_{obs,UVB\text{-}block}$ corrected for light screening ($k_{obs,UVB\text{-}block,photon}$; λ range 280–700 nm) and $[^1O_2]_{ss,bulk}$, depending on association affinities between the virus and NOM. This was not the case for MS2 inactivation in the present study, where we observed a linear relationship between $[^1O_2]_{ss,bulk}$ and MS2 $k_{obs,UVB\text{-}block,photon}$ ($R^2 = 0.91$; Figure 2.6). This finding agrees with Badireddy et al. (2012), who found MS2 inactivation by illuminated fullerenes to be fastest in solutions with the greatest $[^1O_2]_{ss,bulk}$, and Kohn and Nelson (2006), who found a linear relationship between $[^1O_2]_{ss,bulk}$ and MS2 k_{obs} in WSP water. The correlation between MS2 $k_{obs,photon}$ and $[^1O_2]_{ss,bulk}$ observed in this study suggests that there are similar MS2-NOM association affinities among waters, resulting in $[^1O_2]_{ss,bulk}$ being related to the $[^1O_2]_{ss}$ experienced by MS2.

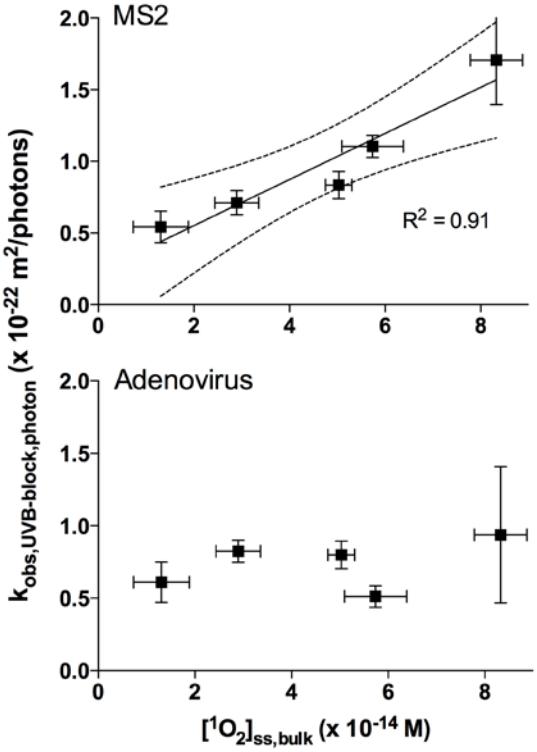

Figure 2.6. Solar simulator inactivation rates determined from UVB-blocking filter experiments and corrected for light screening ($k_{obs,UVB\text{-}block,photon}$) versus bulk-phase, steady-state singlet oxygen concentrations ($[^1O_2]_{ss,bulk}$) for MS2 and HAdV2. Inactivation in PBS was not included. Error bars represent standard error. Solid line in MS2 panel is the linear regression line; dotted lines are the 95% confidence intervals of the regression.

In contrast to MS2, HAdV2 $k_{obs,UVB\text{-}block,photon}$ did not correlate with $[^1O_2]_{ss,bulk}$ ($R^2 = 0.18$; Figure 2.6). Previous research by Dewilde et al. (1996) and Pellieux et al. (2000) investigated HAdV inactivation with exposure to $^1O_2$ released by naphthalene endoperoxides (water-soluble compounds that thermally decompose to release $^1O_2$) and found HAdV-endoperoxide interaction to be important. When exposed to an endoperoxide that did not associate with the virus (1,4-naphthalenedipropanoate), no HAdV inactivation was observed, even when exposed to $^1O_2$ concentrations higher than those used in the present study (Dewilde et al. 1996). However, when exposed to $^1O_2$ released by an endoperoxide containing a nonionic functional group [N,N'-di(2,3-dihydroxypropyl)-1,4-naphthalenedipropanamide], HAdV was inactivated efficiently (Pellieux et al. 2000), likely due to HAdV-endoperoxide association. Differential binding affinity between HAdV2 and constituents in our experimental waters could account for the discrepancy between k_{obs} and $[^1O_2]_{ss,bulk}$.

Water quality conditions that increase virus-NOM binding affinity, such as high ionic strength and low pH (Templeton et al. 2008), have been observed to increase k_{obs}. Sinton et al. (2002) and Kohn et al. (2007), for example, found greater sunlight inactivation rates of F+RNA phage and MS2, respectively, with increased ionic strength, presumably due to increased association between viruses and photosensitizers. Interestingly, we observed the fastest HAdV2 k_{obs} values in waters with highest salinity (TJ and BM), but the same was not true for MS2. It should be noted that halides in seawater can also modify photosensitized processes by increasing both formation and quenching rates of ROS (Grebel et al. 2012).

Viral indicators of sunlight inactivation. Consistent with previous findings in clear water (Love et al. 2010), we observed MS2 to be a conservative indicator for PV3 and HAdV2 inactivation in all experimental waters used in this study (Figure 2.4). Given that HAdV2 has been observed to be the most resistant virus to low pressure UVC light (Hijnen et al. 2006), it is a significant finding that sunlight inactivation rates of MS2 did not exceed those of HAdV2. It has also been reported that MS2 was inactivated more slowly than porcine rotavirus in water with and without the addition of SRNOM (Romero et al. 2011). For monitoring sunlight disinfection in sewage-influenced surface waters, WSP and constructed wetlands, it is not possible to monitor MS2 coliphage alone, but rather F+RNA coliphage in general. Love et al. (2010) found that F+RNA coliphage isolates were inactivated faster than MS2 and HAdV2 in clear water, but slower than PV3, PRD1, F+DNA and somatic coliphage.

The viruses investigated in this study could behave differently in other environmental matrices or in deeper waters. For example, while PV3 was inactivated faster than PRD1, MS2 and HAdV2 in all matrices, MS2 k_{obs} approached PV3 k_{obs} in waters with greater UVB attenuation due to the importance of UVB in PV3 inactivation (Figure 2.4). In water deeper than our reactors (i.e., >5 cm), the inactivation rate of viruses like PV3, which rely heavily on UVB for inactivation, would decrease relative to viruses for which the exogenous mechanism and longer wavelengths contribute more. Additionally, in near-surface waters, the main factor determining $[^1O_2]_{ss,bulk}$ is the absorbance of the photosensitizers in that water, whereas in deeper waters where nearly all light is absorbed, quantum yield is the most important factor in determining $[^1O_2]_{ss,bulk}$ averaged over depth (Haag and Hoigné 1986). The experimental system used in this study approximated near-surface water conditions and, as predicted by Haag and Hoigné (1986), $[^1O_2]_{ss,bulk}$ was highest in the most absorbing water (MEX) and lowest in the least absorbing water (TJ). However, shallow water $[^1O_2]_{ss,bulk}$ may not reflect average $[^1O_2]_{ss,bulk}$ at depth, which could influence k_{obs} of viruses susceptible to exogenous damage.

Because sunlight mediated inactivation of viruses is affected by complex and variable environmental (sunlight spectrum and intensity), water quality (pH, DO, ionic strength, source and concentration of photosensitizers) and virus (genome type and number of sites susceptible to photo-transformation; protein capsid composition and structure) factors, accurately modeling virus inactivation rates is difficult, and the application and comparison of experimental values across studies is a challenge. To better model sunlight inactivation of viruses in the environment, and compare k_{obs} values between organisms in different waters, we need to better understand virus-NOM association, ROS production by NOM, and the photoaction spectra of viruses and NOM. In the meantime, studies should report sunlight spectra and water absorbance spectra, and care must be taken when comparing sunlight inactivation rates across studies. Also, in addition to

reporting k_{obs} in units of inverse time, inactivation rates should be reported in terms of average light irradiance or photon fluence.

Limitations. Due to the time requirements of human virus inactivation experiments, experimental waters were used over the course of 8 months. There was little change in absorbance of these waters over that time, which is consistent with Zepp (1988) who found no change to the absorbance spectrum of swamp water stored in the dark for two years. However, we cannot rule out that some changes occurred to the water matrices over time that affected the inactivation rates measured. Nonetheless, experiments with a particular virus were conducted in all waters at the same time and any changes would have minimal impact on relative inactivation rates.

We were unable to measure whether viruses were aggregated in our experiments. MS2 was reported to exist as dispersed viruses in PBS at neutral pH (Mattle and Kohn 2012; Mattle et al. 2012). While aggregation during the experiment could result in overestimation of k_{obs} attributed to sunlight, viruses already present in aggregates may result in underestimation of k_{obs} because the entire aggregate must be inactivated to prevent plaque formation (Mattle and Kohn 2012; Mattle et al. 2012). In our experiments, viruses were added to reactors and stirred for 15 min in the dark prior to collection of the $t = 0$ sample; controls indicated that minimal aggregation occurred after this time in the dark, but it is possible some aggregation occurred during the sunlight experiments.

Chapter 3

Modeling sunlight inactivation of viruses in water from an open-water, natural wastewater treatment system

Introduction

One of the overarching goals of investigating inactivation of microorganisms in sunlit surface waters is to develop models that predict inactivation rates under different conditions. As discussed in Chapter 2, different waterborne viruses are susceptible to the endogenous and exogenous inactivation mechanisms to different extents, and inactivation rates depend on water characteristics. The goal of this chapter is to investigate the ability of endogenous and exogenous virus inactivation models to predict the sunlight inactivation rates of MS2 and poliovirus type 3 (PV3) in laboratory experiments using water collected from an open-water wastewater treatment wetland.

Fisher et al. (2011) developed photoaction spectra (PAS) for the endogenous inactivation of MS2 and PRD1 coliphage in waters that did not contain light-attenuating or photosensitizing molecules. While the PAS were developed using a solar simulator, Nguyen et al. (in review) determined that the PAS model for MS2 performed well at predicting the inactivation rate of the virus in sensitizer-free water with exposure to natural sunlight in Berkeley, CA during both summer and winter. Nguyen et al. (in review) also found the model to work when accounting for light attenuation due to absorbance by natural organic matter. The present research builds upon the work by Fisher et al. (2011) and Nguyen et al. (in review) by developing and evaluating a model that includes both endogenous and exogenous inactivation mechanisms to predict inactivation rates in natural waters where we must account for both light attenuation and reactive oxygen species (ROS) concentrations. This work is also the first attempt to model human virus sunlight inactivation in a natural surface water. While the models developed here were evaluated through experiments in the laboratory, a larger goal is to develop models that can predict virus inactivation rates in natural surface water bodies with natural sunlight; there is a brief discussion of remaining research needs at the end of the chapter.

Methods

To investigate the ability of the model (discussed in 'Sunlight Inactivation Model Equations' section below) to predict virus inactivation while accounting for the affects of light attenuation on endogenous inactivation and ROS concentration on exogenous inactivation, we conducted solar simulator experiments to compare experimental and modeled inactivation rates of MS2 and PV3. Experiments were conducted in 5-cm and 20-cm deep reactors containing water collected from the Discovery Bay treatment wetland.

Discovery Bay wetland water. Water used for experiments was collected from a pilot-scale open-water unit process wetland located in Discovery Bay, CA (37°54′N, 121°36′W) that receives nitrified, non-disinfected wastewater effluent from the Discovery Bay Wastewater Treatment Plant. The open-water wetland was designed to promote direct and indirect photolysis: the wetland is shallow (approximately 20 cm deep), to allow sunlight penetration, and it is lined with a geotextile fabric and concrete to prevent the growth of emergent vegetation, which would block sunlight. Overlaying the concrete and geotextile fabric is a 2- to 5-cm thick layer of sediment containing a community of photosynthetic and other associated organisms (Nguyen et al. in review). Discovery Bay wetland (DBW) water has a pH between 8.5 and 9 (Nguyen, unpublished data) and a concentration of Mg^{2+} between 1.4 and 1.5 mM (Jasper and Hadgu, unpublished data).

Before use in experiments, the DBW water was filtered using 5-µm, 47-mm diameter polycarbonate membrane filters (Whatman Nucleopore membranes) to remove large particulates that were difficult to maintain in suspension during experiments.

Virus propagation, purification and enumeration. MS2 and PV3 were propagated, purified and enumerated as described in Chapter 2.

Sunlight inactivation experiments. MS2 and poliovirus type 3 (PV3) inactivation rates were investigated in separate experiments. Viruses were inoculated into three types of reactors: (1) 200 mL beaker filled with 100 mL (5 cm deep) clear, sensitizer-free solution (PBS: 16 mM Na_2HPO_4, 4 mM NaH_2PO_4 and 10 mM NaCl); (2) 200 mL beaker filled with 100 mL (5 cm deep) 5-µm filtered DBW water; (3) 4 L beaker filled with 3.5 L (20 cm deep) 5-µm filtered DBW water. All reactors were glass beakers painted black on the outside. The average initial virus concentrations were 5.1×10^4 PFU/mL and 8.5×10^4 PFU/mL for MS2 and PV3, respectively.

Reactors were exposed to full spectrum simulated sunlight as described in Chapter 2.

Singlet oxygen. Bulk-phase, steady-state singlet oxygen concentrations ($[^1O_2]_{ss,bulk}$) were determined for each reactor through photolysis experiments using furfuryl alcohol (FFA) as a probe compound, as described in Chapter 2. FFA photolysis was measured at the same time as inactivation experiments, but FFA and viruses were spiked into different reactors.

Data analysis. First-order, observed inactivation rate constants (k_{obs}) were calculated as the negative slope of the linear regression trend line of $\ln(C_t/C_0)$ versus time, in accordance with the first-order inactivation rate equation:

$$-\ln\frac{C_t}{C_0} = k_{obs} \cdot t \qquad (3.1)$$

where C_0 is the initial virus concentration and C_t is the concentration at time t. All experiments were conducted in duplicate reactors. $\ln(C_t/C_o)$ values were calculated for each time point and each replicate; these values (12 data points = six time points × two replicate experiments) were pooled and used to calculate k_{obs} and the standard error of the slope by linear regression.

Inactivation rates are reported as k_{obs} ± standard error of the slope. Unless noted otherwise, ANOVA with Tukey's post-test were used to determine whether k_{obs} measured in the different reactors were significantly different from each other; inputs were k_{obs}, standard error of the slope and the number of data points. Statistical tests were performed in Prism (v6.0c, GraphPad Software).

Sunlight Inactivation Model Equations

Total inactivation rate. We assume that the first-order, observed sunlight inactivation rate of viruses (k_{obs}) is the sum of inactivation rates caused by the endogenous ($k_{endogenous}$) and exogenous ($k_{exogenous}$) sunlight inactivation mechanisms; while there could be interaction between mechanisms, there is currently no evidence of this. In this study, we use the term k_{obs} to denote experimentally observed inactivation rates and k_{tot} to denote the total modeled inactivation rates, as given in the following equation:

$$k_{tot} = k_{endogenous} + k_{exogenous} \quad (3.2)$$

Modeling endogenous inactivation. Endogenous inactivation was modeled in two ways, both of which depend on the downwelling planar irradiance averaged over a well-mixed water column of depth z [$\langle E_{d,\lambda}\rangle(z)$; W m^{-2}]; the calculation of $\langle E_{d,\lambda}\rangle(z)$ is described later in this section. The first modeling approach uses a photoaction spectrum (PAS), which takes into account the sensitivity of the organism to different wavelengths. The photoaction spectrum for MS2 was determined by Fisher et al. (2011) and used to develop the following model to calculate the endogenous inactivation rate of the virus.

$$k_{endogenous,PAS} = \sum_{\lambda} \langle E_{d,\lambda}\rangle(z) \cdot P_{\lambda} \cdot \Delta\lambda \quad (3.3)$$

P_{λ} (m^2 W^{-1} h^{-1}) is the wavelength- and virus-dependent spectral sensitivity coefficient. Fisher et al. (2011) calculated P_{λ} in 3-nm bins, centered at λ (Table 3.1), so the term $\Delta\lambda$ is equal to 3 nm.

Endogenous sunlight inactivation depends on UVB irradiance absorbed by the virus (Love et al. 2010; Silverman et al. 2013). The second endogenous inactivation modeling approach is based on total UVB irradiance transmitted through the water column and does not account for wavelength-specific sensitivity. While there are limitations to this model (see discussion), a benefit is that it is not necessary to develop a photoaction spectrum; instead, inactivation experiments are conducted in clear water at a few different light intensities, and the correlation between inactivation and intensity is determined. For MS2, we found a linear correlation between the total irradiance in the UVB range (280–320 nm) and k_{obs} measured in clear, sensitizer-free solution (Figure 3.1). While all experiments used to construct the curve in Figure 3.1 were conducted using the same solar simulator, they were conducted by four different

investigators, over a 6-year period and included MS2 stocks that were propagated and purified in both our laboratory and Professor Tamar Kohn's laboratory at École Polytechnique Fédérale de Lausanne, in Switzerland. From linear regression analysis, a slope of 0.12 ± 0.02 m^2 W^{-1} h^{-1} (R^2 = 0.89) was determined and led to the following model for MS2 endogenous inactivation:

$$k^{MS2}_{endogenous,totUVB} = 0.12\ m^2 W^{-1} h^{-1} \cdot \sum_{\lambda=280}^{320} \langle E_{d,\lambda} \rangle (z) \qquad (3.4)$$

Table 3.1. Spectral sensitivity coefficients [P_λ (m^2 W^{-1} h^{-1})] for the MS2 photoaction spectrum (Fisher et al. 2011).

λ (nm)	P_λ (m^2 W^{-1} h^{-1})	λ (nm)	P_λ (m^2 W^{-1} h^{-1})	λ (nm)	P_λ (m^2 W^{-1} h^{-1})
281	2.88	356	0	431	0
284	1.28	359	0	434	0
287	0.320	362	0	437	0
290	0	365	0	440	0
293	0	368	0	443	0
296	0.0669	371	2.65E-06	446	0
299	0.183	374	0.00096	449	0
302	0.299	377	0.00192	452	0
305	0.281	380	0.00287	455	0
308	0.165	383	0.00191	458	0
311	0.0491	386	0.000956	461	0
314	0	389	0	464	0
317	0	392	0	467	0
320	0	395	0	470	0
323	0	398	0	473	0
326	0	401	0	476	0
329	0	404	0	479	0
332	0	407	0	482	0
335	0	410	0	485	0
338	0	413	0	488	0
341	0	416	0	491	0
344	0	419	0	494	0
347	0	422	0	496	0
350	0	425	0		
353	0	428	0		

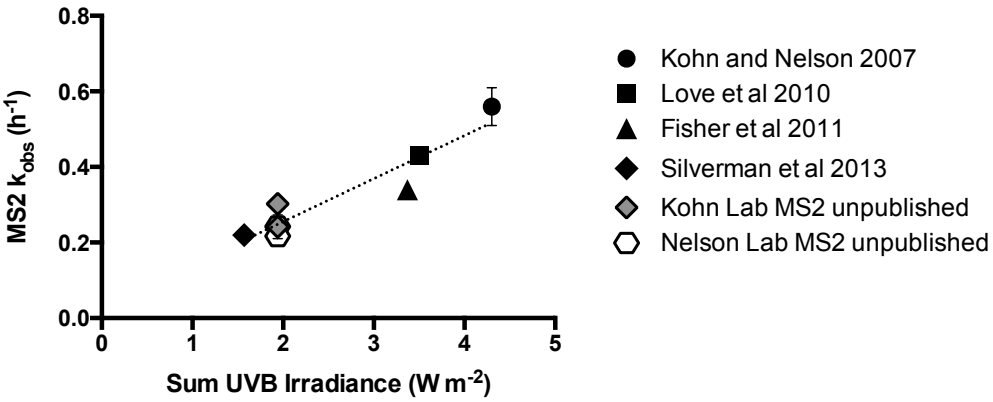

Figure 3.1. Relationship between total UVB irradiance and MS2 k_{obs} in clear, sensitizer-free solution (PBS). Dotted line is the linear regression line (slope = 0.12 ± 0.02 m^2 W^{-1} h^{-1}; R^2 = 0.89). Error bars are standard error; if error bars are not visible, they are smaller than the symbols.

There is currently no photoaction spectrum for PV3. Therefore, we were only able to use the total UVB approach to model endogenous PV3 inactivation. Combining data from Silverman et al. (2013) with more recent data, we found a linear correlation between total UVB irradiance and PV3 k_{obs} measured in PBS (Figure 3.2); the data point measured by Love et al. (2010) was rejected as an outlier and was not included in linear regression analysis (future work should be done to add a point where the total UVB irradiance is equal to approximately 3.5 W m^{-2}). Linear regression analysis was used to determine a slope of 0.98 ± 0.15 m^2 W^{-1} h^{-1} (R^2 = 0.94) and led to the following model for PV3 endogenous inactivation:

$$k^{PV3}_{endogenous,totUVB} = 0.98\ m^2 W^{-1} h^{-1} \cdot \sum_{\lambda=280}^{320} \langle E_{d,\lambda} \rangle (z) \qquad (3.5)$$

Both approaches for modeling endogenous inactivation depend on light intensity transmitted through the water column. Natural waters alter the light field through absorption and scattering, and measurements of light irradiance incident on the water surface must be corrected for these effects in the water column. In our experimental system we used a collimated beam of light, and therefore calculate the downwelling planar irradiance at depth z [$E_{d,\lambda}(z)$] using the following equation:

$$E_{d,\lambda}(z) = E_{d,\lambda}(0) \cdot e^{-K_{d,\lambda} \cdot z} \qquad (3.6)$$

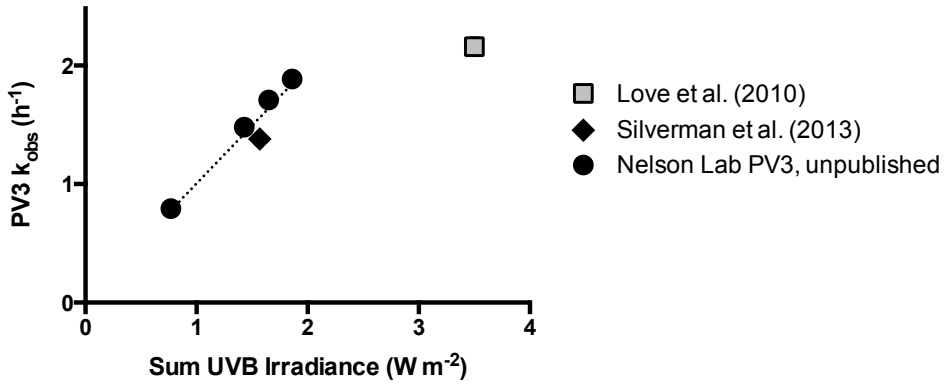

Figure 3.2. Relationship between total UVB irradiance and PV3 k_{obs} in clear, sensitizer-free solution (PBS). Dotted line is the linear regression line (slope = 0.98 ± 0.15 $m^2\ W^{-1}\ h^{-1}$; R^2 = 0.94); the data point from Love et al. (2010) was not included in linear regression analysis. Error bars for standard error are not visible because they are smaller than the symbols.

$E_{d,\lambda}(0)$ is irradiance of light jut below the water surface, $K_{d,\lambda}$ is the attenuation coefficient and z is the depth of the water column. For a collimated beam, with an incident light angle normal to water surface, we assume $E_{d,\lambda}(0)$ to be equal to the incident irradiance ($E_{i,\lambda}$), given that there is no reflection of light off of the water surface, as per Fresnel's equations:

$$E_{d,\lambda}(0) = E_{i,\lambda}\ (1 - R_\lambda) \tag{3.7}$$

$$R_\lambda = \frac{\left(\frac{\sin(\theta - \theta_\lambda')}{\sin(\theta + \theta_\lambda')}\right)^2 + \left(\frac{\tan(\theta - \theta_\lambda')}{\tan(\theta + \theta_\lambda')}\right)^2}{2} \tag{3.8}$$

Where R_λ is the fraction of light reflected, θ is the angle of incident light, and θ' is the angle of transmitted light. θ' is calculated using Snell's equation:

$$\frac{n_{water,\lambda}}{n_{air,\lambda}} = \frac{\sin\theta}{\sin\theta_\lambda'} \tag{3.9}$$

where n is the index of refraction. When using a collimated beam where θ is equal to zero, θ_λ' and R_λ are also equal to zero.

To calculate average light transmitted over a well-mixed depth z [$\langle E_{d,\lambda}\rangle(z)$], $E_{d,\lambda}(z)$ must be integrated over z:

$$\langle E_{d,\lambda}\rangle(z) = \int_0^z E_{d,\lambda}(z)\,\mathrm{d}z = E_{i,\lambda}\left(\frac{1 - e^{-K_{d,\lambda}\cdot z}}{K_{d,\lambda}\cdot z}\right) \tag{3.10}$$

$K_{d,\lambda}$ is the attenuation coefficient, and accounts for light absorption and scattering in the water column. If we assume scattering to have a small affect on light attenuation, $K_{d,\lambda}$ is calculated using the following equation:

$$K_{d,\lambda} = D\ a_\lambda \tag{3.11}$$

Where a_λ is the naperian absorbance coefficient and is derived from UV-visible spectrophotometer measurements (A_λ) and the cuvette pathlength (l) using the following equations (α_λ is the decadic absorbance coefficient):

$$\alpha_\lambda = \frac{A_\lambda}{l} \tag{3.12}$$

$$a_\lambda = 2.303\ \alpha_\lambda \tag{3.13}$$

D is a distribution coefficient that represents the average pathlength of all light vectors in the water column per unit depth. Theoretically, D can vary between 1, for completely clear waters and a solar zenith angle of zero, and 2, for very turbid waters. For naturally sunlit clear waters (Zepp and Cline 1977) and highly absorbing, low scattering, humic waters (Miller and Zepp 1979) D was found to be 1.2. It is not clear from the literature what value of D should be used for a low-scattering humic substance irradiated by a collimated beam of light, therefore we will model light attenuation with two values of D: 1 and 1.2.

Modeling exogenous inactivation. Exogenous sunlight inactivation appears to be important under environmental conditions for some viruses (e.g., MS2) but limited for others (e.g., PV3). While additional reactive oxygen species (ROS) may be involved in exogenous inactivation, the steady state singlet oxygen concentration measured in bulk solution ($[^1O_2]_{ss,bulk}$) has been found to be a good indicator of MS2 exogenous inactivation (Kohn and Nelson 2007; Silverman et al. 2013). Therefore, the exogenous inactivation rate ($k_{exogenous}$; h^{-1}) was modeled using a rate equation that assumes exogenous inactivation to be caused by a first order reaction with singlet oxygen:

$$\mathrm{k_{exogenous}} = \mathrm{k_2}\cdot\left[\ ^1\mathrm{O_2}\right]_{\mathrm{ss,bulk}} \tag{3.14}$$

To determine the values of the apparent rate constant (k_2; M^{-1} h^{-1}) between each virus and $[^1O_2]_{ss,bulk}$, we compiled new and published experimental results for exogenous inactivation of MS2 and PV3 in natural waters and solutions with model photosensitizers (Figure 3.3). These experiments were conducted using an optical filter that only transmitted light with wavelengths greater than 320 nm; with no incident UVB light we assume that all observed inactivation is caused by the exogenous mechanism ($k_{obs,exogenous}$). According to Equation 3.14, k_2 is equal to the slope of linear regression line between $k_{obs,exogenous}$ and $[^1O_2]_{ss,bulk}$. Using this approach, MS2 k_2 was calculated to be $(4.1 \pm 0.56) \times 10^{12}$ M^{-1} h^{-1} (Figure 3.3A; $R^2 = 0.85$) and PV3 k_2 was calculated to be $(2.9 \pm 0.39) \times 10^{11}$ M^{-1} h^{-1} (Figure 3.3C; $R^2 = 0.88$).

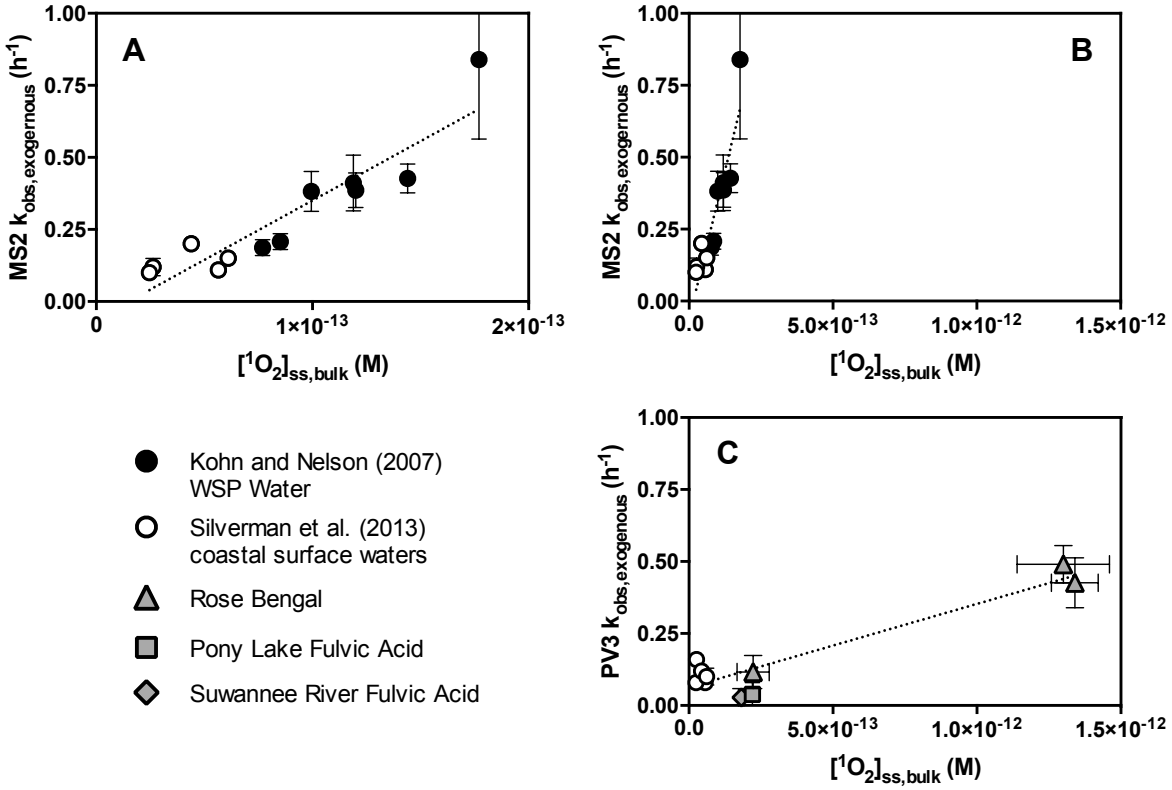

Figure 3.3. Relationship between $[^1O_2]_{ss,bulk}$ and MS2 (panels A and B) and PV3 (panel C) $k_{obs,exogenous}$ in various surface waters, Rose Bengal, or standard NOM. Pony Lake and Suwannee River fulvic acid solutions were at concentrations of 25 mg C/L; Rose Bengal concentrations were 80 nM and 160 nM. Panel B is the same data as panel A, but with a different scale for better comparison to panel C. Dotted lines are linear regression lines, the slope of which are MS2 and PV3 k_2 [MS2: slope = $(4.1 \pm 0.56) \times 10^{12}$ M^{-1} h^{-1}; $R^2 = 0.85$. PV3: slope = $(2.9 \pm 0.39) \times 10^{11}$ M^{-1} h^{-1}; $R^2 = 0.88$]. Error bars are standard error; if error bars are not visible, they are smaller than the symbols.

Results

Light attenuation. The absorbance spectra of DBW water (Figure 3.4) was used in conjunction with Equations 3.10 to 3.13 to calculate the average light irradiance transmitted through well-mixed water columns with different total depths, ranging from 2 to 50 cm (Figure 3.5). The difference in irradiance calculated using $D = 1$ and $D = 1.2$ is small for DBW water.

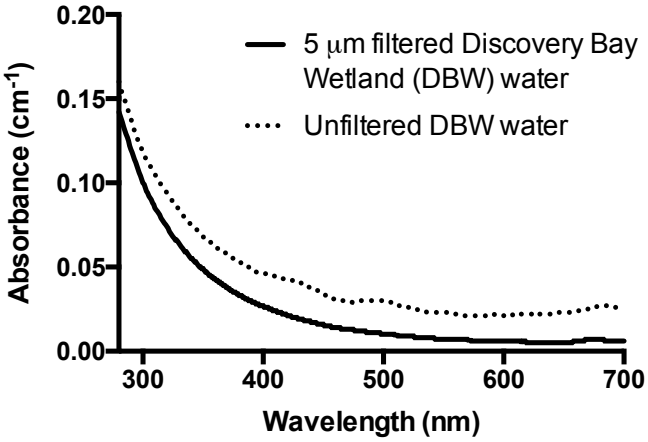

Figure 3.4. Decadic absorbance spectra (α_λ) of filtered and unfiltered DBW water; $l = 1$ cm.

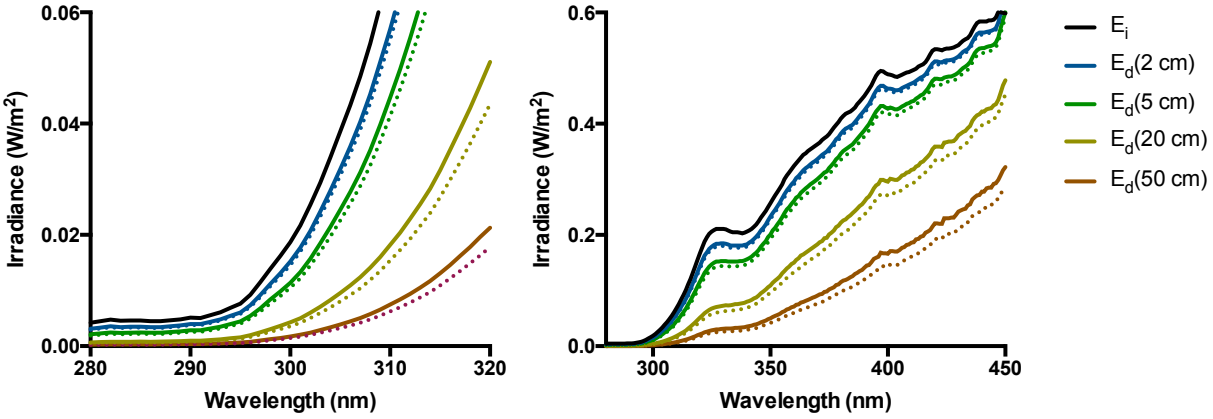

Figure 3.5. Measured light irradiance incident on the water surface (E_i, black line), and modeled average irradiance transmitted through well-mixed water columns. Light attenuation by 5-μm filtered DBW water was calculated using Equations 3.10 to 3.13 and two values of D: 1 (solid line) and 1.2 (dotted line). The left panel is the same data as the panel on the right, but is a close-up of the UVB range.

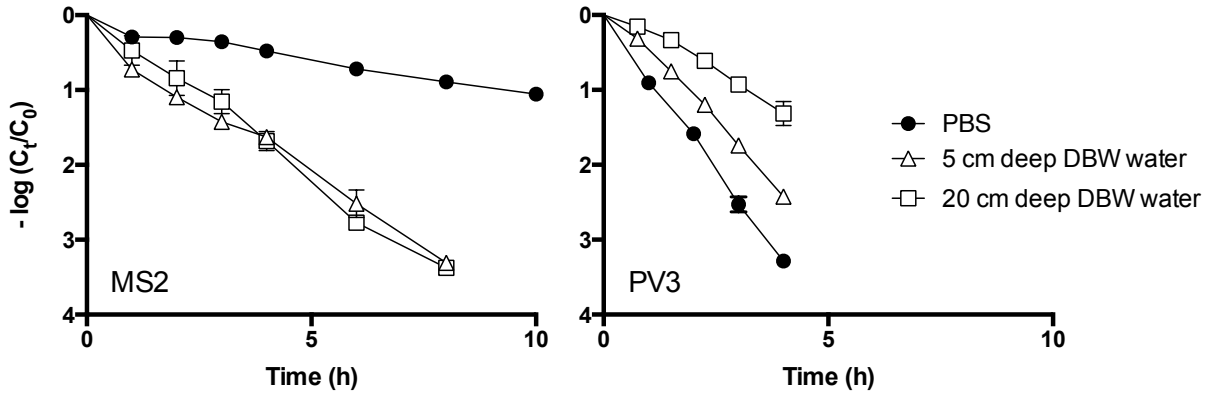

Figure 3.6. MS2 and PV3 inactivation curves in clear, sensitizer-free solution (PBS), and 5-cm and 20-cm deep 5-µm filtered DBW water ($n = 2$ for each time point). Error bars are standard error; if error bars are not visible, they are smaller than the symbols.

Singlet oxygen concentration. $[^1O_2]_{ss,bulk}$ was $(7.86 \pm 0.54) \times 10^{-14}$ M (based on FFA degradation, $R^2 = 0.98$) in 5-cm deep DBW water and $(6.65 \pm 0.27) \times 10^{-14}$ M (FFA degradation $R^2 = 0.99$) in 20-cm deep DBW water.

Observed virus inactivation in DBW water. MS2 inactivation in PBS ($k_{obs} = 0.23 \pm 0.01$; $R^2 = 0.96$) was significantly slower than inactivation in DBW water ($k_{obs} = 0.90 \pm 0.04$ and 0.99 ± 0.04 for 5- and 20-cm depths, respectively; $R^2 = 0.98$ for both; ANOVA, Tukey's post-test, $p < 0.001$). There was no significant difference between inactivation in DBW water at the two depths.

PV3 inactivation in PBS ($k_{obs} = 1.89 \pm 0.04$; $R^2 = 0.99$) was significantly faster than inactivation in DBW water ($k_{obs} = 1.42 \pm 0.05$ and 0.77 ± 0.05 for 5- and 20-cm depths, respectively; $R^2 = 0.99$ and 0.96). The PV3 inactivation rate in 5-cm deep DBW water was significantly faster than the rate in 20-cm deep DBW water (ANOVA, Tukey's post-test, $p < 0.001$).

The dark inactivation rate in DBW water (k_{dark}) was 0.07 ± 0.03 h^{-1} for MS2 ($R^2 = 0.34$) and 0.18 ± 0.05 h^{-1} for PV3 ($R^2 = 0.76$).

Discussion

In the following section, the term k_{obs} will be used to denote experimentally observed inactivation rates, while $k_{endogenous}$ and $k_{exogenous}$ will be used to denote modeled endogenous and exogenous inactivation rates, respectively. k_{tot} is the total modeled inactivation rate, equal to the sum of $k_{endogenous}$ and $k_{exogenous}$ (Equation 3.2).

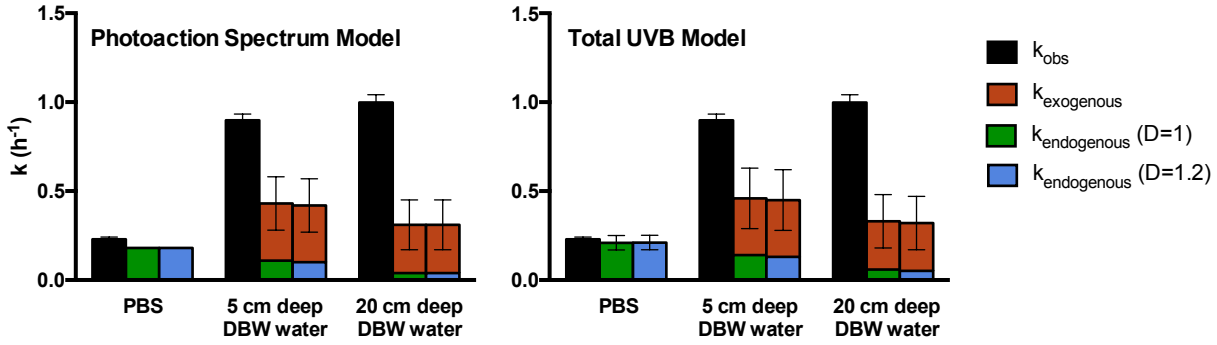

Figure 3.7. MS2 inactivation rates measured (k_{obs}) and modeled ($k_{endogenous}$ and $k_{exogenous}$) in clear, sensitizer-free solution (PBS), and 5-cm and 20-cm deep DBW water. Two models (the photoaction spectrum model, Equation 3.3, and the total UVB model, Equation 3.4) and two values for *D* (1 and 1.2) were used. Error bars are standard error; standard error on photoaction spectrum modeled values are from $k_{exogenous}$ while error on total UVB modeled values are combined error from $k_{endogenous}$ and $k_{exogenous}$.

Modeling MS2 inactivation in DBW water. The sunlight inactivation rate of MS2 was modeled using two approaches for $k_{endogenous}$ (Equations 3.3 and 3.4), and Equation 3.14 to model $k_{exogenous}$. Equations 3.10 to 3.13 were used to model light attenuation, with two values of *D*: 1 and 1.2.

The two MS2 $k_{endogenous}$ models (i.e., the PAS and total UVB models), predicted similar $k_{endogenous}$ (Figure 3.7), and the two *D* values used to quantify light attenuation gave similar results. Modeled values of $k_{endogenous}$ were very similar to k_{obs} measured in PBS. PBS is the clear water, sensitizer-free control, in which we assume only endogenous sunlight mechanisms contribute to virus inactivation; therefore similar k_{obs} and $k_{endogenous}$ in PBS provide evidence that the endogenous models predict reasonable estimates.

k_{tot} calculated for MS2 in DBW under-predicted k_{obs} in both 5-cm and 20-cm depths. The discrepancy between measured and modeled inactivation rates likely lies in the prediction of the exogenous inactivation rate. The exogenous sunlight inactivation mechanism is more important than the endogenous mechanisms for MS2, as seen by faster MS2 inactivation rates in waters containing photosensitizers than in PBS (Silverman et al. 2013a; Kohn and Nelson 2007). The importance of the exogenous mechanism is also seen in similar k_{obs} in the two well-mixed DBW water depths, despite more light attenuation in the 20-cm deep reactor. The $k_{exogenous}$ model is a simple one, relying on only two variables – k_2 and $[^1O_2]_{ss,bulk}$. Given that $[^1O_2]_{ss,bulk}$ was a measured value, we used the following equations to calculate a DBW water-specific k_2 ($k_{2,DBW}$) from measured k_{obs} and $[^1O_2]_{ss,bulk}$, and modeled values of $k_{endogenous}$ (using the PAS model):

$$k_{exogenous} = k_{obs} - k_{endogenous} \quad (3.15)$$

$$k_{2,DBW} = \frac{k_{exogenous}}{\left[{}^1O_2 \right]_{ss,bulk,DBW}} \quad (3.16)$$

$k_{2,DBW}$ was found to be (1.00 ± 0.08) × 10^{13} M^{-1} h^{-1} and (1.44 ± 0.09) × 10^{13} M^{-1} h^{-1} when calculated using data from the 5-cm deep and 20-cm deep DBW water reactors, respectively. An additional experiment was conducted with the UVB blocking filter and 5-µm filtered DBW water collected on two additional days. Using measured values of $k_{obs,exogenous}$ (n = 2) and $[^1O_2]_{ss,bulk}$, and Equation 3.14, we found two additional $k_{2,DBW}$ values of (1.60 ± 0.06) × 10^{13} M^{-1} h^{-1} and (9.5 ± 1.0) × 10^{12} M^{-1} h^{-1}. Taking the average of four values, $k_{2,DBW}$ was found to be (1.25 ± 0.16) × 10^{13} M^{-1} h^{-1} (n = 4).

When using the DBW water-specific $k_{2,DBW}$ in the inactivation rate model, k_{tot} better predicted MS2 k_{obs} in DBW water at both depths (Figure 3.8). $k_{2,DBW}$ is 3.5 times larger than the average MS2 k_2 calculated using the data in Figure 3.3A, meaning that water in the Discovery Bay treatment wetland is more effective at inactivating MS2, as compared to other water sources investigated by Silverman et al. (2013a) and Kohn and Nelson (2007). A possible reason for the larger $k_{2,DBW}$ could be that photosensitizers [e.g., natural organic matter (NOM), algae-derived chromophores] in DBW water have better access to targets of oxidation. $^1O_2$ is a short-lived ROS due to reaction with NOM and quenching by water, which results in a higher $^1O_2$ concentration closer to the source of production than in bulk solution (Wershaw 2006; Latch and McNeill 2006); association between NOM and viruses, therefore, would result in virus exposure to a larger concentration of $^1O_2$ than we measure in bulk solution. One hypothesis as to why $k_{2,DBW}$ was larger than the average k_2 is that there was a higher divalent cation concentration in DBW water. While both viruses and NOM are net negative at high pH (pH of DBW water was between 8.5 and 9.0) DBW water contained between 1.4 and 1.5 mM Mg^{2+}, which can promote association through cation bridging (Gerba 1984; Kohn et al. 2007). After addition of 2 mM Mg^{2+} to solutions containing model photosensitizers, for example, Kohn et al. (2007) found an increase in MS2 $k_{obs,exogenous}$ that ranged between 1.2- and 4.1-fold, for Suwanee River humic acid (SRHA) and Pony Lake fulvic acid (PLFA), respectively.

A second hypothesis is that NOM size may affect MS2 k_2. The MS2 capsid contains 32 pores that are 1.8 nm in diameter and allow access to the virus interior (Hooker et al. 2004). Kovacs et al. (2007), for example, was able to decorate the interior of RNA-free MS2 capsids with fluorescent anilines (MW = 600 Da), using capsid pores for entry. Organic matter derived from wastewater and wastewater treatment processes, referred to as effluent organic matter (EfOM), has a similar size range as DOM derived from microbial sources, which are smaller in size than NOM derived from terrestrial sources, such as SRHA. The hydrophobic and transphilic fractions of EfOM isolated from wastewater collected from five Connecticut wastewater treatment plants, for example, were found to have number-averaged molecular weights that ranged in size from 290 to 390 Da (Quaranta et al. 2012), whereas those for terrestrially-derived NOM, including

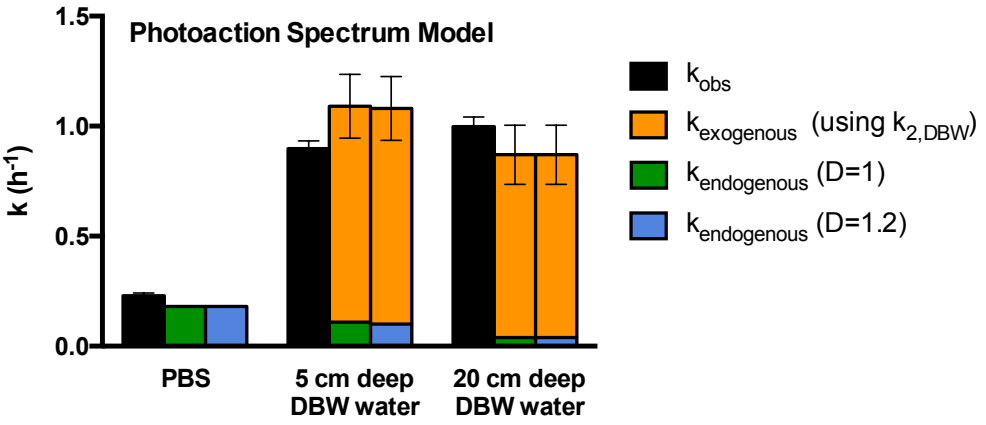

Figure 3.8. Measured (k_{obs}) and modeled ($k_{endogenous}$ and $k_{exogenous}$) MS2 inactivation rates, with $k_2 = k_{2,DBW}$. Error bars are standard error; standard error on modeled values are from $k_{exogenous}$.

SRHA, ranged from 710 to 2310 Da (Cabaniss et al. 2000). EfOM is comparable in size to the florescent aniline used by Kovacs et al. (2007), and could potentially pass through MS2 capsid pores to interact with the virus' RNA. Wigginton et al. (2012) found MS2's RNA to be the main target of damage with exposure to $^1O_2$, which we hypothesize is due to the ability of $^1O_2$ to access the virus interior through capsid pores; Wigginton et al. (2012) used Rose Bengal as a sensitizer (MW ≅ 1000 Da). If low molecular weight sensitizers can access RNA through capsid pores it would result in a higher concentration of $^1O_2$ closer to this important target of inactivating damage. One consideration, however, is that small NOM molecules, such as EfOM, do not absorb as much light as larger NOM molecules.

The interaction between sensitizers and RNA is even more likely with a high concentration of divalent cations that can bridge between negatively charged organic matter and RNA. One interesting finding by Kohn et al. (2007) is that when 2 mM Mg^{2+} was added to solutions containing MS2 and 5 mg C/L solutions of NOM, MS2 $k_{obs,exogenous}$ increased more in solution with PLFA than it did in solution with SRHA, Fluka humic acid or Aldrich humic acid; PLFA is derived from microbial sources and likely to have a smaller size than the other three NOM studied. The effects of divalent cation concentration, and NOM type and size on exogenous inactivation rates need to be further investigated.

Modeling PV3 inactivation in DBW water. PV3 $k_{endogenous}$ was modeled using the total UVB approach (Equation 3.5), and $k_{exogenous}$ was modeled using Equation 3.14. Equations 3.10 to 3.13 were used to model light attenuation, with two values of *D*: 1 and 1.2.

The modeled value of $k_{endogenous}$ was similar to k_{obs} measured in PBS (Figure 3.9), providing evidence that the total UVB model for endogenous inactivation worked well for solar simulator inactivation of PV3. The exogenous mechanism is not important for PV3 sunlight inactivation, as seen by Silverman et al. (2013a) and in the present study; this was reflected by a relatively

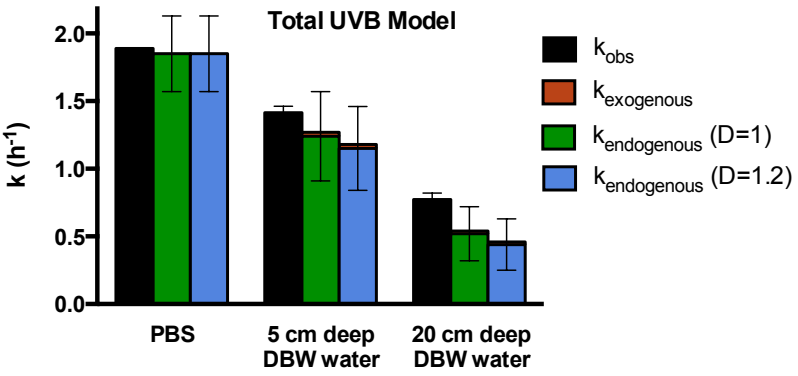

Figure 3.9. PV3 inactivation rates measured (k_{obs}) and modeled ($k_{endogenous}$ and $k_{exogenous}$) in clear, sensitizer-free solution (PBS), and 5-cm and 20-cm deep DBW water. Error bars are standard error; standard error on total UVB modeled values are combined error from $k_{endogenous}$ and $k_{exogenous}$.

small k_2 between PV3 and $[^1O_2]_{ss,bulk}$, and the insignificant $k_{exogenous}$ in DBW water predicted by the PV3 exogenous inactivation model. $k_{endogenous}$ under-predicted k_{obs} in 5- and 20-cm deep DBW water, though k_{obs} was within the standard error of $k_{endogenous}$. It is not clear whether the under-prediction of k_{obs} was due to the endogenous model, or an under-prediction of $k_{2,DBW}$ for PV3, as was seen for MS2. Further investigation of sunlight inactivation of PV3 in DBW water should be conducted using the UVB-blocking filter to measure $k_{2,DBW}$.

Challenges with the total UVB model. The total UVB model predicted $k_{endogenous}$ in PBS within 10% of measured inactivation rates for both viruses. However, given that shorter wavelength UVB light is likely to be more damaging to viruses than longer wavelength light, there is an inherent bias in the total UVB model, which weighs all UVB light equally, regardless of wavelength. Different solar simulators, or sunlight at different latitudes or times of year, may have different ratios of short to long wavelength UVB light (e.g., the ratio of $\Sigma I_{280-300}$ to $\Sigma I_{300-320}$), which could result in a relationship between k_{obs} and $\Sigma I_{280-320}$ that differs from the ones observed in Figures 3.1 and 3.2. This was exemplified in experiments conducted by Nguyen et al. (in review), in which MS2 inactivation in PBS was determined with exposure to natural sunlight. As part of this work, MS2 k_{obs} was measured for each hour interval during a summer and winter day and compared to the sum of UVB irradiance during that hour, and resulted in a slope of 0.04 $m^2\ W^{-1}\ h^{-1}$ (Figure 3.10). This value is 1/3 the magnitude of the slope used in the present study to relate the sum of UVB irradiance to predicted $k_{endogenous}$ (0.12 $m^2\ W^{-1}\ h^{-1}$), which would have resulted in an over-prediction of natural sunlight k_{obs}.

A second potential issue for the total UVB model is in modeling inactivation at depth. In natural waters, shorter wavelength light is absorbed faster than longer wavelength light (Figure 3.4), which means that the ratio of $\Sigma I_{280-300}$ to $\Sigma I_{300-320}$ would decrease with depth of the water column, and total UVB models developed using irradiance data from light incident on the water

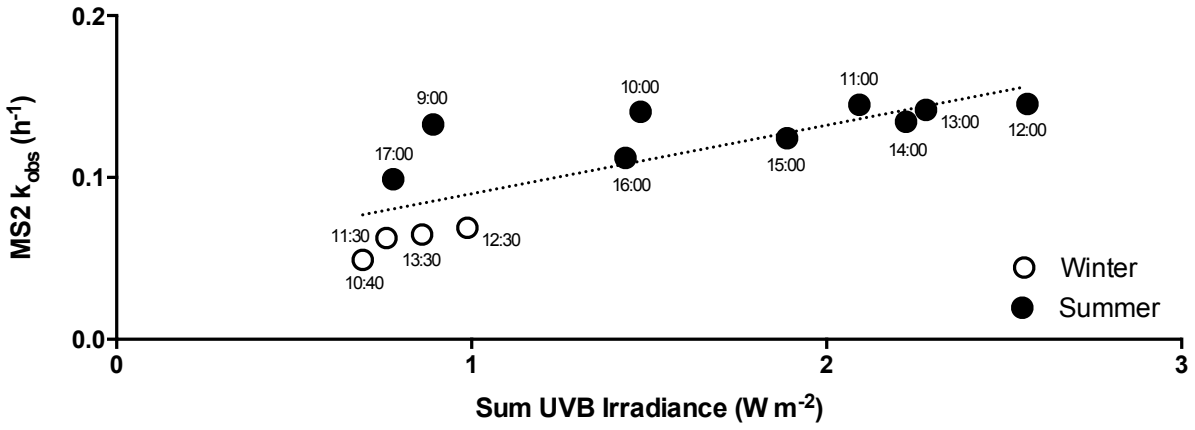

Figure 3.10. Relationship between total UVB irradiance and MS2 k_{obs} in clear, sensitizer-free solution (PBS) for 1 h intervals with exposure to natural sunlight. Dotted line is the linear regression line (slope = 0.04 ± 0.01 m^2 W^{-1} h^{-1}; R^2 = 0.64). Numbers next to data points are the time of day the sample and irradiance spectrum were taken. Data is from Nguyen et al. (in review).

surface would probably not hold for inactivation at depth in strongly absorbing waters. As an example, in the present study, the ratio of $\Sigma I_{280\text{-}300}$ to $\Sigma I_{300\text{-}320}$ was 0.093 for incident light, and an average of 0.080, 0.067, and 0.065 for well-mixed depths of 5 cm, 20 cm and 1 m. Longer wavelengths dominate the total UVB relationship and a decrease in shorter UVB wavelengths due to light attenuation is not represented as strongly as it should be. This, however, does not explain the underestimation of PV3 $k_{endogenous}$ by the total UVB model; if anything, the affect of light attenuation on total UVB model predictions of $k_{endogenous}$ would be to over-predict inactivation, given the dominance of longer wavelength light in Equation 3.5.

Comparison between modeled MS2 and PV3 inactivation rates in DBW water. A comparison of modeled values of k_{tot} for MS2 and PV3 across different well-mixed water column depths is presented in Figure 3.11; the total UVB model with D = 1 was used to model $k_{endogenous}$. To calculate $k_{exogenous}$, $[^1O_2]_{ss,bulk}(z)$ was modeled using the absorbance at 410 nm, as suggested by Haag and Hoigné (1986) in the following equation:

$$\left[{}^1O_2 \right]_{ss,bulk}(z) = \left[{}^1O_2 \right]_{ss,bulk}(0) \left(\frac{1 - e^{-a_{410nm} \cdot z}}{a_{410nm} \cdot z} \right) \quad (3.17)$$

$[^1O_2]_{ss,bulk}(0)$ was an average of values that were back-calculated using $[^1O_2]_{ss,bulk}$ measured in 5- and 20-cm deep reactors. $k_{2,DBW}$ was used to model MS2 $k_{exogenous}$.

While PV3 $k_{endogenous}$ in PBS is around 8 times faster than that of MS2, PV3 inactivation in DBW is only 1.3 times faster than that of MS2 in shallow, well-mixed water depths (i.e., 0–2 cm deep

water columns) due to the contribution of $k_{exogenous}$ to the MS2 inactivation rate. Because PV3 sunlight inactivation is dominated by the endogenous mechanisms, PV3 k_{tot} decreases quickly with depth, whereas, for MS2, the contribution of the exogenous mechanism compensates for the decrease in $k_{endogenous}$ caused by light attenuation. At well-mixed water column depths of 7 cm and deeper, MS2 k_{tot} was greater than that of PV3, and MS2 can no longer be considered a conservative indicator of poliovirus sunlight inactivation. For example, under the conditions used to model the data in Figure 3.11 and at 20 cm depth, total MS2 inactivation over the course of 10 h would be 10 times greater than that of PV3. This finding is also reflected in the experimentally observed MS2 and PV3 inactivation rates in 20-cm deep reactors (Figure 3.11). While human adenovirus type 2 (Silverman et al. 2013a) and human rotavirus (group A, strain Wa; Romero et al. 2013) were also found to be susceptible to exogenous sunlight inactivation, further work should investigate whether these and other human viruses are more or less susceptible to exogenous inactivation than MS2, and how it affects their inactivation rates at different depths.

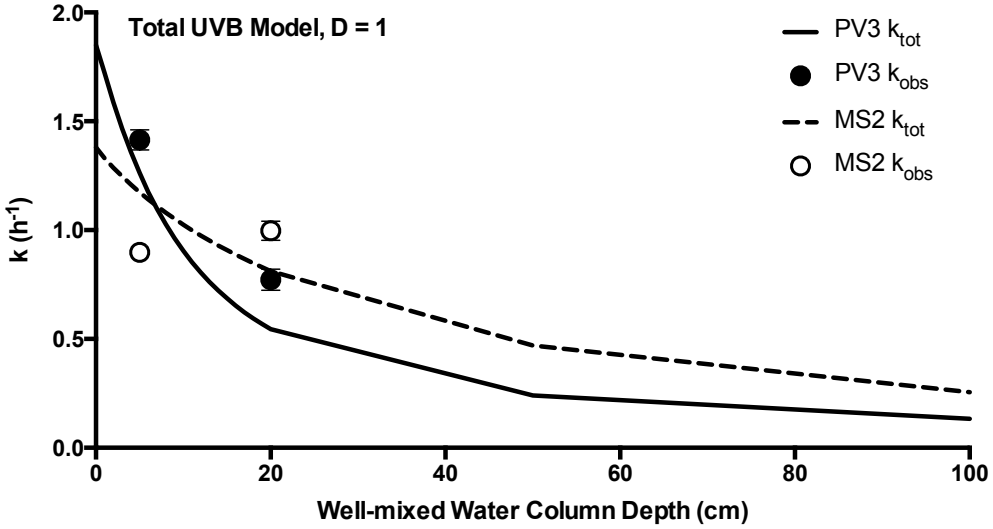

Figure 3.11. Comparison of modeled values of k_{tot} for MS2 and PV3 across different well-mixed water column depths. $k_{endogenous}$ was modeled using the total UVB approach with $D = 1$. For the $k_{exogenous}$ model, $[^1O_2]_{ss,bulk}(z)$ was calculated using Equation 3.17 and $k_{2,DBW}$ was used for MS2. Circles represent experimentally derived k_{obs}. Error bars are standard error; if error bars are not visible, they are smaller than the symbols.

Research needs for translating sunlight inactivation models from the laboratory to the environment. While we were able to evaluate the sunlight inactivation model's ability to predict virus inactivation rates in the laboratory, the overall goal of this work is to model virus inactivation in the environment. To do this, some pieces need to be further developed. To begin with, we need to develop a better model for k_2 that takes into account water quality and NOM characteristics. To expand the model to the environmental scale with natural sunlight, we also need to develop the models to take into account the solar zenith angle, annual and diurnal variation in irradiance, and wetland hydraulics. If we plan to use the total UVB approach to model $k_{endogenous}$, we must figure out how to weight the spectrum to overcome bias presented by higher-intensity, longer-wavelength UVB light, as discussed above. Additionally, it would be beneficial to have a model that can predict $[^1O_2]_{ss,bulk}$ based on optical characteristics and water depth. Some research into this has already been done; Peterson et al. (2012), for example, found a correlation between the naperian absorbance at 300 nm and $[^1O_2]_{ss,bulk}$ in water collected from Lake Superior.

Finally, there are many sources of variability in real environmental systems. It is possible that some of the sources of error in modeling sunlight inactivation rates are not significant when compared to sources of variability in the environment (e.g., residence time distribution, mixing with depth, thermal stratification, sunlight irradiance). A sensitivity analysis will need to accompany future modeling work.

Chapter 4

The effect of sunlight on the protein capsid function of poliovirus type 3

Introduction

While it has been established that sunlight can inactivate viruses (Davies-Colley et al. 1999; Kohn and Nelson 2007; Kohn et al. 2007; Love et al. 2010; Romero et al. 2011, 2013; Silverman et al. 2013a; Sinton et al. 1999, 2002) and different viruses have different rates of sunlight inactivation (Davies-Colley et al. 1999; Love et al. 2010; Romero et al. 2011, 2013; Silverman et al. 2013a; Sinton et al. 1999, 2002), we do not know exactly where virions are damaged with exposure to sunlight nor which aspects of virus composition or structure account for the difference in inactivation rates. The objective of this work is to begin to investigate the target of sunlight damage to virions by determining whether damage to the protein capsid contributes to endogenous sunlight inactivation of poliovirus type 3, as measured by inhibition of virus attachment to host cells. By exploring the location of inactivating damage, we aim to better understand why viruses have different rates of sunlight inactivation and, potentially, predict sunlight susceptibility of viruses not yet studied (Wigginton and Kohn 2012).

The general virus life cycle consists of (1) virus attachment to host cells, (2) delivery of nucleic acids into host cells, (3) protein synthesis, (4) nucleic acid replication, (5) virion assembly, and (6) cell lysis. Endogenous sunlight inactivation mechanisms have the potential to interrupt the virus life cycle through damage to the protein capsid (interrupting life cycle steps 1 or 2) or nucleic acids (interrupting steps 3 or 4). As viruses are obligate parasites and require host cell entry to reproduce, host cell attachment is critical for the other life cycle processes to occur. Capsid proteins are responsible for virus attachment and nucleic acid entry into cells – any damage that disrupts these capsid processes will render the virus inactive. While it is possible that sunlight may damage both capsid and nucleic acids, if viruses are unable to attach to host cells, the state of the nucleic acids no longer matters for infectivity.

Light in the sunlight spectrum can be absorbed by capsid amino acids, and result in damage via direct or indirect photolysis. Tyrosine (Tyr), tryptophan (Trp) and cystine disulfide bonds, for example, absorb light in the UVB range (Davies and Truscott 2001). Dissolved Tyr and Trp amino acids have been found to undergo direct photolysis with exposure to simulated sunlight (Boreen et al. 2008) and cystine is susceptible to direct photo-dissociation (Davies and Truscott 2001). In addition to chemical modification (such as photo-ionization), excited triplet states of Tyr and Trp can transfer energy to nearby amino acid side chains (Davies and Truscott 2001). Energy transfer, for example, can dissociate disulfide bonds and modify the capsid conformation, given the important role of disulfide bonds in protein folding and stability. Additionally, products of Trp oxidation are good photosensitizers and can generate singlet oxygen ($^1O_2$) within the capsid in the presence of sunlight and oxygen (Davies and Truscott 2001). Proteins are a major target of oxidation by $^1O_2$: the amino acids amino acids cysteine (Cys), histidine (His), methionine (Met), Tyr, and Trp, for example, are readily susceptible to $^1O_2$ oxidation at neutral

pH due to their sulfur-residues or aromatic groups (Boreen et al. 2008; Remucal and McNeill 2011).

Given the potential for sunlight damage to the capsid, and the capsid's role in host cell entry, we investigated the role of protein capsid damage in endogenous sunlight inactivation of poliovirus type 3 (PV3), as measured by inhibition of virus attachment to host cells.

Methods

Preparation of PV3 and MS2 stocks. PV3 (ATCC VR-300) was propagated on 90% confluent HeLa cells (ATCC CCL-2) in T-150 flasks: cells were washed with 30 mL 1X Dulbecco's Modified Eagle Medium (DMEM; Invitrogen), 2 mL PV3 with an MOI between 0.01 and 0.1 was added to the flask, which was then incubated at 37 °C and 5% CO_2 for 1 h, and rocked every 15 min. After 1 h, 30 mL 1X DMEM amended with 1X penicillin and streptomycin (pen/strep) and 10% (vol/vol) fetal bovine serum (FBS) was added to the flask, which was then incubated for 4 d. After incubation, viruses were released from cells by three freeze-thaw cycles using an ethanol-dry ice bath and 37 °C water bath.

MS2 (ATCC 15597-B1) was propagated by broth enrichment using tryptic soy broth, *E. coli* F_{amp} (ATCC 700891) host and 1X ampicillin-streptomycin antibiotics (0.015 g/L, w/v, each).

To purify crude virus stocks, PV3 and MS2 stocks were first chloroform extracted to remove cell debris: chloroform was added at a 1:3 (vol/vol) concentration, the solution was vortexed for 2 min, then centrifuged at 2000 ×*g* for 10 min. To remove broth constituents, the supernatant was polyethylene glycol (PEG) precipitated overnight at 4 °C (9% PEG, 0.3 M NaCl), centrifuged at 20,000 ×*g* for 15 min to produce virus pellets that were resuspended in phosphate buffered saline (PBS; 10 mM NaCl, 20 mM phosphate), chloroform extracted as above and filtered through a 0.22 μm filter. Virus stocks were stored at -80 °C.

Experimental setup. Experiments were conducted using a 1000-W solar simulator (Oriel #91194) with an ozone-free Xe bulb (Newport #6271), 1.5:G:A global airmass filter (Newport #81388) and an atmospheric attenuation filter (Newport #81017) to mimic the solar spectrum. Bulb irradiance was measured at the start of each experiment using a spectroradiometer (EPP2000C-SR-100 with CR2 cosine receptor, Stellarnet) and the power was adjusted to ensure consistent light spectrum across experiments. The average total irradiance was 198 W/m^2 (280-700 nm); irradiance in the UVB region of the spectrum (280–320 nm) was 1.54 W/m^2. The solar simulator spectrum is presented in Figure 4.1.

Experimental reactors consisted of 100-mL or 10-mL glass beakers painted black on the outside. Reactors were filled with 50 mL or 2 mL PBS (10 mM NaCl, 20 mM phosphate; ionic strength 62 mM), respectively, and inoculated with purified PV3 stock; the average, initial PV3 concentrations were 3.4×10^5 and 6.9×10^6 PFU/mL, respectively. Reactors were constantly mixed using a stir plate and sterile stir bars, located in a water bath cooled by a recirculating chiller to maintain a temperature of 20 °C, and exposed to simulated sunlight for 8 h. Two milliliter samples were removed from 100-mL reactors every 2 h; for 10-mL reactors, each time

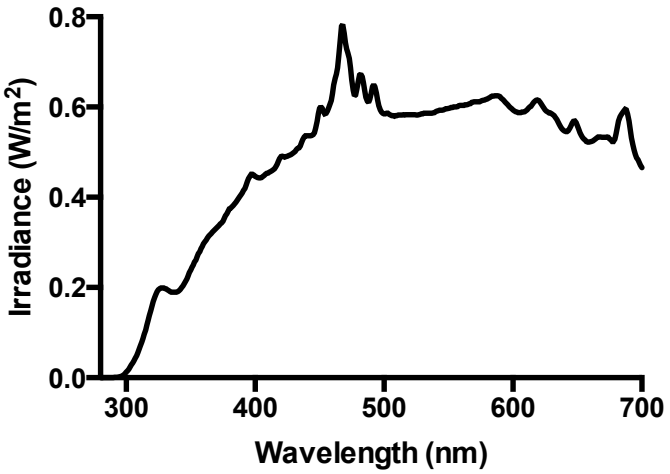

Figure 4.1. Average solar simulator irradiance (n = 2).

series consisted of five reactors, which were sacrificially sampled every 2 h. Samples were immediately aliquoted into sub-samples and frozen at -80 °C until analysis; the aliquots were used for subsequent infectivity, cell attachment, and quantitative PCR (qPCR) control assays described below. Dark control reactors were maintained in the same way, but were covered with aluminum foil.

Infectivity assay. Virus plaque assays were performed to determine the concentration of infectious PV3. Plaque assays were performed in duplicate on 6-well plates of 90% confluent HeLa cells with 100 µL sample inocula and an agar overlay [1.5% wt/vol low melting point agarose (Fisher Scientific #BP165), 1X DMEM, 1X pen/strep, and 10% FBS]. Plates were incubated at 37 °C and 5% CO_2 for 3 d. After incubation, agar overlays were removed and cells stained with crystal violet in order to count plaque forming units (PFU).

Cell attachment assay. Attachment assays were conducted using 6-well plates of 90% confluent HeLa cells. Three versions of the cell attachment assay were conducted (see Table 4.1 for a flow chart of each method). Method A: Maintenance media was removed from each well, which was then inoculated with 100 µL undiluted sample. Plates were incubated at 37 °C and 5% CO_2 for 1 h, with shaking every 15 minutes. After 1 h, inoculum was aspirated and cells were washed 3X with 150 µL 1X DMEM, which was aspirated and discarded after each wash. After washing, each well received 150 µL 1X DMEM and cells were scraped using a cell lifter (Fisher Scientific #08-100-240), which was then rinsed into the well with an additional 150 µL 1X DMEM. The scraped cell-DMEM mixture was aspirated and saved as the cell-attached fraction. Wells were rinsed one more time with 150 µL 1X DMEM, the liquid aspirated and added to the cell-attached fraction (for a total of 450 µL). The cell-attached fraction was frozen at -80 °C until RNA extraction and RT-qPCR to quantify the attached virus concentration (see 'RNA extraction and quantitative PCR' below).

Table 4.1. Workflow of the attachment assays and qPCR control assay.

Exposure to Simulated Sunlight			
Inoculate onto HeLa Cells	Inoculate onto HeLa Cells	Inoculate onto HeLa Cells	
Incubate 1 h at 37°C and 5% CO_2	Incubate 1 h at 25°C	Incubate 1 h at 37°C and 5% CO_2	
Wash cells 3X	Wash cells 3X	Wash cells 3X	
	Add MS2 control	Add MS2 control	Add MS2 Control
Scrape cells, collect as cell-attached fraction	Scrape cells, collect as cell-attached fraction	Scrape cells, collect as cell-attached fraction	
Add MS2 Control			
3X freeze-thaw and chloroform extract	3X freeze-thaw and chloroform extract	3X freeze-thaw and chloroform extract	
		RNase Treatment	
Extract RNA	Extract RNA	Extract RNA	Extract RNA
RT-qPCR	RT-qPCR	RT-qPCR	RT-qPCR
Attachment Assay Method A	**Attachment Assay Method B**	**Attachment Assay Method C**	**qPCR Control**
to measure all cell-attached PV3 (with intact qPCR target)	**to measure all cell-attached PV3 (with intact qPCR target)**	**to measure cell-attached PV3 unable to release genome (with intact qPCR target)**	**to measure all sunlight-exposed PV3 (with intact qPCR target)**

Method B was exactly the same as method A above, but with incubation at 25 °C, to inhibit genome injection into host cells (see 'Virus-host Attachment Assay Theory' below for information on the rationale behind the attachment assay). Method C was performed to quantify viruses that were attached to HeLa cells but unable to release RNA into the host. Method C involved incubation at 37 °C and 5% CO_2, then RNase treatment of the cell-attached fraction after the freeze-thaw and chloroform extraction steps outlined below, but before RNA extraction. RNase treatment protocol is as follows: RNase A (Fermentas) was added to samples at a final concentration of 100 µg/mL, followed by incubation for 30 min in a 37 °C water bath.

qPCR control assay. The qPCR control assay was conducted to determine whether a reduction in the attachment assay RT-qPCR signal after sunlight exposure was due to a reduction in attachment or due to sunlight-induced damage to the RT-qPCR target. For this assay, samples from solar simulator experiments were subjected directly to RNA extraction and RT-qPCR without any upstream sample preparation.

RNA extraction and quantitative PCR. All samples analyzed by RT-qPCR first underwent three freeze-thaw cycles (alternating ethanol dry-ice bath and 25 °C water bath) and chloroform extraction, to ensure release of viruses or injected RNA from HeLa cells. Chloroform extraction was performed as described above. After chloroform extraction, RNA was extracted from viruses using the QIAamp Viral RNA Extraction Kit (Qiagen); a 140 µL aliquot of each sample was extracted following manufacturer instructions and with a final 2 x 40 µL elution step.

MS2 was used as an internal control for the cell attachment and qPCR control assays. For the qPCR control assay and cell attachment assay method A, 10 µL MS2 solution, corresponding to 2.2×10^3 PFU, was added to cell-attached samples before the chloroform extraction step. For cell attachment assay methods B and C, 10 µL MS2 was added to each well of the 6-well plate before scraping the cells with the cell lifter (for future work, this is the recommended method for the MS2 control).

RT-qPCR was used to quantify PV3 and the MS2 control in the cell attachment assay and qPCR control samples. RT-qPCR reactions included 1X TaqMan RNA-to-C_t 1-Step kit Master Mix and 1X RT Enzyme Mix (Applied Biosystems), the appropriate concentrations of primers and probe, 5 µL template, and nuclease-free water to obtain a final 25-µL volume. The PV3 RT-qPCR assay included EV probe [(FAM)-ACGGACACCCAAAGTAGTCGGTTC-(BHQ-1); 200 nM; Gregory et al. 2006; Walters et al. 2009], and EVupstream (CCTCCGGCCCCTGAATG; 400 nM) and EVdownstream (ACCGGATGGCCAATCCAA; 400 nM) primers (DeLeon et al. 1990; Walters et al. 2009). The MS2 RT-qPCR assay included GJW-P probe [(FAM)-CCGTACCTCGGGTTTCCGTCTTGCT-(BHQ-1); 250 nM], and GJW-F (CGGCTGCTCGCGGATA; 900 nM) and GJW-R (ACTTGCGTTCTCGAGCGATAC; 900 nM) primers (Williams 2009). Reactions were run on an Applied Biosystems StepOnePlus Real-Time PCR system. Cycling conditions for both assays were as follows: 30 min hold at 48 °C, 10 min at 95 °C, and 45 cycles of 95 °C for 15 s and 60 °C for 1 min (Walters et al. 2009; Williams 2009). Samples were analyzed in triplicate wells, and all RT-qPCR plates included a standard curve and a no-template control consisting of nuclease-free water.

Whole, extracted PV3 and MS2 genomes were used to create RT-qPCR standard curves. Virus stock solutions were first treated with RNase to destroy extra-viral RNA: RNase A was added for a final concentration of 100 µg/mL, and incubated for 30 min at 37 °C. RNA was extracted using guanidinium thiocyanide lysis buffer (1:1, v/v): the sample-lysis buffer solution was vortexed for 5 s, incubated at room temperature for 10 min, then applied to a silica spin column (Qiagen); RNA was eluted with 50 µL 1X TE. RNA concentrations were measured using the ribogreen assay (Molecular Probes) on a NanoDrop ND-3300 fluorospectrophotometer (Nanodrop Technologies). Standard curves were constructed using ten-fold serial dilutions of RNA in nuclease-free water.

Data analysis. First-order observed rate constants (k; h^{-1}) were calculated as the slope of the linear regression trend line of $-\ln(C_t/C_0)$ versus time. To account for inefficiencies in sample extraction and RNA amplification, PV3 concentrations measured by RT-qPCR were corrected using the MS2 internal standard. The following equation was used to correct $-\ln(C_t/C_0)$ data:

$$-\ln {}^{C_t}/_{C_0} = -\ln \left[\left[\frac{C_{\mathrm{PV3},t}}{C_{\mathrm{MS2},t}}\right] \Big/ \left[\frac{C_{\mathrm{PV3},0}}{C_{\mathrm{MS2},0}}\right] \right]$$

$$= \ln C_{\mathrm{PV3},0} - \ln C_{\mathrm{PV3},t} + \ln C_{\mathrm{MS2},t} - \ln C_{\mathrm{MS2},0} \qquad (4.1)$$

$$= -\ln \left[\frac{C_{\mathrm{PV3},t}}{C_{\mathrm{PV3},0}}\right] + \ln \left[\frac{C_{\mathrm{MS2},t}}{C_{\mathrm{MS2},0}}\right]$$

Statistical tests were performed in Prism (v6.0c, GraphPad Software).

Virus-host Attachment Assay Theory

The poliovirus infection cycle begins with virus attachment to the host cell's poliovirus receptor (i.e., Pvr, also known as CD155; Mendelsohn et al. 1989). Upon attachment, poliovirus undergoes conformational changes to convert from the native particle (called the 160S particle, based on its sedimentation rate in sucrose density gradient centrifugation) to the A particle (also known as the 135S particle), which is thought to be a cell-entry intermediate (Hogle 2002 and ref. within). After some time post-infection, the concentration of A particles decreases while a new altered poliovirus particle – the 80S particle – starts to emerge (Hogle 2002 and ref. within); one theory is that the 80S particle is an empty capsid that remains after poliovirus RNA is released into the host cell cytoplasm (Hogle 2002).

At 37 °C, poliovirus attachment to, and RNA release into, HeLa cells is fast and efficient. Yafal et al. (1993) found maximal native-to-A particle conversion within 1 h when poliovirus was incubated with soluble Pvr, and determined that Pvr remains attached to the virus during that time. Brandenburg et al. (2007) found poliovirus RNA release into HeLa cells to occur with a $t_{½}$ of 22 ± 3 min. We therefore assume that after 1 h incubation, all PV3 that has the ability to attach to host cells has done so. After washing the cells, and discarding wash water, the assumption is that only cell-attached viruses remain in our sample.

While PV3 attachment to host cells occurs between 4 and 40 °C, temperatures greater than 33 °C are required for A particle conversion and subsequent genome release into the host (Yafal et al. 1993); this is likely due to A particle conversion acting as a rate-limiting step to infection at lower temperatures (Huang et al. 2000). Brandenburg et al. (2007), for example, observed attachment of PV3 to HeLa cells at 24 °C, but no RNA release. In attachment assay method B, which involves incubation of inoculated cells at 25 °C, we assume that RNA is not released into host cells, and instead remains within the virus. This differs from method A (with incubation at 37 °C), where it is assumed that attached viruses that retain the ability to release RNA into the host cell will do so within the 1 h incubation time. By keeping all RNA in its encapsulated form in method B, we hope to better protect it from degradation until quantification by RT-qPCR.

While both methods A and B were designed to quantify all cell-attached PV3, regardless of its ability to release RNA into the host cell, method B was performed to ensure no loss of RT-qPCR signal occurred due to degradation of un-encapsulated RNA.

Attachment assay method C was performed as an indirect way to quantify the decrease in ability of PV3 to release its genome into host cells. Method C involved incubation of PV3-inoculated HeLa cells at 37 °C (to allow PV3 attachment and RNA release), cell washing and scraping (to isolate the cell-attached PV3 fraction), freeze-thaw and chloroform extraction (to disrupt HeLa cell membranes and release viruses and naked viral RNA from within the cell) and RNase treatment (to degrade naked RNA). 135S particles are not susceptible to RNase (Curry et al. 1996), therefore after RNase treatment we assume all RNA quantified by RT-qPCR to be RNA that remained encapsulated (i.e. within PV3 particles that were able to attach to host cells, but unable to release RNA).

Results and Discussion

To assess the contribution of protein damage to sunlight inactivation of PV3 – as manifested as the inhibition of attachment of the virus to host cells – we conducted infectivity and cell attachment assays with sunlight-exposed PV3. The infectivity assay, a plaque assay performed with HeLa cells, allowed us to determine the reduction in virus infectivity and calculate the first-order observed inactivation rate constant for the virus (k_{obs}). The cell attachment assays, quantified by RT-qPCR, were conducted to determine the extent and rate of attachment inhibition (k_{attach}); all viruses quantified by this assay were assumed to be attached to host cells, however, given the use of RT-qPCR for quantification, it is possible that a portion were not infectious. A third assay, the qPCR control assay, was conducted to determine the extent of RT-qPCR signal decrease attributed to sunlight degradation of the RT-qPCR target.

Using the infectivity assay (Figure 4.2A, circles), we calculated PV3 k_{obs} to be 1.54 h^{-1} (n = 4; 95% confidence interval 1.41 to 1.66 h^{-1}; R^2 = 0.98), which is similar to that measured by Silverman et al. (2013a; k_{obs} = 1.38 h^{-1}). This rate would change with different UVB light intensity, as was modeled in Chapter 3.

As determined by attachment assay method A (Figure 4.2A, triangles), inhibition of PV3 attachment to host cells at t = 2 h was not significantly different from zero (n = 3; t-test, P = 0.17). Between t = 2 and 8 h, there was a log-linear decrease in PV3 attachment, corresponding to first-order decay, and k_{attach} was 0.51 h^{-1} (R^2 = 0.96).

None of the average $-\ln(C_t/C_0)$ values determined via the qPCR control assay were found to be significantly different from zero (Figure 4.2A, squares; n = 3; t-test, P = 0.08-0.78), although the mean $-\ln(C_t/C_0)$ at t = 8 h was 0.92. This result indicates that most of the reduction in the RT-qPCR signal measured by the attachment assays can be attributed to a reduction in the number of attached PV3 particles, not damage to the RT-qPCR target. However, there is potential for sunlight-induced modification of the RT-qPCR amplicon, given that it contains adjacent uracil and cytosine bases (Hogle et al., 1985), which are targets for the formation of pyrimidine dimers with exposure to UV light.

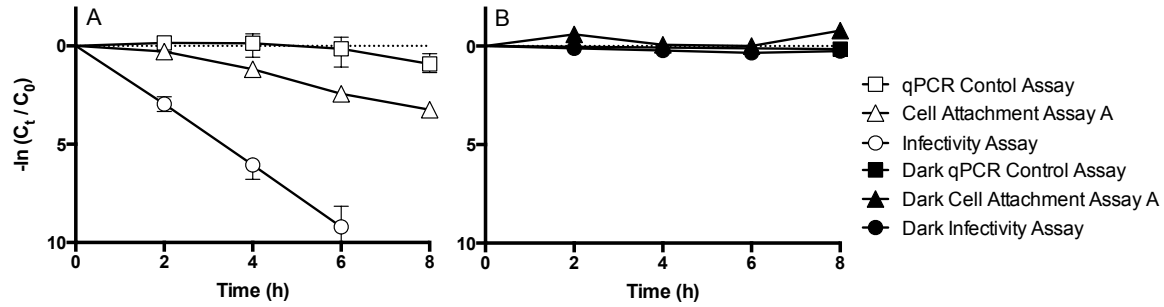

Figure 4.2. Average -ln(C_t/C_0) values determined by the infectivity, cell attachment (method A) and qPCR control assays conducted with samples exposed to simulated sunlight (A) or collected from dark control reactors (B). $n = 4$ for light infectivity assay, $n = 3$ for light cell attachment assay and qPCR control assay, $n = 2$ for dark infectivity assay and cell attachment assay, $n = 1$ for dark qPCR control assay. Error bars are the range of values.

None of the dark control -ln(C_t/C_0) values determined by the infectivity, cell attachment or qPCR control assays were found to be greater than zero (Figure 4.2B).

The lag in cell attachment inhibition leads to two discussion points. First, the shoulder in the attachment inhibition curve at t = 2 h suggests that this process is governed by a multiple-hit kinetic model. The applicability of a multiple-hit model makes sense: the PV3 capsid is composed of 60 copies of each of four proteins (Hogle et al. 1985), and theoretically has 60 points where it can attach to the host cell's poliovirus receptor. If some attachment locations are damaged, the virion may have other intact anchor points that could be used. Cell attachment assay method B was conducted with undiluted and 10-times diluted sample and found to have similar -ln(C_t/C_0) versus time curves (Figure 4.3), indicating that the shoulder was due to a lag in virus attachment inhibition and not a saturation of host cell attachment sites at t = 0 h.

Second, while a shoulder was observed in the cell attachment curve, none was seen in the inactivation curve. This, along with a slower rate of attachment inhibition than inactivation (0.51 versus 1.54 h^{-1}), demonstrates that attachment inhibition plays a minor role, if any, in PV3 sunlight inactivation. Two other potential mechanisms of PV3 sunlight inactivation remain. The first is damage to RNA, resulting in an inhibition of transcription or translation. The second is protein damage that inhibits RNA delivery into the host cell. One long-standing hypothesis about genome delivery is that virus capsids are assembled under tension, and that the stored energy is required for genome injection (Kuzmanovic et al. 2006). Capsid damage, such as cleavages, that dampen this tension could result in lower energy available for genome deliver (Wigginton et al. 2012).

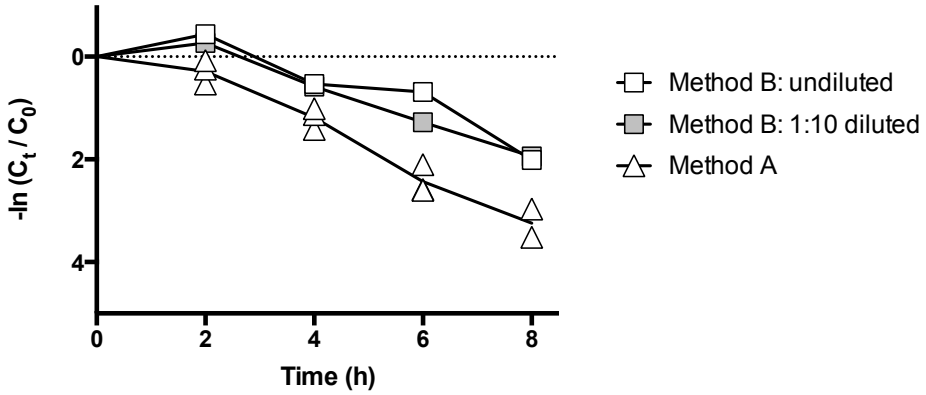

Figure 4.3. Comparison of attachment assay methods A and B. $n = 3$ for method A and $n = 1$ for method B, both diluted and undiluted.

To test the latter, we conducted an experiment to measure the percentage of attached viruses that were unable to inject their genome into the host cell. To do this we used cell attachment assay methods B and C where PV3 samples were inoculated onto two sets of HeLa cells: one set (method B) was incubated for 1 h at 25 °C, to allow attachment but prevent RNA delivery into host cells, and the other (method C) at 37 °C, to promote RNA delivery. Before extracting RNA from the attached PV3 fraction, samples incubated at 37 °C were subjected to host cell disruption and RNase treatment, with the assumption that all RNA delivered to the host was released to bulk solution and then destroyed by RNase, while RNA that remained encapsulated (i.e., within the fraction of viruses unable to deliver RNA) was protected. Therefore, viruses quantified by attachment assay method C were those that were unable to deliver RNA into host cells. One limitation of this assay is that we assume that only RNA injected into host cells was destroyed by RNase, however, we do not know whether encapsulated RNA within sunlight-exposed viruses is more susceptible to RNase than that within unexposed viruses (in future work, to determine this, an additional attachment assay control should be conducted at 25 °C, followed by RNase treatment of attached viruses before RNA extraction).

Attachment assay methods B and C were only conducted once, as a preliminary experiment, so the following analysis should be taken lightly. The $-\ln(C_t/C_0)$ versus time curve for method B was similar to that for method A (Figure 4.3), although method B had a slower rate of attachment inhibition. This result suggests that method B may better protect against degradation of un-encapsulated RNA. Preliminary results from attachment assay method C suggest that there is a linear decrease in the number of PV3 virions that attached to host cells but did not inject their genomes ($R^2 = 0.97$; Figure 4.4, black diamonds). These data were used to calculate the concentration of viruses that delivered RNA to host cells ($C_{\text{PV3,release RNA}}$; Figure 4.4, crosses) using the following equation:

$$C_{PV3,release\ RNA} = C_{PV3,attached,total} - C_{PV3,attached,no\ release} \quad (4.2)$$

where $C_{PV3,attached,total}$ is the concentration of PV3 measured using attachment assay method B and $C_{PV3,attached,no\ release}$ is that measured using attachment assay method C. The MS2 internal control correction only works with measurements relative to t = 0 [e.g., -ln(C_t/C_0)], so was not used here.

$C_{PV3,release\ RNA}$ was used to compute the percentage of attached viruses that were able to inject RNA into the host cell using the equation:

$$Percent\ Attached\ PV3\ that\ injected\ RNA = \frac{C_{injected}}{C_{PV3,attached,total}} \cdot 100\% \quad (4.3)$$

Preliminary results using attachment assay methods B and C suggest that most attached viruses were also able to deliver their genome into the host cell (Table 4.2; Figure 4.4): approximately 40% of attached viruses were able to deliver their genome at t = 0 (i.e., before sunlight exposure), while 78 to 91% of attached viruses were able to do so between t = 2 and 8 h.

Table 4.2. Percent of attached viruses that injected genomes into the host.

Time (h)	Percent attached PV3 that injected RNA into host cell (%)
0	41
2	87
4	78
6	91
8	90

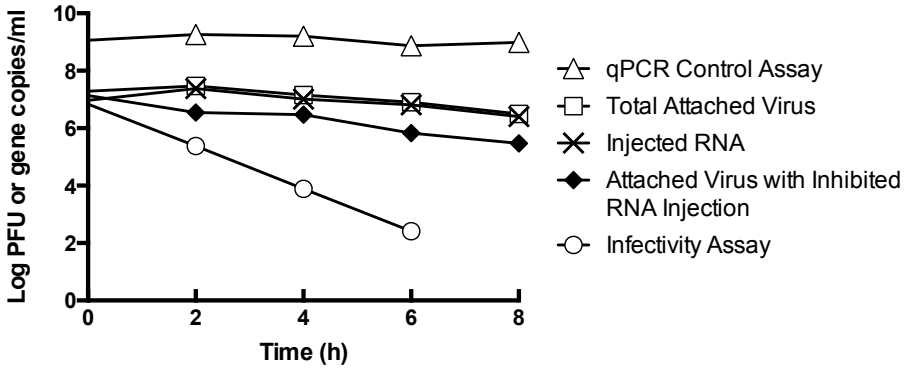

Figure 4.4. Log concentration data using attachment assays B and C. $n = 1$ for all.

Attachment assay methods B and C should be conducted again to ensure that results are reproducible. If the data are correct, they indicate that the inhibition of genome delivery in sunlight exposed PV3 is insignificant, leaving genome damage as the main hypothesized cause of sunlight inactivation of PV3. Further research should be conducted to quantify genome damage, to help determine why some viruses are inactivated at faster rates than others. Quantitative PCR, as seen in our study and others (Pecson et al. 2011 and ref. within), typically underestimates virus inactivation and is a poor proxy for whole genome damage, due to the small size of the amplification target as compared to the length of the entire genome. There are three potential approaches that can be taken in the future to study genome damage. The first is to conduct long-range qPCR, using longer amplicons that are more likely to contain a target of sunlight-induced damage (Simonet and Gantzer 2006). Second is to use a theoretical framework developed by Pecson et al. (2011) that quantifies damage to the whole genome based on PCR amplification of several smaller sections. And a third is to use an assay that quantifies sites of sunlight modification on the genome, such as the endonuclease sensitive site assay that can quantify pyrimidine dimers (Oguma et al. 2001; Sutherland and Shih 1983). No matter which method is chosen to study genome degradation it will be important to relate that information to RNA composition and conformation, as well as infectivity data.

Chapter 5

Quantification of human norovirus GII, human adenovirus, and fecal indicator organisms in wastewater used for irrigation in Accra, Ghana

The following chapter is adapted from Silverman et al. (2013) Quantification of human norovirus GII, human adenovirus, and fecal indicator organisms in wastewater used for irrigation in Accra, Ghana. *J. Wat. Health* 11, 473-488, with permission from Mark O. Akrong, Philip Amoah, Pay Drechsel, and Kara L. Nelson.

Introduction

The use of untreated wastewater in urban and peri-urban irrigated agriculture is prevalent around the world. Increasing urban populations use more freshwater and produce a greater volume of wastewater that is, in many cases, discharged to the environment without treatment. Scarcity of (unpolluted) freshwater resources and year-round access to wastewater create conditions that encourage wastewater irrigation (Scott et al. 2004). Ghana's capital city, Accra, provides an example of wastewater irrigation practiced on a wide-scale. Accra has an estimated 100 ha of land under irrigated vegetable production (Obuobie et al. 2006). Due to limited functional wastewater collection and treatment infrastructure (Murray and Drechsel 2011), as well as leaky septic systems and open defecation, untreated greywater and sewage (collectively 'wastewater') flow directly and indirectly into open drains and streams, which are the primary sources of water used by farmers in Accra to irrigate vegetables. The term 'wastewater irrigation,' therefore, encompasses the use of water along the whole trajectory from raw wastewater to contaminated surface water. Alternative water sources are rare, making wastewater irrigation necessary for farmers who want to reap the benefits of urban or peri-urban agriculture. Year-round farming in proximity to Accra's markets offers a significant livelihood opportunity for small-scale farmers while supplying the city with most of its perishable vegetables (Raschid-Sally and Jayakody 2008). Additionally, municipalities and landowners benefit when farmers act as informal caretakers: farmers protect land from solid waste dumping and illegal land development, and farmed land can contribute to stormwater management (Lydecker and Drechsel 2010), an issue particularly important for Accra, which experiences annual flooding.

Despite the benefits, there are health risks associated with wastewater irrigation due to the potential presence of human pathogens. The connection between illness and agricultural use of human and animal waste has been shown; epidemiological studies have demonstrated that the use of inadequately treated waste in agriculture can lead to an increased risk of viral, protozoan, intestinal helminth, and bacterial infection for farmers, their families, and consumers (Blumenthal and Peasey 2002; Ensink et al. 2006; Jiménez 2006). In an effort to reduce the health risks associated with water reuse, regulatory and health agencies, such as the United States

Environmental Protection Agency and the World Health Organization (WHO), have developed water quality guidelines for the reuse of water for agricultural purposes (Blumenthal et al. 2000; US EPA 2004; WHO 2006). The 2006 WHO Guidelines for the safe use of wastewater, excreta and greywater in agriculture (hereafter referred to as the 'WHO Guidelines') stresses the development of location-specific, health-based water quality targets, and the use of water quality assessment and quantitative microbial risk assessment (QMRA) to determine health risks due to pathogens in wastewater. After estimating health risks, regulators can determine water treatment objectives to meet health-based targets.

QMRA models rely on estimates of pathogen exposure (e.g., estimates of pathogen concentration and rates of ingestion) and appropriate dose-response models. Due to the complexity and expense of pathogen analyses, actual pathogen concentrations are often not measured. Instead, water quality is assessed using indicator organisms – typically fecal indicator bacteria (FIB) such as *E. coli*, enterococci or thermotolerant coliforms – and simple relationships between FIB and pathogens are used to predict the concentration of the target pathogen. However, relationships between indicator organism and pathogen concentrations are complex. Different organisms and classes of organisms (e.g., viruses, bacteria, protozoa and helminths) are excreted in different ratios by varying proportions of the population depending on their health status, and have different fate and transport processes in the environment. While bacterial pathogens can cause disease associated with wastewater irrigation, research using QMRA modeling has found viral pathogens such as rotavirus and norovirus to present greater health risks in wastewater irrigation than *Campylobacter*, which was used as an 'index' bacterial pathogen (WHO 2006). Viruses tend to be more persistent than bacteria in the environment and have been named some of the most important causes of food- and waterborne disease. Norovirus, for example, has been found to be *the* leading cause of foodborne illness in the United States (Widdowson et al. 2005), and a study conducted in the city of Tamale, in Northern Ghana, found rota-, adeno-, noro- or astroviruses to be present in the stool of 73% of children aged 0–12 years suffering from diarrhea (Reither et al. 2007).

Previous researchers investigating irrigation water quality in Accra have quantified coliforms (Mensah et al. 2001; Keraita et al. 2003; Amoah et al. 2005), but not human viruses. To provide data that can be used to refine QMRA model inputs, irrigation waters from major farm sites around Accra were sampled and analyzed for concentrations of two types of human viral pathogen (human adenoviruses and norovirus genogroup II) and six fecal indicator organisms (human-specific *Bacteroidales*, *E. coli*, enterococci, thermotolerant coliform, and somatic and F+ coliphages). Norovirus and adenovirus are important waterborne viruses. Norovirus genogroup II was chosen over genogroup I given that genogroup II is a more prevalent etiology of disease in both Ghana (Armah et al. 2006; Silva et al. 2008) and around the world (Siebenga et al. 2009). Measured concentrations were used to determine relationships among fecal indicator microorganisms, and compute ratios between *E. coli* and human virus concentrations.

Methods

Site selection and sample collection. Sampling sites were farming areas located within the Accra Metropolitan Assembly (Table 5.1). Water samples were collected in July 2010, from

locations where farmers collect irrigation water and at a time when farmers were using the water (between 8:30 and 11:30 am). Each site was sampled on two separate days (except for La Drain and Odaw River which were each sampled once) for a total of twenty samples at eleven locations. Samples were collected using a bucket sterilized with 70% ethanol, wiped dry and rinsed with sample water before use. Water was poured from buckets into sterile, opaque cubitainers and transported to the laboratory on ice. All samples were analyzed within 6 h of collection.

Table 5.1. Farm sites and sample locations.

Site	Water Samples	Irrigation Water Used
Dzorwulu/ Roman Ridge	Dzorwulu Drain Roman Ridge Drain Onyansa Stream	Piped water, open drains, and the Onyansa stream, which is contaminated by effluent from the non-functioning Roman Ridge wastewater treatment plant
La Fulani	La Drain La WSP Influent La WSP Effluent	Irrigation water sources include a drain containing sewage from the military base and WSP water
Marine Drive	Marine Drive Stream	Stream water
Korle Bu	Korle Bu Drain	Drain water, potentially from adjacent housing complexes
Nima Creek	Nima Creek	Nima Creek, which receives wastewater flows from houses along its course
Ghana Broadcasting Corporation (GBC)	GBC Drain	Main water source is an unlined drain that runs through the center of the site
Odaw River	Odaw River	The Odaw is the main river running through Accra and serves to drain an area of approximately 250 km^2, including the most urbanized areas of the city. While not a farm site per se, farmers located on the Odaw's banks use its water for irrigation

Culture-based microbiological analyses. *Fecal Indicator Bacteria.* Water samples were analyzed for *E. coli* and enterococci concentrations by membrane filtration using 47-mm diameter, 0.45-µm pore size, mixed cellulose ester HA filters (Millipore). *E. coli* were quantified using both mI (BD) and chromocult agars (Merck KGaA), with incubation at 37 °C for 24 h.

Enterococci concentrations were quantified using mEI agar (BD), with incubation at 41 °C for 24 h. *E. coli* and enterococci were enumerated as colony forming units (CFU).

Thermotolerant coliform, also referred to as fecal coliform, were quantified by the multiple tube fermentation, most probable number (MPN) method with 1 mL sample inoculums, 5 mL sterile MacConkey broth (Merck KGaA), and three replicates of each dilution; tubes were incubated at 41 °C for 48 h. Replicates were marked as positive for thermotolerant coliform if color change or gas production was detected.

Coliphage. Water samples were concentrated for coliphage enumeration by membrane filtration using HA filters. $MgCl_2$ (0.05 M final concentration) was added to water samples to facilitate virus adsorption to filters (Lukasik et al. 2000); samples were mixed and held for 5 min before filtration. Between 15 and 150 mL of sample was subsequently filtered (at a rate approximately 100 mL/3 min), depending on water turbidity and filter clogging. Filters were preserved until elution by freezing at -20 °C on 300 µL of 50% glycerol [1:1 vol/vol with phosphate buffered saline (PBS)].

Coliphage were eluted from filters by adding 3% Beef Extract (pH 9; 30 g/L Beef Extract, 30 mL/L Tween 80, 0.3 M NaCl) and swirling for 10 min. Filter eluent was assayed for coliphage using the double agar layer (DAL) method with 100 µL and 1 mL sample inoculums, modified Tryptic Soy Agar (TSA) top and bottom agars, and appropriate hosts and antibiotics. F+ coliphage were assayed using *E. coli* F_{amp} host bacteria with 1X ampicillin and streptomycin antibiotics (0.0015 g/L of each); somatic coliphage were assayed using *E. coli* CN13 host with nalidixic acid (0.01 g/L). Modified TSA agar consists of: BactoAgar [0.75% (top agar) or 1.5% (bottom agar) wt/vol; BD], 30 g/L tryptic soy broth (BD), and 0.002 M $CaCl_2$. Eluted filters were plated, face down, on top agar augmented with 0.3% Tween 80. Plates were incubated at 37 ºC for 18–24 h and enumerated as plaque forming units (PFUs). Total phage concentrations were calculated by adding counts from the DAL and filter plates.

Correlation between organisms. Correlation coefficients (R^2) between pairs of FIB and coliphage were determined using log-transformed concentrations.

(RT-)qPCR analyses. Human-specific *Bacteroidales*, human adenovirus (HAdV; all 51 types) and norovirus genotype II (NV-GII) were concentrated, extracted and then quantified by quantitative PCR (qPCR) or reverse transcription qPCR (RT-qPCR).

Sample concentration. Bacteria and viruses were concentrated from water samples in the same manner as described above for coliphage, but with a $MgCl_2$ concentration of 0.025 M. For DNA/RNA preservation, filters were covered with 500 µL RNAlater (Qiagen), allowed to sit for 1 min, and then excess liquid was removed by vacuum. Filters were aseptically rolled and placed in 5 mL DNA/RNA-free tubes, stored at 4 °C overnight to allow RNAlater to further soak into the filter, then frozen at -20 °C until transported to University of California, Berkeley for analysis; once there, filters were stored at -80 °C until extracted.

Preparation of recovery controls. MS2 (ssRNA bacteriophage) and *Pseudomonas syringae* pv. *phaseolicola* (pph6; gram-negative bacteria) were used as control spikes to evaluate the

combined efficiency of nucleic acid extraction and amplification for RNA and DNA, respectively.

MS2 was propagated by broth enrichment with *E. coli* F_{amp} host and 1X ampicillin and streptomycin, then purified through chloroform extraction and polyethylene glycol precipitation, resuspended in PBS and frozen at -80 °C in single use aliquots. The concentration of culturable MS2 in the control spike was determined by DAL with *E. coli* F_{amp} host and 1X ampicillin and streptomycin.

Pph6 was cultured in modified King's B media (10 g/L tryptone, 10 g/L peptone, 10 mL/L glycerol, 8.3 mM $MgSO_4$, 5.7 mM K_2HPO_4) and incubated at 28 °C for 48 h. Freshly cultured cells were centrifuged for 10 min at 5400 ×*g* at 4 °C, the supernatant discarded, and then rinsed three times by resuspending with PBS, centrifuging and discarding the supernatant. After the final wash, the cells were resuspended in 15% glycerol-0.01 M $MgSO_4$. The cell suspension was frozen at -80 °C in single use aliquots.

Fifty microliters of the 10^{-6} dilution of the MS2 spike (approximately 11 MS2 PFU) or the 10^{-1} dilution of the pph6 spike (approximately 1.5×10^5 gene copies) was spiked into each RNA or DNA sample tube, respectively, prior to nucleic acid extraction, but after sample concentration and tube transport. Identical control spikes were also added to extraction blanks, which did not contain filters. Extraction/amplification efficiency of each sample was calculated by comparing MS2 or pph6 concentration in that sample with the concentration in the extraction blank, and classified as poor (–; <25%), acceptable (+; 25-50%) or good (++; >50%); sample concentrations were not adjusted in relation to recovery efficiency. MS2 and pph6 recoveries do not include information on efficiency of the concentration step or potential loss during sample transport. Additionally, given variability in virus composition and structure, as well as interactions with sample matrices, MS2 may not behave exactly like the human viruses in extraction and amplification steps. Likewise, pph6 may not be a perfect proxy for extraction and amplification of human-specific *Bacteroidales* and HAdV in the irrigation water samples.

Nucleic acid extraction. DNA and RNA were extracted from separate filters. As mentioned above, extraction/amplification control spikes (MS2 and pph6) were added to samples prior to extraction. DNA and RNA were extracted using the PowerWater DNA and RNA isolation kits (MoBio, Carlsbad, CA), respectively, following manufacturer protocols and one modification: final DNA/RNA elution buffer was preheated to 95 °C before use to improve recovery (Viau et al. 2011). Extracted DNA and RNA were aliquoted in single-use aliquots and frozen at -80 °C.

(RT-)qPCR assays. Previously published primers, hydrolysis probes and assays were used for (RT-)qPCR analyses (Table 5.2); probes were 5' labeled with a 6'FAM reporter dye and 3' labeled with a Black Hole 1 quencher. For qPCR assays [human-specific *Bacteroidales* (BacHum target), HAdV, and pph6], reactions included 1X TaqMan Fast Universal PCR Master Mix with no AmpErase UNG (Applied Biosystems), the appropriate concentrations of primers and probe, 6 µL template, and nuclease-free water to obtain a final 20 µL volume. For RT-qPCR analyses (NV-GII and MS2), reactions included 1X TaqMan One Step RT-PCR Master Mix, 1X RT Enzyme Mix (Applied Biosystems), the appropriate concentrations of primers and probe, 6 µL template, and nuclease-free water to obtain a final 20 µL volume. A 1:10 dilution of extracted DNA/RNA was used as template for all samples. Preliminary experiments found that 1:10

Table 5.2. (RT-)qPCR targets, primers, probes, and thermocycling conditions. Hydrolysis probes were 5' labeled with a 6'FAM reporter dye and 3' labeled with a Black Hole 1 quencher. Primer and probe concentrations are presented in parenthesis. Degenerate bases: N, any nucleotide; R, A or G; W, A or T.

Target Organism (gene)	Primers/Probe (concentration in nM)	Oligonucleotide Sequence (5'-3')	Position	Thermo-cycling Conditions
Bacteria				
Human-specific *Bacteriodales*[1] (16s Gene)	BacHum-160f (400)	TGAGTTCACATGTCCGCATGA	160-180	95°C, 10 min 45 Cycles: 95°C, 15 s 60°C, 1 min
	BacHum-241r (400)	CGTTACCCCGCCTACTATCTAATG	241-218	
	BacHum-193p (80)	TCCGGTAGACGATGGGGATGCGTT	193-217	
Viruses				
Adenovirus[2] (hexon)	JTVXF (250)	GGACGCCTCGGAGTACCTGAG	18895-18915	95°C, 10 min 45 Cycles: 95°C, 15 s 55°C, 1 min
	JTVXR (250)	ACNGTGGGGTTTCTGAACTTGTT	18990-18968	
	JTVXP (150)	CTGGTGCAGTTCGCCCGTGCCA	18923-18944	
Norovirus GII[3] (ORF1-ORF2 Junction)	QNIF2d (200)	ATGTTCAGRTGGATGAGRTTCTCWGA	5012-5037	50°C, 15 min 95°C, 10 min 45 Cycles: 95°C, 15 s 55°C, 1 min
	COG2R (200)	TCGACGCCATCTTCATTCACA	5100-5080	
	QNIFS (200)	AGCACGTGGGAGGGGATCG	5042-5061	
Extraction Controls				
MS2[4] (replicase β chain)	GJW-F (900)	CGGCTGCTCGCGGATA	3165-3180	48°C, 30 min 95°C, 10 min 45 Cycles: 95°C, 15 s 60°C, 1 min
	GJW-R (900)	ACTTGCGTTCTCGAGCGATAC	3228-3208	
	GJW-P (250)	CCGTACCTCGGGTTTCCGTCTTGCT	3182-3206	
Pseudomonas syringae[5] (pph6) (Avr PphE)	Pph-409f (900)	CAGGCCCTAGCGTGGAAAC	409-427	95°C, 10 min 40 Cycles: 92°C, 15 s 60°C, 1 min
	Pph-465r (900)	GGTTCTGGGCCGATGATG	465-448	
	Pph-428p (250)	CACTGAAAAGGCTGTTCA	428-445	

[1] (Kildare et al. 2007)
[2] (Jothikumar et al. 2005)
[3] (Kageyama et al. 2003; Loisy et al. 2005; Viau et al. 2011)
[4] (Williams 2009)
[5] (Silkie and Nelson 2009)

dilution of extracted DNA/RNA from pond water and primary sewage effluent reduced inhibition; further dilution did not provide an additional anti-inhibitory effect (data not shown). Reactions were run on an Applied Biosystems StepOnePlus Real-Time PCR system. Thermocycling conditions varied for each target based on previously published methods (Table 5.2). All (RT-)qPCR plates included a standard curve and a no-template control consisting of nuclease-free water.

Generation of standards and calibration curves. Linearized plasmid standards were used for quantification of BacHum, HAdV, pph6 and NV-GII targets. *E. coli* containing the plasmid standard for the BacHum target was obtained from Professor Stefan Wuertz at the University of California, Davis (Kildare et al. 2007). *E. coli* containing plasmid standards for HAdV and NV-GII were obtained from Professor Alexandria Boehm at Stanford University (Viau et al. 2011). *E. coli* containing the plasmid standard for pph6 was from Silkie and Nelson (2009). Plasmids were extracted using a QIAprep Spin MiniPrep kit (Qiagen). pph6, HAdV and NV-GII plasmid standards were linearized using restriction enzyme BamHi; the BacHum plasmid standard was linearized using restriction enzyme PstI. Linearized plasmids containing the NV-GII target were invitro-transcribed to RNA using MAXIscript (Ambion) and purified using MEGAclear (Ambion). A whole genome RNA standard was used for quantification of MS2. MS2 RNA was extracted from purified culture using guanidinium thiocyanide lysis buffer and a silica spin column (Qiagen), as described by Love et al. (2008).

DNA standard concentrations were quantified using the PicoGreen assay (Molecular Probes) for dsDNA on a NanoDrop ND-3300 fluorospectrophotometer (Nanodrop Technologies); RNA standard concentrations were quantified using the RiboGreen assay (Molecular Probes). Ten-fold serial dilutions of DNA and RNA standards in nuclease-free water were used to construct calibration curves to relate cycle thresholds (C_t) to concentrations (gene copies/μL). Calibration curves were pooled if an assay was run more than once.

Data analysis. Nucleic acid extract from each sample was analyzed in triplicate reactions. If C_t of all three reactions fell within the linear range of the calibration curve, C_t values were used to calculate the average concentration and standard deviation for that sample's nucleic acid extract; to calculate the *sample* concentration, this value was multiplied by the volume of extracted DNA/RNA and normalized by the volume of water concentrated for that sample. If none of the replicates amplified within 45 cycles, the sample concentration was designated as 'less than the limit of detection (<LOD).' If at least one replicate amplified, but it or other replicates had a C_t value greater than the highest C_t on the standard curve, that sample was designated as 'positive, but below the limit of quantification (+BLOQ).'

Results

Fecal indicator bacteria and coliphage. Average FIB and coliphage concentrations at each site are presented in Figure 5.1. Thermotolerant coliform concentrations ranged from 6.0 to 9.0 log MPN/100 mL. *E. coli* concentrations measured using mI and chromocult agars were similar: only four out of twenty samples had measured concentrations that differed by more than 0.1 log CFU/100 mL and the largest difference was 0.25 log CFU/100 mL. The correlation coefficient

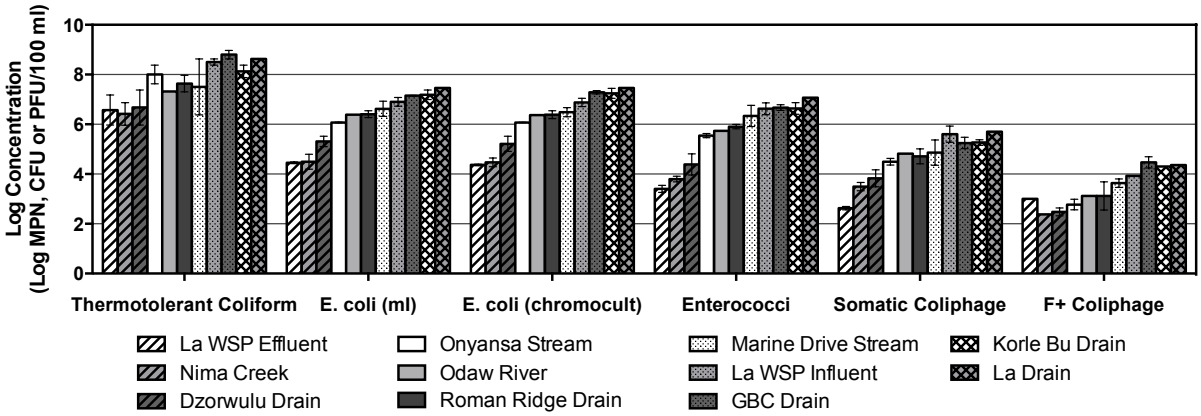

Figure 5.1. Average FIB and coliphage concentrations. $n = 2$ for all samples, except for all organisms in La Drain and Odaw Stream, and F+ coliphage in Nima Creek, La WSP Influent and Korle Bu Drain, where $n = 1$. Error bars designate the range of values.

(R^2) between *E. coli* concentrations measured using the two media was 0.99. *E. coli* concentrations ranged from 4.2 to 7.5 log CFU/100 mL. Enterococci concentrations ranged from 3.3 to 7.1 log CFU/100 mL. Somatic coliphage concentrations ranged from 2.6 to 5.9 log PFU/100 mL, and F+ coliphage concentrations from 2.3 to 4.7 log PFU/100 mL. The ranking of indicator organisms from that with the highest concentration to least was in the following order for all samples, except the La waste stabilization pond (WSP) effluent: thermotolerant coliform concentration > *E. coli* > enterococci > somatic coliphage > F+ coliphage. In the La WSP effluent, the F+ coliphage concentrations were greater than somatic coliphage concentrations. No organisms were detected in negative controls.

Virus and human-specific Bacteroidales concentrations. Samples positive for NV-GII, HAdV, and human-specific *Bacteroidales* are indicated in Figure 5.2; the locations of these samples are presented in Figure 5.3. Measured virus and human-specific *Bacteroidales* concentrations, as well as extraction/amplification recoveries, are presented in Table 5.3.

Recovery efficiencies of pph6, the DNA extraction/amplification control, ranged from 0 to 115% (mean = 46%), with one and seven out of twenty samples categorized as having acceptable and good efficiency, respectively. Recovery efficiencies of MS2, the RNA extraction/amplification control, ranged from 0 to 145% (mean = 62%), with six and nine out of twenty samples categorized as having acceptable and good efficiency, respectively. Poor extraction/amplification control recovery in some samples could be due to poor nucleic acid extraction and/or (RT-)qPCR inhibition. Microorganism concentrations measured by (RT-)qPCR, therefore, may not reflect actual virus concentrations, but conservative estimates. Additionally, because recovery efficiency varied from sample to sample, the relative concentrations between samples may not be accurate.

Sixteen samples (80%) were positive for NV-GII: eleven were quantifiable and five classified as +BLOQ. Of the samples with quantifiable concentrations of NV-GII, concentrations ranged

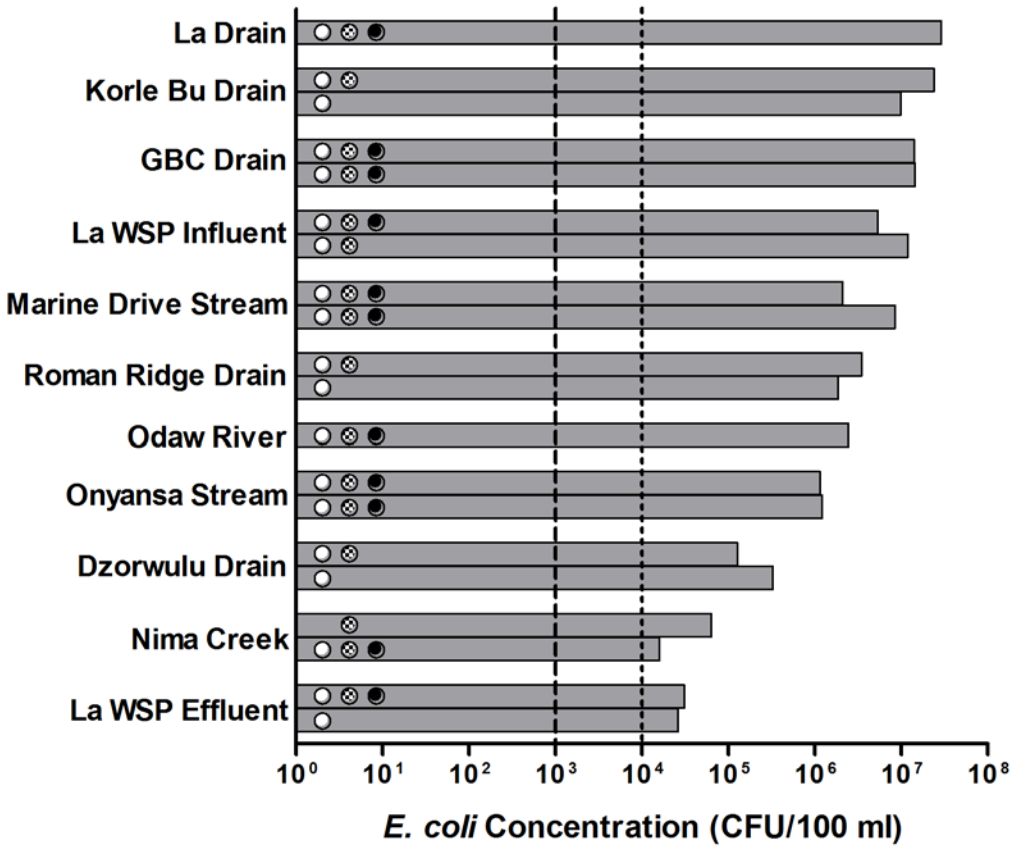

Figure 5.2. *E. coli* concentrations; each bar represents water sampled from the denoted site on one day. White circles indicate samples positive human-specific *Bacteroidales*, black-and-white-check circles indicate samples positive for norovirus GII, and black circles indicate samples positive for human adenoviruses. The dashed line (10^3 *E. coli* CFU/100 mL) designates water quality criteria suggested by 2006 WHO Guidelines for irrigation of root crops while the dotted line (10^4 *E. coli* CFU/100 mL) designates that for irrigation of leaf crops.

between $(4.75 \pm 2.20) \times 10^2$ and $(1.58 \pm 0.28) \times 10^4$ gene copies/100 mL. Eleven samples (55%) were positive for HAdV: seven were quantifiable and four classified as +BLOQ. Of the samples with quantifiable concentrations of HAdV, concentrations ranged between $(2.80 \pm 0.92) \times 10^2$ and $(6.50 \pm 0.60) \times 10^4$ gene copies/100 mL. NV-GII was detected more frequently than HAdV. Eleven samples contained both viruses, five samples contained NV-GII only, and four samples contained neither virus (Figure 5.2). All sites contained either NV-GII or HAdV in at least one sample.

Human-specific *Bacteroidales* was quantified in fifteen out of twenty samples and classified as <LOD in only one sample (from Nima Creek); the samples classified as +BLOQ and <LOD for

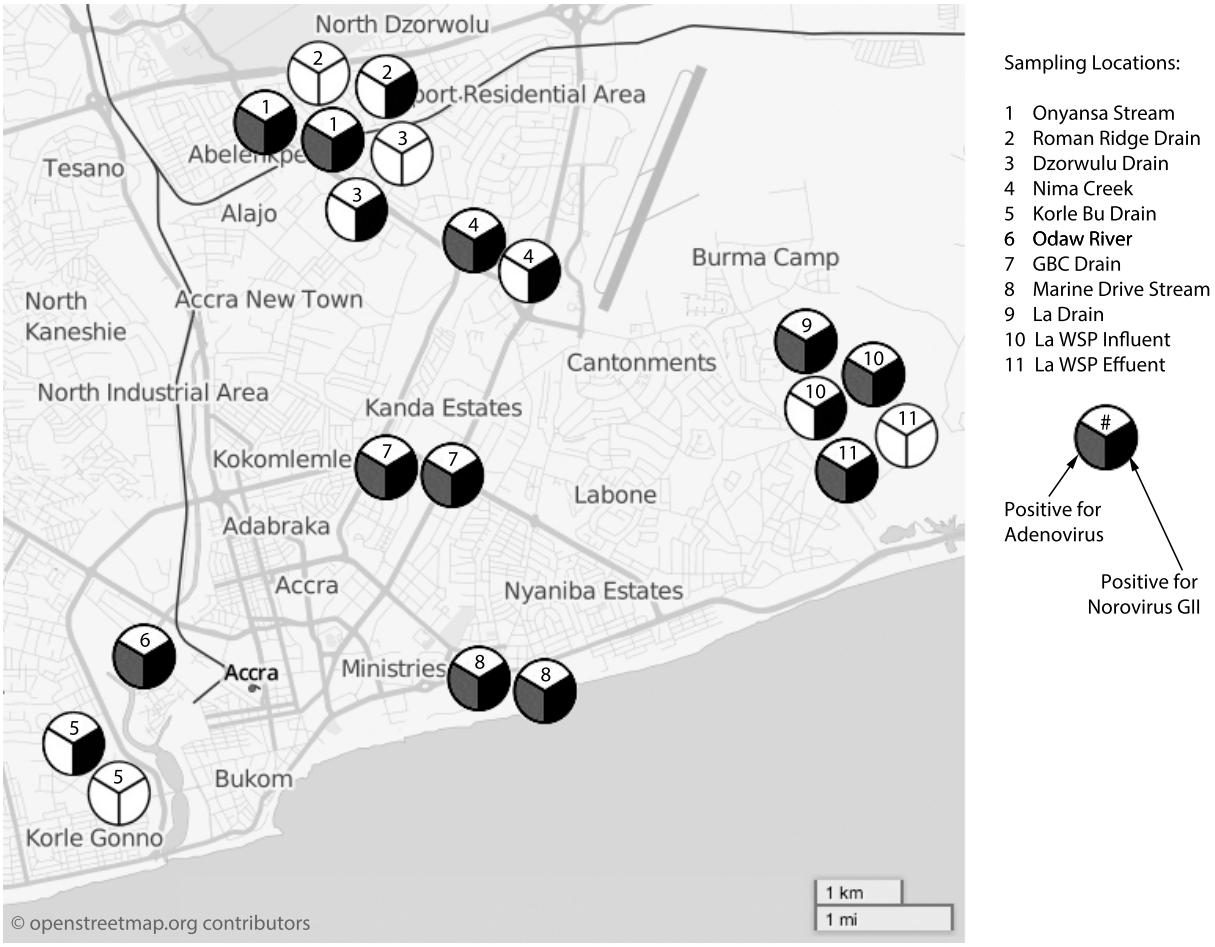

Figure 5.3. Location of samples positive for human adenoviruses and norovirus GII.

human-specific *Bacteroidales* were also classified as having poor DNA extraction/amplification efficiency. Measured human-specific *Bacteroidales* concentrations ranged from $(9.7 \pm 5.0) \times 10^2$ gene copies/100 mL in La WSP effluent to $(4.9 \pm 0.02) \times 10^6$ gene copies/100 mL in La drain water.

Negative controls that captured the entire analysis chain (from sample concentration to amplification), and no-template (RT-)qPCR amplification controls were negative.

Limitations. While (RT-)qPCR is a sensitive tool for the quantification of microorganisms, its limitations could result in an under- or overestimation of pathogen concentrations and health risks. (RT-)qPCR does not differentiate between infectious and non-infectious pathogens, and could overestimate the risk of infection presented by a particular organism. Conversely, the method employed to concentrate samples before extraction did not allow for the concentration of large volumes of water. This resulted in LOQs that were high compared to the infectious doses of the human virus targets: 18 virus particles for NV (Teunis et al., 2008), and unknown but

Table 5.3. Human-specific *Bacteroidales*, human adenovirus and norovirus GII concentrations. Concentrations listed as 'below the limit of detection (<LOD)' or 'positive, but below the limit of quantification (+BLOQ)' are followed, in parentheses, by the LOQ of that particular sample for that particular assay. Concentrations are listed as gene copies/100 mL. Recovery efficiency categories are as follows: – poor (<25%), + acceptable (25-50%), and ++ good (>50%)

Sample	Date	DNA Target Concentrations (gene copies/100 mL)			RNA Target Concentration (gene copies/100 mL)	
		Human-specific *Bacteroidales* (Mean ± SD)	Human Adenovirus (Mean ± SD)	Pph6 Recovery Efficiency	Human Norovirus GII (Mean ± SD)	MS2 Recovery Efficiency
Streams						
Marine Drive Stream	7/21/10	$3.58 \pm 0.36 \times 10^5$	$3.97 \pm 1.01 \times 10^2$	–	$4.48 \pm 2.35 \times 10^3$	++
	7/27/10	$5.86 \pm 0.11 \times 10^5$	$2.80 \pm 0.92 \times 10^2$	++	+BLOQ ($<6.26 \times 10^2$)	–
Odaw River	7/22/10	$3.64 \pm 0.17 \times 10^5$	$1.70 \pm 0.44 \times 10^4$	++	$2.62 \pm 0.14 \times 10^3$	++
Onyansa Steam	7/26/10	$1.50 \pm 0.06 \times 10^6$	$3.77 \pm 1.26 \times 10^2$	++	$1.04 \pm 0.47 \times 10^3$	++
	7/28/10	$1.27 \pm 0.04 \times 10^6$	$3.71 \pm 0.34 \times 10^2$	++	$2.18 \pm 0.58 \times 10^3$	++
Nima Creek	7/19/10	$2.28 \pm 0.26 \times 10^3$	+BLOQ (<27.2)	++	+BLOQ ($<3.13 \times 10^2$)	+
	8/02/10	<LOD ($<2.05 \times 10^2$)	<LOD (<35.3)	–	$4.75 \pm 2.20 \times 10^2$	++
Drains						
La Drain	7/21/10	$4.86 \pm 0.02 \times 10^6$	$2.06 \pm 0.48 \times 10^4$	+	$8.04 \pm 2.22 \times 10^3$	++
Korle Bu Drain	7/22/10	+BLOQ ($<1.02 \times 10^3$)	<LOD ($<1.77 \times 10^2$)	–	<LOD ($<1.88 \times 10^3$)	–
	7/28/10	$6.08 \pm 3.79 \times 10^3$	<LOD ($<1.77 \times 10^2$)	–	$2.01 \pm 1.46 \times 10^3$	+
GBC Drain	7/21/10	$2.82 \pm 0.61 \times 10^5$	+BLOQ ($<2.35 \times 10^2$)	–	$1.58 \pm 0.28 \times 10^4$	++
	7/28/10	$1.23 \pm 0.14 \times 10^5$	+BLOQ ($<1.18 \times 10^2$)	–	+BLOQ ($<1.25 \times 10^3$)	++
Roman Ridge Drain	7/20/10	+BLOQ ($<4.10 \times 10^2$)	<LOD (<70.6)	–	<LOD ($<7.51 \times 10^2$)	–
	7/26/10	$1.46 \pm 0.22 \times 10^5$	<LOD (<58.8)	–	$9.89 \pm 3.64 \times 10^2$	++
Dzorwulu Drain	7/20/10	+BLOQ ($<3.41 \times 10^2$)	<LOD (<58.8)	–	<LOD ($<6.26 \times 10^2$)	–
	7/26/10	+BLOQ ($<2.56 \times 10^2$)	<LOD (<44.1)	–	+BLOQ ($<4.69 \times 10^2$)	+
WSP						
La WSP Influent	7/21/10	$6.63 \pm 4.86 \times 10^3$	<LOD ($<1.18 \times 10^2$)	–	$4.39 \pm 0.63 \times 10^3$	+
	7/27/10	$2.75 \pm 0.11 \times 10^6$	$6.50 \pm 0.60 \times 10^4$	++	$1.26 \pm 0.56 \times 10^3$	+
La WSP Effluent	7/21/10	$6.29 \pm 1.27 \times 10^3$	<LOD (<39.2)	++	<LOD ($<4.17 \times 10^2$)	–
	7/27/10	$9.66 \pm 5.02 \times 10^2$	+BLOQ (<39.2)	–	+BLOQ ($<4.17 \times 10^2$)	+

assumed to be low for waterborne HAdV. Samples found to be <LOD could potentially contain virus concentrations capable of causing infection.

There are additional uncertainties in virus and human-specific *Bacteroidales* concentrations measured by (RT-)qPCR. We were unable to measure the efficiency of sample concentration in the field, and the extraction/amplification controls used in this study (pph6 and MS2) may not perfectly model extraction and amplification of the (RT-)qPCR targets. This is due to physical and chemical properties that can differ between microorganisms, and may be particularly different between pph6 and HAdV given that the size and structure of bacteria and viruses are quite different. Inefficient sample concentration would lead to *measured* virus concentrations that are less than *actual* concentrations in source waters; the use of measured virus concentrations in risk assessment could underestimate the health risks associated with using these waters for irrigation.

Pathogen concentrations in wastewater and the environment can vary both spatially and temporally depending on local conditions that include climate, weather, the health status of the population, the availability and condition of wastewater infrastructure, and the environmental fate and transport of a particular microorganism. This limitation may make generalization and extrapolation of study findings to wider contexts difficult.

Discussion

Water quality and the WHO Guidelines. The 2006 WHO Guidelines call for the use of QMRA to develop location-specific, health-based water quality standards for irrigation water. The Guidelines used an illustrative example, with rotavirus as an 'index' viral pathogen, to determine that an *E. coli* concentration of no more than 10^3/100 mL (for root crops) or 10^4/100 mL (for leaf crops) would meet the health-based target of no more than 10^{-6} disability-adjusted life years (DALYs) lost per person per year for farmers practicing wastewater irrigation. This recommendation was also deemed appropriate to protect the health of consumers of raw vegetables as long as post-water treatment control measures (such as the use of drip irrigation, pathogen die-off in the field, and vegetable washing and disinfection) are employed. While Seidu et al. (2008) employed QMRA to determine health risks associated with wastewater irrigation in Accra (using measured fecal coliform concentrations and an assumed ratio between concentrations of fecal coliform and rotavirus), QMRA has not yet been conducted with actual virus concentrations measured in Accra, nor has it been used to establish Accra- or Ghana-specific health-based water quality standards.

None of the irrigation water samples analyzed in this study met the water quality standards suggested by the 2006 WHO Guidelines (Figure 5.2): all samples contained *E. coli* concentrations greater than 10^4/100 mL, with some samples (La, Korle Bu, and GBC drains) containing *E. coli* concentrations over three orders of magnitude higher than this limit. Additionally, thermotolerant coliform concentrations in all samples greatly exceeded the limit of 10^3 thermotolerant coliforms/100 mL set by the 1989 WHO Guidelines for irrigation of vegetables that could be eaten raw (WHO 1989). Similar results were found by Mensah et al. (2001), Keraita et al. (2003) and Amoah et al. (2005). Amoah et al. (2005) analyzed irrigation

water samples collected from streams and drains in Accra and Kumasi, Ghana over the course of a year and found all but two samples to have fecal coliform concentrations that exceeded the 1989 WHO Guidelines, despite considerable variation over time.

A challenge with the use of the fecal indicator bacteria *E. coli*, enterococci and thermotolerant coliforms is that they can have animal fecal sources as well as environmental sources and reservoirs. While FIB have been observed to multiply in tropical environments (Field and Samadpour 2007 and ref. within), bacteria in the order *Bacteroidales* are strict anaerobes, and are less likely to grow outside human and animal hosts (Kreader 1995; Kildare et al. 2007; Walters and Field 2009). The molecular marker BacHum was designed to detect human-specific *Bacteroidales* (Kildare et al. 2007), however some cross-reactivity with animal feces has been observed (Kildare et al. 2007; Silkie and Nelson 2009). All but one sample contained detectable levels of human-specific *Bacteroidales*, an indication that the water sources sampled were contaminated with human feces. While one of the Nima Creek samples had a human-specific *Bacteroidales* concentration <LOD, this sample had poor DNA extraction/amplification efficiency and contained $(4.75 \pm 2.20) \times 10^2$ NV-GII gene copies/100 mL, indicating that this water source also had human fecal contamination. Overall, the BacHum qPCR target was a sensitive marker for sewage, similar to studies conducted in California (Kildare et al. 2007; Silkie and Nelson 2009), but different from that of Jenkins et al. (2009) who found limited sensitivity of the BacHum qPCR target to detect human-specific *Bacteroidales* in human feces and sewage in Kenya. The levels of BacHum in Accra samples ranged from $<10^{2.3}$ to $10^{6.7}$ gene copies/100 mL, which is lower than the concentrations reported for sewage samples in California: $10^{8.0}$–$10^{9.8}$ gene copies/100 mL (Silkie and Nelson 2009) and $10^{7.8}$–$10^{9.9}$ gene copies/100 mL (Van De Werfhorst et al. 2011). One reason for the lower concentrations is that the Accra samples were likely more diluted than pure sewage, as the concentrations of culturable *E. coli* were also lower in Accra samples: $10^{4.2}$–$10^{7.5}$ CFU/100 mL compared to $10^{6.1}$–$10^{6.8}$ MPN/100 mL observed in Californian sewage (Silkie and Nelson 2009). Lower BacHum concentrations in Accra could also be attributed to a lower concentration of the BacHum target in human feces in Accra than in California, or to DNA extraction/amplification efficiencies less than 100%.

The greatest indicator organism concentrations were observed in the La, Korle Bu and GBC drains. Some drains, like the Roman Ridge and Dzorwulu drains, were likely built to channel greywater and stormwater, not untreated sewage; however, given the presence of human-specific *Bacteroidales* and NV-GII, it is likely that untreated human waste was discharged into these drains as well. The streams sampled as part of this study also contained human-specific *Bacteroidales* and human viruses, highlighting the fact that, in Accra, many streams act as de facto drains.

Samples were collected from the inlet and outlet of a WSP on the La Fulani farm site. WSPs remove microorganisms from wastewater through sedimentation, predation, competition, and sunlight inactivation, with sunlight inactivation playing an important role (Curtis et al. 1992; Davies-Colley et al. 1999, 2000; Shilton 2005; Sinton et al. 2002). Although we had a limited sample size for evaluating the La WSP ($n = 2$), microorganism concentrations were observed to decrease between the WSP influent and effluent – measured *E. coli*, enterococci, thermotolerant coliform, somatic and F+ coliphage concentrations decreased by 2.5, 3.3, 1.6, 3.1 and <1 log, respectively – and water samples collected at the outlet of the La WSP had lower concentrations

of *E. coli*, enterococci, thermotolerant coliform and somatic coliphage than other water sources. However, La WSP effluent still did not meet the WHO recommended limit for *E. coli* in irrigation water. Additionally, we observed little reduction in F+ coliphage concentrations between the WSP inlet and outlet, possibly due to slower rates of F+RNA coliphage inactivation than the other organisms in sunlit WSP water (Sinton et al. 2002). Viruses have different rates of sunlight inactivation depending on their composition and structure (Love et al. 2010; Silverman et al. 2013a) and, generally, have slower inactivation rates than bacteria. The WHO Guidelines include WSPs on the list of health protection measures that can be used to achieve water quality targets. While bacteria, and some virus, removal occurred in the WSP, additional treatment would be required to meet WHO recommended bacteria levels and remove or inactivate persistent viruses.

Correlation between indicator organisms. Log concentrations of indicator organisms were compared to determine correlations between them. *E. coli* was generally correlated with enterococci and somatic coliphage (n = 20; R^2 = 0.97 and 0.89, respectively), and less so with thermotolerant coliform and F+ coliphage (n = 20 and 17; R^2 = 0.68 and 0.62, respectively). R^2 between enterococci and somatic coliphage log concentrations was 0.91 (n = 20). Thermotolerant coliform and F+ coliphage were the least correlated with other fecal indicators (Table 5.4).

When looking at correlation charts between F+ coliphage and *E. coli*, enterococci and somatic coliphage, the most apparent outlying points are those sampled from the La WSP effluent (circled in Figure 5.4). The outlying points could be caused by the longer persistence of F+ coliphage in WSP (as compared to FIB and somatic coliphage), which would result in higher relative concentrations of F+ coliphage in WSP effluent than in fresher wastewater. When the La WSP effluent samples are removed from analysis, the correlation coefficients between F+ coliphage and *E. coli*, enterococci and somatic coliphage increase to 0.82, 0.74 and 0.66, respectively. These results serve as a reminder that when making comparisons between microorganism concentrations, it is important to consider the environmental conditions and processes the samples have been exposed to, as fate and transport in the environment can differ among organisms.

Table 5.4. R^2 between microorganism log concentrations (n = 20 for all except n = 17 for those with F+ coliphage). Values in parentheses in F+ coliphage column are R^2 values determined with the exclusion of La WSP effluent samples.

	E. coli (chromocult agar)	**Enterococci**	**Somatic Coliphage**	**Thermotolerant Coliform**	**F+ Coliphage**
E. coli (mI agar)	0.99	0.97	0.89	0.68	0.62 (0.82)
E. coli (chromocult agar)		0.96	0.88	0.68	0.64 (0.83)
Enterococci			0.91	0.67	0.58 (0.74)
Somatic Coliphage				0.69	0.43 (0.66)
Thermotolerant coliform					0.46 (0.49)

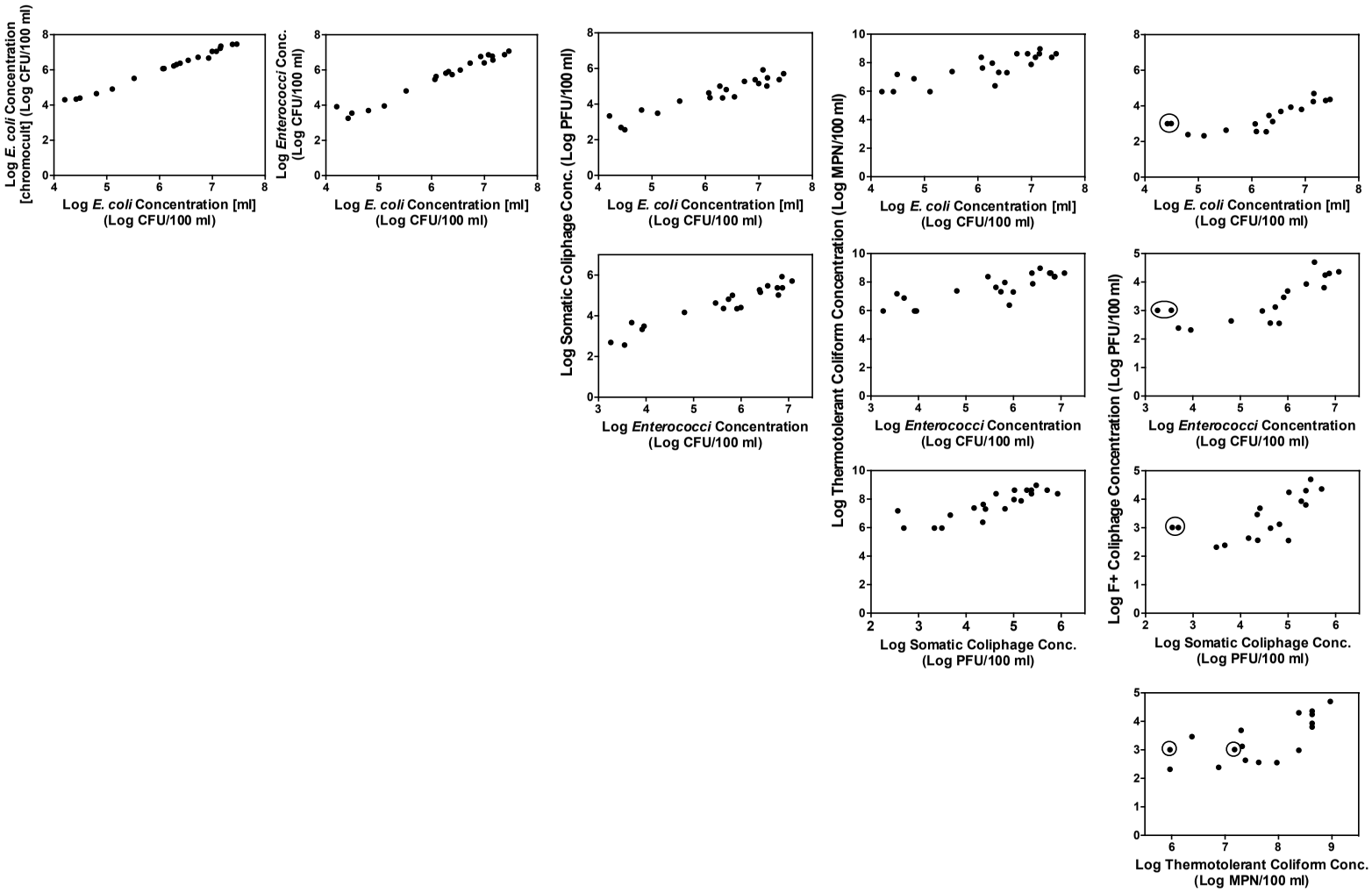

Figure 5.4. Correlation between microorganism log concentrations. Data points circled in the rightmost column correspond to La WSP effluent samples.

QMRA assumptions: the ratio between norovirus and E. coli. The 2006 WHO Guidelines employed rotavirus as an index organism for QMRA used to make recommendations for health-based water quality standards. However, with the generation of dose-response data for norovirus (Teunis et al. 2008), some [including Mara and Sleigh (2010) and Mara et al. (2010)] have called for the use of norovirus in these models. While norovirus and rotavirus are both highly infectious, norovirus is frequently associated with food and waterborne outbreaks and is capable of infecting people of all ages (Widdowson et al. 2005), whereas rotavirus predominantly infects children under the age of five.

As viruses are not regularly quantified in water samples, QMRA models frequently employ assumptions of virus concentration based on the concentration of FIB. Shuval et al. (1997), Seidu et al. (2008), and the 2006 WHO Guidelines used the assumption that wastewater contains 0.1–1 rotavirus particles per 10^5 fecal coliforms based on work by Schwartzbrod (1995), who employed a literature review to determine that enteric viruses exist in untreated wastewater at concentrations ranging from 10^2 to 10^3 PFU/L. The majority of studies cited by Schwartzbrod were conducted in the United States and Europe. Mara et al. (2007) used an assumption of 0.1–1 rotavirus particles per 10^5 *E. coli* with the reasoning that *E. coli* is a better indicator of fecal contamination; Mara et al. (2007) also cited work by Oragui et al. (1986) in northeastern Brazil, though this publication measured concentrations of fecal coliform, not *E. coli*, and found a ratio of four rotaviruses per 10^5 fecal coliforms in raw wastewater. In recent QMRA modeling, Mara and Sleigh (2010) and Mara et al. (2010) assumed a ratio of 0.1–1 noroviruses per 10^5 *E. coli*, a ratio likely carried over from the rotavirus assumption and lack of other information on norovirus concentrations.

In the present study, in samples with quantifiable concentrations of NV-GII, we found an average of one NV-GII per $10^{3.2\pm1.1}$ *E. coli* or $10^{4.8\pm1.0}$ thermotolerant coliform ($10^{\text{mean}\pm95\%\text{ confidence interval}}$; $n = 11$). Samples that did not have quantifiable NV-GII concentrations include five that had poor RNA extraction/amplification efficiency and three that had low concentrations of *E. coli*, which would correspond to NV-GII concentrations below the LOQ; one sample (GBC drain) had good extraction/amplification efficiency and a sufficiently high concentration of *E. coli*, but did not contain a quantifiable NV-GII concentration. The NV-GII to thermotolerant coliform ratio found here is similar to the rotavirus to fecal coliform ratio used previously (Shuval et al. 1997; Seidu et al. 2008; WHO 2006); however, our NV-GII to *E. coli* ratio is larger than the norovirus to *E. coli* ratio assumed in recent publications (Mara and Sleigh 2010; Mara et al. 2010). The larger NV-GII to *E. coli* ratio could be attributed to (1) the use of *E. coli* instead of thermotolerant coliform in the ratio, since thermotolerant coliform concentrations are usually greater than those for *E. coli*, (2) a difference in the number of norovirus infections at the time of sample collection, or, (3) the virus quantification method employed. Virus concentrations determined through (RT-)qPCR are greater than those determined by culture based methods, because total particle to PFU ratios can range from 100–1000 to 1 (Flint et al. 2004). Given that no fully permissive cell culture system for norovirus exists at present, norovirus must be measured by RT-qPCR or direct particle count. The use of RT-qPCR to quantify norovirus and membrane filtration to quantify *E. coli* could be preferred in this context given that RT-qPCR was used to quantify norovirus used in dose-response work (Teunis et al. 2008), and membrane filtration is regularly used to quantify *E. coli* in environmental samples. Although there are uncertainties surrounding the use of RT-qPCR in norovirus quantification – such as the exclusion of norovirus genogroup I from analysis, and imperfect sample concentration, RNA extraction,

and amplification – any correction of these limitations would act to further increase the norovirus to *E. coli* ratio.

As discussed above, pathogen concentrations, and the ratios between pathogens and fecal indicator organisms, can change spatially and temporally depending on local conditions. While the ratio of NV-GII to *E. coli* or thermotolerant coliform is likely to differ over place and time, it is an important finding that the current assumption of 0.1–1 norovirus particles per 10^5 *E. coli* would underestimate virus dose with exposure to the wastewater and surface waters sampled in Accra by approximately 2–3 orders of magnitude. The use of the NV-GII to *E. coli* ratio determined in the present study would result in a higher estimate of health risk.

The ratios of HAdV to fecal indicator bacteria were similar to those of NV-GII, but more variable. The ratio of HAdV to *E. coli* was one to $10^{3.2\pm1.7}$ and the ratio of HAdV to thermotolerant coliform was one to $10^{4.6\pm2.0}$ ($10^{\text{mean}\pm95\%\text{ confidence interval}}$; $n = 7$).

Conclusion

No water sources sampled as part of this study met water quality criteria recommended by either the 1989 or 2006 WHO Guidelines, and all but one contained detectable concentrations of human-specific *Bacteroidales*, suggesting human fecal contamination. NV-GII was detected in 16/20 samples and HAdV in 11/20 samples. Given that wastewater irrigation can be beneficial to farmers and municipalities, it is unlikely, and potentially inadvisable, for water reuse in agriculture to cease. Instead, health risks should be addressed by treating wastewater before use on farms. The 2006 WHO Guidelines suggest the use of the 'multi-barrier approach' to reduce microbial contamination from 'farm to fork'; this approach can utilize measures such as WSPs, on-farm wastewater treatment ponds (Keraita et al. 2008a; Amoah et al. 2011) and produce disinfection (Amoah et al. 2011). While the La WSP reduced concentrations of indicator microorganisms, the WSP effluent did not meet WHO recommended limits, highlighting the importance of multiple barriers.

As the WHO Guidelines and QMRA models are implemented and updated, it is important to have reasonable estimates of virus concentrations to use as inputs to these models. In the present study we found an average of one NV-GII per $10^{3.2\pm1.1}$ *E. coli*. While this ratio is expected to vary depending on local conditions, such as the health status of the contributing population, it could be used to calculate an informed estimate of virus concentration for modeling health risks associated with wastewater irrigation in Accra.

Chapter 6

On-farm treatment of wastewater used for vegetable irrigation: bacteria and virus removal in small ponds in Accra, Ghana

Introduction

Urban agriculture in Ghana's capital city, Accra, is an important example of wastewater-irrigated agriculture practiced on a wide scale. Due to limited financial resources, maintenance, institutional capacity, and accountability, the majority of wastewater treatment facilities in the city are not in operation (Murray and Drechsel 2011). As a result, untreated greywater and sewage (collectively 'wastewater') flow directly and indirectly into open drains and streams, which are the primary sources of water used by farmers in Accra to irrigate vegetables. Irrigation waters used by urban farmers in Ghana contain fecal indicator bacteria concentrations that exceed the limit suggested by the World Health Organization (WHO) for the use of wastewater in agriculture (Mensah et al. 2001; Keraita et al. 2003; Amoah et al. 2005), as well as human viruses at concentrations that present health risks (Silverman et al. 2013b). Wastewater irrigation can be beneficial for both farmers and municipalities (Drechsel et al. 2006; Lydecker and Drechsel 2010), and on-farm wastewater treatment has been suggested as a way to reduce health risks associated with the practice (Keraita et al. 2008a; WHO 2006; Cofie et al. 2010).

A common method of irrigation in Accra is manual watering with watering cans. In an effort to shorten the distance that water must be carried between the water source and crop bed, many farmers in Accra dig small reservoirs adjacent to their farm plots (volumes ranging from 0.5 to 12 m^3) into which they pump and store irrigation water (Drechsel et al. 2006; Keraita et al. 2008a; Reymond et al. 2009); it is from these small ponds that farmers fill watering cans (a typical on-farm pond is shown in Figure 6.1). Keraita et al. (2008a) and Reymond et al. (2009) reported that on-farm ponds in Ghana reduced thermotolerant coliform and helminth egg concentrations, leading some to suggest that small on-farm ponds (Cofie et al. 2010) be included as a component of the WHO's multi-barrier approach to reduce health risks associated with wastewater irrigation (WHO 2006). Similar to larger waste stabilization ponds (WSP) that are designed to treat wastewater at a low cost and with minimal maintenance, it is hypothesized that small ponds reduce pathogen and fecal indicator organism concentrations through predation, sedimentation, and inactivation by sunlight-mediated processes (Mayo 1995; Davies-Colley 2005).

This study builds upon research by Keraita et al. (2008a) and Reymond et al. (2009) by investigating the reduction in concentration of two additional groups of fecal indicator bacteria (*E. coli* and enterococci) and two viral indicators (somatic and F+ coliphage) in a typical on-farm pond in Accra. The goals of this study were to: (1) better understand the factors that influence bacteria and virus removal within the pond; and (2) determine microorganism inactivation rates. Based on the results of this and previous studies, we provide recommendations for possible operating schemes for on-farm treatment ponds.

Figure 6.1. A farmer using watering cans to collect irrigation water from a typical small, on-farm pond.

Methods

Experimental design and sampling. Two independent experiments were conducted with slightly different sampling methodology. Both experiments were conducted using a farmer-dug pond located on an urban farm in Accra's Airport Residential neighborhood. The experimental pond was typical of those used by urban farmers in Ghana (Keraita et al. 2008a; Reymond et al. 2009). The pond was approximately 3 m in diameter by 0.5 m deep, and was used regularly by farmers to store irrigation water; a pond of this size can hold approximately three days of irrigation water. The pond was filled the night before experiments began with stream water augmented with effluent from a nearby, non-functioning wastewater treatment facility (approximately 3.5% of pond volume). Pond water sat undisturbed for 12 h prior to the start of experiments, during which time viruses and bacteria associated with large particles may have settled out of the water column. Each experiment was conducted over the course of three days. The pond had no inlet or outlet, was operated as a batch reactor with no manual mixing, and farmers did not collect water from the pond during the course of the experiments.

In Experiment 1, samples were collected from two regions of the pond – an open water region and a dark column – and at two depths in each: 10 cm below the pond surface (shallow samples) and 10 cm above the pond sediment (deep samples); a diagram of the pond and sampling locations is presented in Figure 6.2. The dark column consisted of a covered, 40-cm

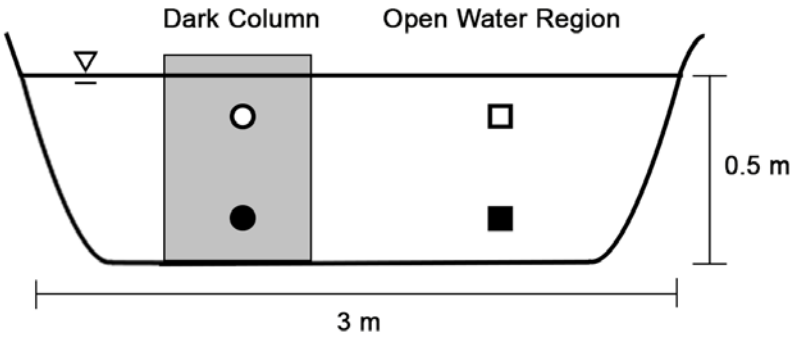

Figure 6.2. Diagram of the small, on-farm pond used for experiments. Open and closed symbols indicate shallow and deep water sampling locations, respectively.

diameter pipe inserted into the pond to create a column of water with the same characteristics as the rest of the pond, but without exposure to sunlight. Dark control samples collected from the dark column were analyzed to help distinguish mechanisms of bacteria and virus removal: the dark column eliminated the potential for sunlight-mediated inactivation, but retained the possibility of removal due to sedimentation and predation; however, there is a possibility that conditions in the dark column were not exactly the same as those in the rest of the pond (e.g., temperature, mixing, and the effect of air movement above the pond) and could have potentially enhanced sedimentation compared to the rest of the pond. Deep water samples were collected using sampling ports installed in the pond, which consisted of L-shaped plastic pipes that allowed water collection at a consistent depth without disruption of pond stratification. The top of the sampling ports extended out of the top of the pond to allow for the insertion of sampling tubes, and the bottom was located 10 cm above the bottom of the pond. The dark column and sample ports were installed after filling the pond. The sunlit region of the pond was sampled every four hours starting at sunrise and ending at sunset (at 06:00, 10:00, 14:00, and 18:00). The dark column was sampled at 06:00 and 18:00. Samples were collected using a hand-operated vacuum pump connected to sterile PVC tubing and polypropylene collection bottles; two tube volumes were pumped and discarded before collecting each sample.

In Experiment 2, water was collected from the pond in a manner that sampled the entire water column, and there was no dark column. A bucket was sterilized with 70% ethanol, wiped dry and rinsed with pond water before use. The bucket was used to scoop water from the pond, with an effort made to not resuspend sediments. Samples were poured into acid-washed, opaque, plastic cubitainers for transport.

For both experiments, samples were placed on ice in the dark, transported to the lab and analyzed immediately. A negative control consisting of sterile deionized water was analyzed each day for all microbiological assays.

Bacteria analyses. All water samples were analyzed for *E. coli* and enterococci concentrations by membrane filtration with 47-mm diameter, 0.45-μm pore size, mixed cellulose ester HA filters (Millipore). *E. coli* concentrations were quantified by plating filters on mI agar (BD) and incubating for 24 h at 37 °C. Enterococci concentrations were quantified by plating filters on mEI agar (BD) and incubating for 24 h at 41 °C. *E. coli* and enterococci plates were enumerated as colony forming units (CFU).

Coliphage analyses. Water samples collected at 06:00 and 18:00 during Experiment 1 were concentrated for coliphage enumeration using membrane filtration with 47-mm diameter, 0.45-μm pore size, mixed cellulose ester HA filters. Before filtration, water samples were amended with $MgCl_2$ (0.05 M final concentration) and held for 5 min to facilitate virus adsorption to filters (Lukasik et al. 2000). Between 15 and 150 mL of sample was filtered, depending on water turbidity and filter clogging. Filters were preserved until elution by freezing at -20 °C on 300 μL of 50% glycerol [1:1 vol/vol with phosphate buffered saline (PBS)].

Coliphage were eluted from filters by adding 3% Beef Extract (pH 9; 30 g/L Beef Extract, 30 mL/L Tween 80, 0.3 M NaCl) and swirling for 10 min. Filter eluent was assayed for coliphage using the double agar layer (DAL) method with 100-μL and 1-mL sample inoculums, a modified Luria Bertani (LB) top agar (0.75% wt/vol) and bottom agar (1.5% wt/vol), and appropriate hosts and antibiotics. F+ coliphage were assayed using *E. coli* F_{amp} host bacteria with ampicillin and streptomycin antibiotics (0.0015 g/L of each); somatic coliphage were assayed using *E. coli* CN13 host with nalidixic acid (0.01 g/L). Modified LB consists of: bacto agar (0.75% or 1.5% wt/vol; BD), 10 g/L bacto tryptone (BD), 0.137 M NaCl, 1 g/L yeast extract (EMD Chemicals), 0.0055 M dextrose (EMD Chemicals), 0.002 M $CaCl_2$ (Fisher Scientific). Eluted filters were plated, face down, on top agar augmented with 0.3% Tween 80. Plates were incubated at 37 ºC for 18–24 h and enumerated as plaque forming units (PFUs). Total phage concentrations were calculated by adding counts from the DAL and filter plates. Coliphage samples were concentrated and plated in duplicate.

Environmental parameters. Total UVB irradiance (280-320 nm) was measured every 15 to 30 min during daylight hours using a hand-held meter (Solartech, Inc.); total daily UVB fluence was calculated by taking the sum of UVB irradiance multiplied by the time between measurements. Pond water absorbance was measured at the beginning of the experiment using a UV-visible spectrophotometer (Jenway model 6705 spectrophotometer); absorbance was measured at 280, 300, 320, 360, 400, 550 and 700 nm wavelengths. The depth of 99% light attenuation at each wavelength was calculated using the Beer-Lambert law.

Data analysis. First-order, observed inactivation rate constants (k_{obs}) for each organism and sampling location were calculated for each day between the hours of 06:00 and 18:00. k_{obs} was calculated as the negative slope of the linear regression trend line of $\ln(C_t/C_0)$ versus time. Bacteria k_{obs} values for inactivation in the sunlit region of the pond were calculated using four data points, while dark k_{obs} were calculated using two data points. Average k_{obs} over the course of an experiment were calculated as the mean of three daily k_{obs}. Statistical analysis and graphs were made using GraphPad Prism (v6.0c)

Results and Discussion

Environmental and pond water characteristics. Experiments were conducted during the rainy season in southern Ghana (August 2010 and September 2011), however there was no precipitation during experiments; cloud cover ranged from partly cloudy to overcast. UVB irradiation measured at the pond surface is presented in Figure 6.6. Pond water was green in color and pond pH increased from an average of 7.9 at 06:00 to an average of 9.6 at 14:00, indicating high rates of photosynthesis by algae. Absorbance measurements indicated that the pond water attenuated light: 99% of 300 and 550 nm light was attenuated at depths of 2.9 and 7.4 cm, respectively (Figure 6.3).

Bacteria removal. In Experiment 1, bacteria concentrations were observed to decrease faster in the open water region than in the dark column (Figure 6.4). The overall decrease in concentration of bacteria in the open pond over the course of three days in Experiment 1 was 1.7 log for *E. coli* and 1.8 log for enterococci. Overall bacteria removal in the dark column was 0.95 log for *E. coli* and 1.1 log for enterococci, which account for only 20% of the bacteria removal observed in the sunlit section of the pond. Little bacteria removal occurred in the dark column until the third day and night. The dark column was designed to allow sedimentation to occur, but not sunlight exposure; enhanced rates of bacteria removal in the open water region are attributed to sunlight inactivation, while all bacteria removal in the dark column is attributed to dark processes such as predation, sedimentation, and loss of viability due to environmental stress.

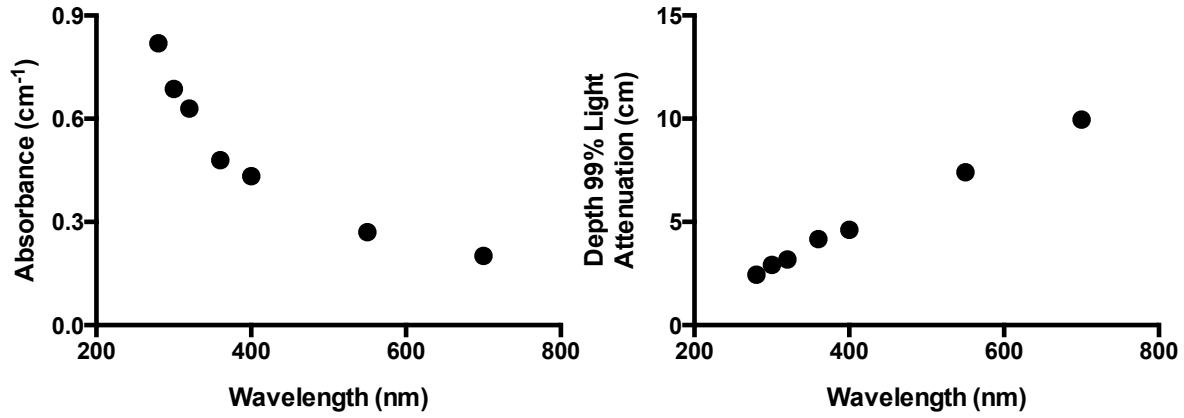

Figure 6.3. Pond water absorbance and depths of 99% light attenuation.

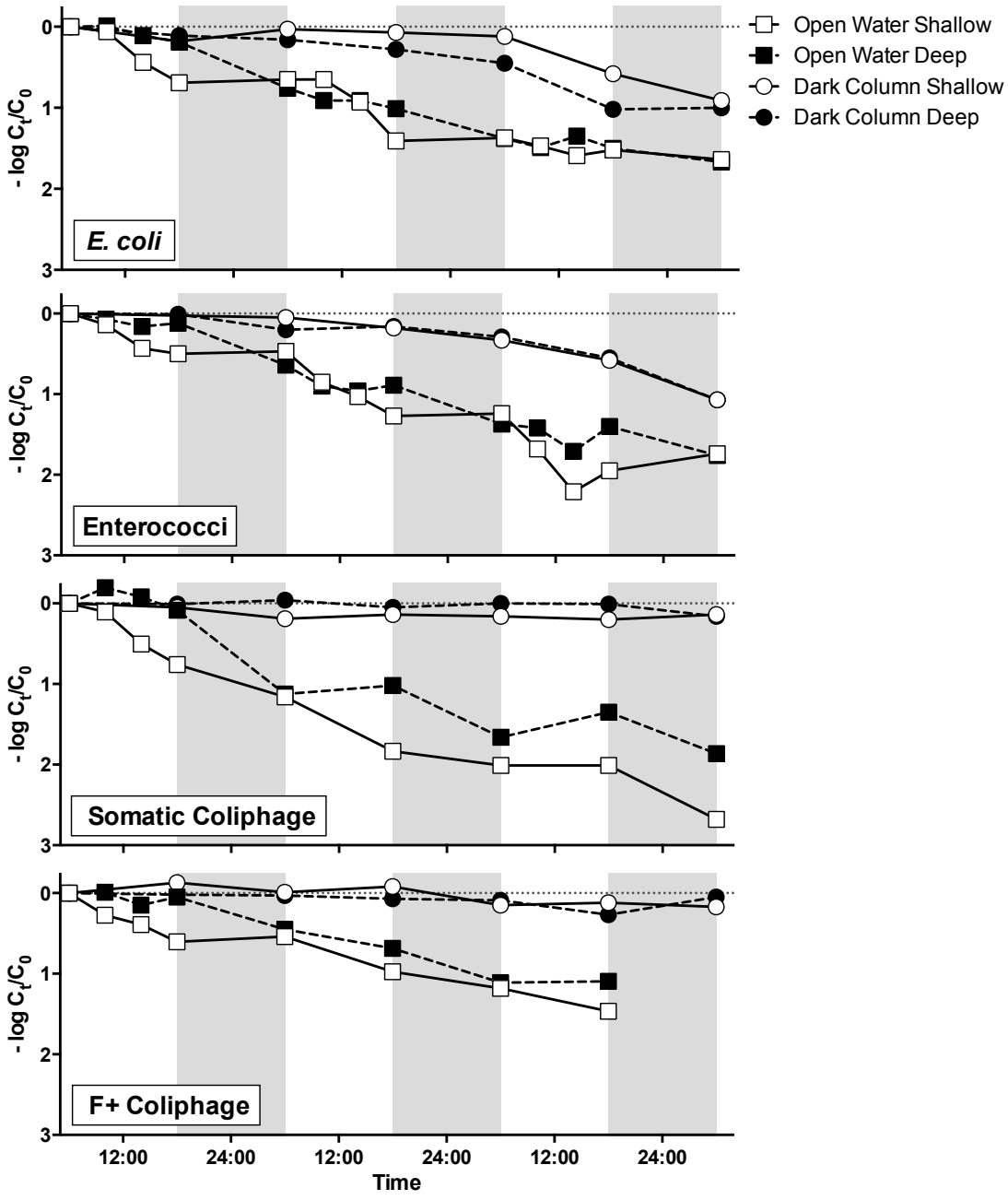

Figure 6.4. Microorganism concentrations measured in the shallow and deep regions of the open pond and dark column during Experiment 1. Shaded areas represent nighttime.

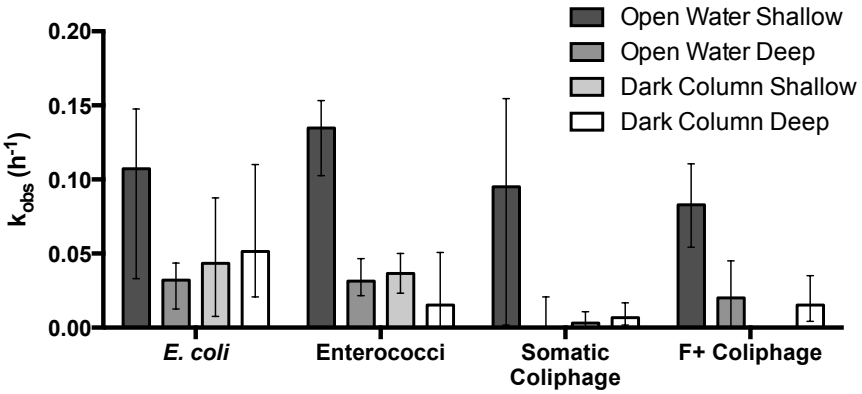

Figure 6.5. Average daytime k_{obs} (h^{-1}) at each sample location during Experiment 1 (n = 3). k_{obs} were measured between the hours of 6:00 and 18:00. Error bars indicate the range of k_{obs} values.

While the *overall* rates of inactivation observed in the shallow and deep portions of the open water region were similar, the trend during daylight hours was different at the two depths (Figures 6.4 and 6.5). For the shallow samples, the greatest decrease in bacteria concentrations occurred during the day, with little to no decrease at night. For the deep samples, the decrease in bacteria concentrations was slower during the day than in the shallow samples, followed by an additional decrease overnight. The most likely explanation for these trends is that the pond was thermally stratified during the day, followed by whole pond mixing overnight. Water sampled from the top and bottom of the pond had different colors and smells in the afternoon, suggesting stratification. During the day, a combination of light attenuation and thermal stratification may have confined sunlight disinfection to the top layer of the water column; similar results have been observed in larger scale WSP by Mayo (1989; 1995). At night, the apparent inactivation in the deep samples may have been a result of deep water mixing with shallow water that contained lower bacteria concentrations; the fact that the bacteria concentrations at the top and bottom of the water column at 06:00 were similar supports this explanation.

The effect of sunlight was also observed when comparing the inactivation rates reported above with those from Experiment 2, which was conducted during a period with greater insolation (Figure 6.6). There was more bacterial inactivation during the second experiment, with an overall 3.2-log and 2.7-log reduction of *E. coli* and enterococci, respectively, over the course of the three-day experiment. After pooling data from both experiments, a correlation was observed between the *E. coli* and enterococci k_{obs} measured each day between 06:00 and 18:00 (average of sunlit shallow and deep inactivation rates for Experiment 1 data) and that day's total UVB fluence (Figures 6.7A and B; R^2 = 0.94 for *E. coli* and 0.79 for enterococci, n = 6). Note that in the relationships between k_{obs} and total daily UVB fluence, an approximate 40% increase in UVB fluence lead to an approximate 10-fold increase in k_{obs}. If inactivation was due to direct sunlight inactivation mechanisms alone we would assume that a two-fold increase in UVB

fluence would result in a two-fold increase in k_{obs}. However, ponds are complicated systems, and one hypothesis as to why we observed a greater increase in k_{obs} is that indirect sunlight inactivation mechanisms or other sunlight-mediated processes added to bacteria inactivation; for example, greater sunlight intensity would result in higher water temperatures, a greater concentration of reactive intermediates, and higher pH and greater dissolved oxygen concentrations in algae-laden waters, all of which could affect *E. coli* and enterococci k_{obs} (Kadir and Nelson 2013; Davies-Colley et al. 1999). Solar irradiance changes throughout the year. The total daily UVB fluence (i.e., UVB irradiance integrated over time) for the 21st day of

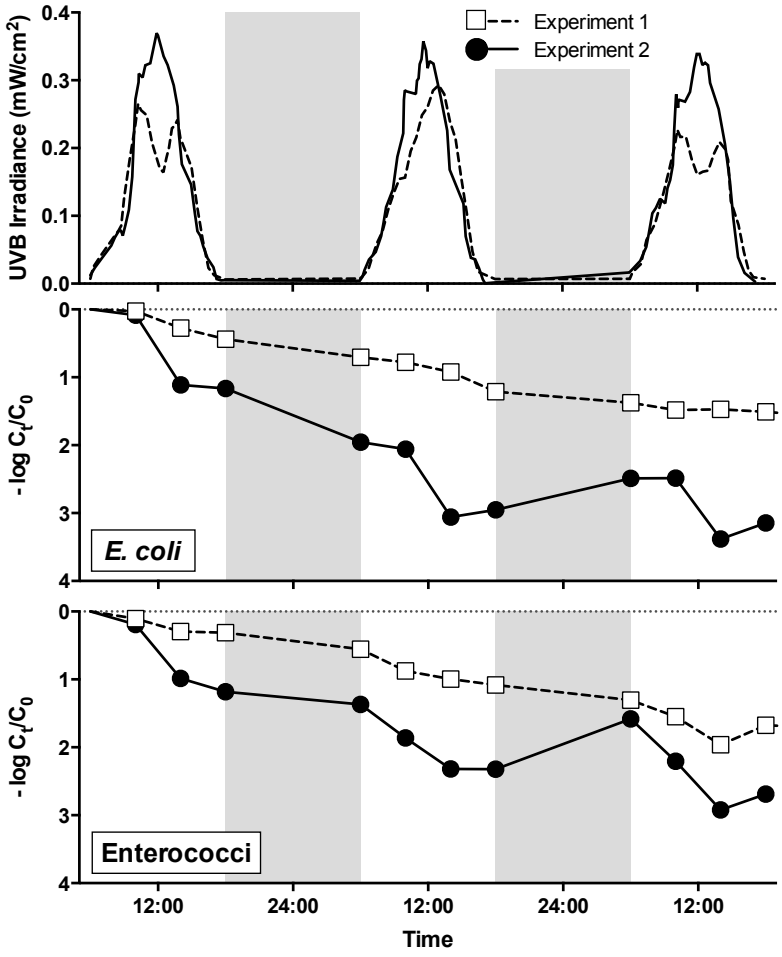

Figure 6.6. Comparison of sunlight UVB irradiance and *E. coli* and enterococci inactivation during two independent experiments. Experiment 1 (data also presented in Figure 3) is denoted by a dotted line and open squares, and represents the average of inactivation data from the shallow and deep sunlit regions of the pond. Experiment 2 is denoted by a solid line and filled circles.

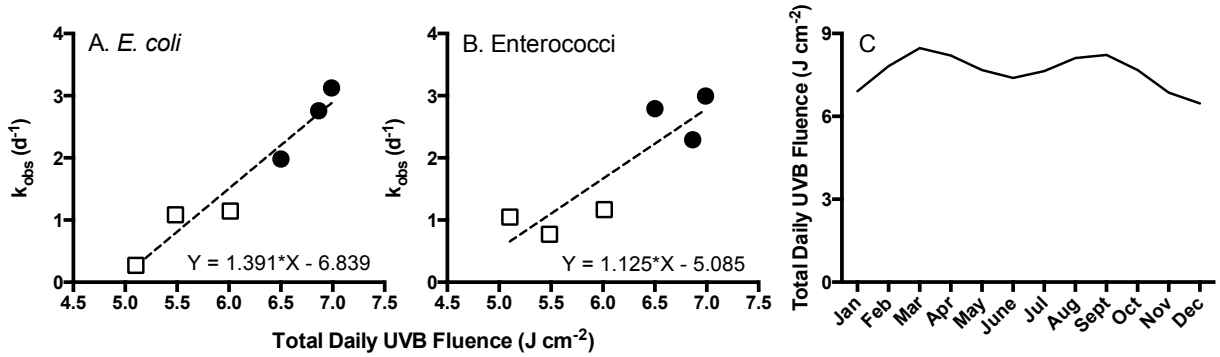

Figure 6.7. A and B: Daytime k_{obs} (measured between 6:00 and 18:00) plotted versus total UVB fluence measured on that day. Each point represents data obtained on one day; data is from Experiments 1 (white squares) and 2 (black circles). *E. coli* $R^2 = 0.94$; enterococci $R^2 = 0.79$. C: Total UVB fluence predicted for the 21st day of each month by the SMARTS radiative transfer model (Gueymard 2005).

each month in Accra under clear sky conditions is presented in Figure 6.7C; hourly irradiance spectra were predicted by the SMARTs radiative transfer model (Gueymard 2005) as global horizontal irradiance. Under clear sky conditions, inactivation rates would be highest in March and September, and lowest in December and June; however other climatic conditions, such as cloud cover, air pollution and atmospheric dust (e.g., from the seasonal Harmattan wind), also act to decrease irradiance and therefore microorganism inactivation.

Keraita et al. (2008a) studied fecal coliform removal from small farmer-dug farms in Kumasi, Ghana and found an average k_{obs} of 1.6 d^{-1} during the first six days of treatment during the dry season. This value falls within the two, three-day average *E. coli* k_{obs} measured in the present study: 1.5 and 2.8 d^{-1} [calculated as the negative slope of $\ln(C_t/C_o)$ versus time (d^{-1}) using all *E. coli* data points for each three day experiment; Experiment 1 combined $\ln(C_t/C_o)$ data from the top and bottom of the pond]. Keraita et al. (2008a) also found more inactivation in the dry season than the wet season, which they attributed to greater insolation during the dry season.

In a review of 186 full-size WSP, von Sperling (2005) found a median range (25–75 percentile) of overall coliform removal of 1.4–2.3 log units for primary facultative ponds and 0.5–1.7 log units for maturation ponds. The overall reductions in *E. coli* concentration observed in the present study were 1.7 and 3.2 log units for Experiments 1 and 2, respectively, which fall within and exceed the range for primary facultative ponds (the influent water quality of the experimental ponds more closely resembles that of a primary facultative pond than a maturation pond). It is difficult to compare k_{obs} between large and small ponds because larger facultative ponds have hydraulic residence times (HRT) on the order of weeks (Shilton and Walmsley 2005), as compared to three days for the on-farm ponds, which would result in much lower average k_{obs} for facultative ponds. Faster inactivation rates in the smaller on-farm ponds are

likely due to shallower depth and operation as batch reactors, which have more efficient kinetics than completely mixed flow reactors such as conventional WSPs.

The 2006 WHO Guidelines for the safe use of wastewater, excreta and greywater in agriculture recommend that irrigation water contain no more than 10^3 *E. coli*/100 mL for the irrigation of root crops and 10^4 *E. coli*/100 mL for the irrigation of leafy crops (WHO 2006). The ability of small ponds to disinfect contaminated irrigation water to an extent that meets the WHO recommendation depends on k_{obs}, the HRT, and the initial *E. coli* concentration (which in turn depends on the water source). The *E. coli* concentrations measured at the end of each experiment were quite different: the final *E. coli* concentration for Experiment 1 was 8.2×10^4 CFU/100 mL while that of Experiment 2 was 82 CFU/100 mL, due to a lower initial *E. coli* concentration and faster inactivation rate. All natural treatment systems have variability in their treatment efficiency; while treatment variability in small ponds can result in a final *E. coli* concentration greater than the WHO recommendation, the ponds can still play a role in the multi-barrier approach to reducing risks from wastewater irrigation outlined in the 2006 WHO Guidelines. Pond design recommendations to improve treatment efficiency are provided below.

Coliphage removal. Previous evaluations of small on-farm treatment ponds (Keraita et al. 2008a; Reymond et al. 2009) did not investigate virus removal. In the present study, we observed a 2.0-log and 1.5-log reduction of somatic and F+ coliphage, respectively, in the shallow open water region of the pond by 18:00 on the third day of Experiment 1; the total reduction was 1.4 log and 1.1 log for somatic and F+ coliphage, respectively, in samples collected from the deep open water region. However, the bulk of the coliphage removal seen in the deep open water region occurred at night, with insignificant inactivation occurring during the day (Figures 6.4 and 6.5). Like the trend seen in bacteria removal from the pond, this could be due to thermal stratification of the pond during the day and mixing at night. Interestingly, reductions in coliphage concentration were also seen in the shallow open water region at night (nights 1, 2 and 3 for somatic coliphage and night 2 for F+ coliphage). There are two possible explanations for this finding: continued inactivation or removal of the viruses at night, or error or variability in virus concentration measurements given that measurements at night are based on only two time points.

Insignificant coliphage removal was observed in the dark column, indicating that dark processes (e.g., sedimentation and predation) did not contribute to coliphage removal and that sunlight was essential for coliphage removal/inactivation.

Pond Management Suggestions and Challenges

Some conclusions from this and previous research can be used to make suggestions for management of small on-farm ponds to maximize disinfection. We found that sunlight is important for reducing bacteria and virus concentrations, and faster inactivation rates were measured in water at the pond surface compared to deeper water. Other researchers found an inverse relationship between total WSP depth and fecal coliform inactivation rates (Sarikaya et al. 1987; Saqqar and Pescod 1991; Mayo 1995; Pearson et al. 1995; von Sperling 1999; 2005). Therefore, ponds should be shallow to allow for light penetration, though not less than 0.4 m

deep to avoid growth of emergent plants (Davies-Colley 2005). Additionally, shallower ponds are less likely to become permanently stratified (i.e., stratified during the day with no mixing at night), which would isolate deeper waters and limit sunlight disinfection. As an example, deep water storage reservoirs, such as those used in Israel to store wastewater for irrigation, have limited treatment efficiency compared to conventional WSP (Dor et al. 1987; Juanico and Shelef 1994), partially due to their depth (e.g., 5.5 to 15 m deep) and stratification (Liran et al. 1994). The 0.5 m pond used in the present study appeared to be stratified during the day and mixed overnight.

Ponds should be kept clear of emergent and floating plants, and vegetation growing on pond embankments should be cut frequently. While floating vegetation, such as duckweed and water lettuce, can aid in nutrient removal, this is not necessary for irrigation water; nitrate concentrations measured in on-farm ponds by Keraita et al. (2008a), for example, were in the range suggested by the Food and Agriculture Organization of the United Nations for vegetable irrigation (Ayers and Westcot 1985). The disadvantage of emergent and floating plants is that they block sunlight penetration into pond waters, have been observed to reduce rates of bacteria removal (Pearson et al. 1995; Awuah et al. 2004), and can provide a habitat for insect larvae, such as mosquitos (Lloyd 2005). Given the concern that urban agriculture and WSP can increase the risk of malaria and other vector-borne disease (Drechsel et al. 2006 and ref. within), efforts must be made to reduce vector habitats, especially in regions endemic for diseases such as malaria, dengue fever and schistosomiasis. Additional vector management strategies include introducing fish that eat mosquito larvae and building ponds with steep walls (Knight et al. 2003).

Conversely, suspended algae can be beneficial for pond disinfection. Algae photosynthesis increases pond water pH and dissolved oxygen concentrations, which can increase microorganism inactivation rates (Davies-Colley et al. 1999). Algae may also be a source of photosensitizers that cause exogenous sunlight inactivation, to which enterococci and F+ RNA coliphage are susceptible (Davies-Colley et al. 1999; Kadir and Nelson 2013). Algae in finished water used for irrigation is beneficial for crop production, acting as a soil conditioner and slow release fertilizer (Pearson 2005). While not currently utilized in Accra, even drip irrigation systems can be used with waters containing algae; Taylor et al. (1995) found that microalgae did not clog drip irrigation systems, and that simple filtration systems can be used to remove non-algal solids responsible for system clogging. While we observed algae growth in ponds in this study, Reymond et al. (2009) did not, possibly due to the use of a different water source (i.e., drain water versus contaminated stream water) or HRT.

Operating ponds as batch reactors can reduce hydraulic inefficiencies. However, the operation of just one batch reactor with a sufficiently long HRT (Scheme 1, Figure 6.8) is difficult given that farmers use the ponds and water stored within everyday. This problem can be overcome if farmers have more than one pond and operate them in a fill-rest-use cycle, as suggested by Cofie et al. (2010) and Mara et al. (2010; Scheme 2, Figure 6.8).

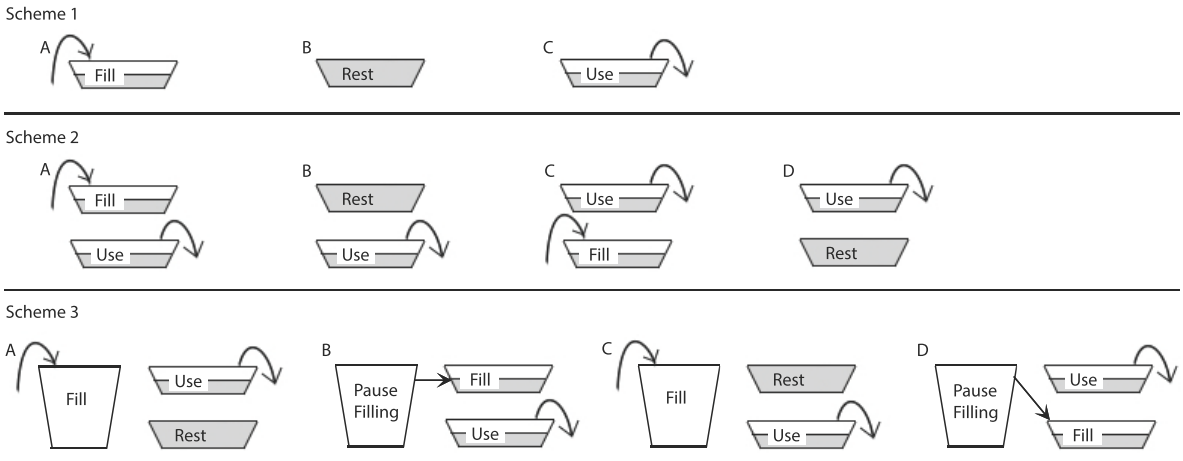

Figure 6.8. Options for treatment pond configuration and operation.

When operating small ponds as batch reactors, reliance on solar radiation for disinfection combined with short HRT (e.g., on the order of days) can lead to variability in final irrigation water quality, as was demonstrated by the variability in daily k_{obs} values measured in this study. Longer retention times can help reduce variability in final water quality, and can be achieved by increasing the volume, and therefore surface area, of the ponds. Pond volumes can be increased by making individual ponds larger, or by combining a few farmers' small ponds into larger shared ponds, which should be operated in a fill-rest-use cycle. Larger shared ponds can also address the challenge of requiring each farmer to be a pond manager, as management groups can share operation and maintenance responsibilities. However, larger ponds that are shared among a group may not be located conveniently for all farmers.

In addition to the risks posed by bacterial and viral pathogens, helminths are important etiologies of disease associated with wastewater irrigation (e.g., Blumenthal et al. 2001; Blumenthal and Peasey 2002; Ensink et al. 2005). While we did not measure helminth egg concentrations or removal in the current study, Keraita et al. (2008a) found helminth egg removal in farmer-dug ponds to be similar during the wet and dry seasons, indicating sedimentation as the main removal mechanism; the researchers also found that the ponds achieved a helminth egg concentration of <1 egg/L within three days. This finding is consistent with *Ascaris lumbricoides* and hookworm egg sedimentation rates of 0.65 and 0.39 m/h, respectively (Mara 2004); at these rates helminth eggs should settle out of the 0.5 m deep ponds within one day under quiescent conditions.

Helminth eggs and other pathogens that settle out of the water column accumulate in the pond sediment (Nelson 2003; Keraita et al. 2008a), and can be resuspended when farmers collect irrigation water (Keraita et al. 2008a). This challenge can be addressed in Schemes 1 and 2 by the addition of simple infrastructure to allow water collection without stirring up sediment, such as stairs built into the pond to help farmers avoid stepping in sediment (Reymond et al. 2009; Cofie et al. 2010). An additional option is to build a deeper pond upstream of the parallel batch

reactors in Scheme 2, with the express purpose of allowing sedimentation (Scheme 3, Figure 6.8): the pond should be designed to allow for complete removal of helminth eggs before undergoing treatment in the batch reactors. For all schemes, an operation and maintenance plan is needed that includes specifications for pond desludging and treatment of the sludge to reduce pathogen concentrations after removal (Nelson et al. 2004). If Scheme 3 is properly designed and managed, only the single upstream sedimentation pond would require desludging.

No matter which treatment scheme is deemed most appropriate, overarching challenges with on-farm wastewater treatment include limited land availability, insecure land tenure, and lack of incentives to change current irrigation practices (Keraita et al. 2008b; Flynn-Dapaah 2002). Most farmers do not have formal land tenure (Flynn-Dapaah 2002), and many do not consider the health risk associated with wastewater irrigation as a priority (Keraita et al. 2008b); these factors reduce farmers' ability and desire to make monetary or labor investments into water treatment infrastructure. Keraita et al. (2008b) suggested two routes that could be taken to provide incentives for farmers to participate in on-farm wastewater treatment: (1) market incentives that could include "higher economic returns for safer vegetables which could be achieved through the establishment of distinct marketing channels of safer produce," and (2) "institutional support from government institutions like provision of extension services in exotic vegetable farming, loans, awards and land tenure security" in exchange for the use of treated irrigation water. A next step would be to target specific incentive routes for on-farm wastewater treatment and implement pilot projects to test if interventions work from institutional, management and water treatment perspectives.

Chapter 7

Conclusions

An overarching goal of this dissertation was to develop models that can predict the inactivation rates of waterborne viruses in natural surface waters and engineered treatment systems. Through the course of this research, we determined that the sunlight inactivation rates of human poliovirus type 3 (PV3) and bacteriophage PRD1 in environmentally sourced water relied mostly on endogenous inactivation mechanisms, while MS2 and human adenovirus type 2 were also affected by the exogenous mechanism. Inactivation rates differed among virus types and for viruses in different water matrices, depending on light attenuation and natural organic matter in the water source (Chapter 2). We used these data in combination with data from other researchers to develop and test models that predict the inactivation rates of MS2 and PV3 in water collected from an open-water wetland (Chapter 3).

Sunlight-mediated inactivation of microorganisms is ubiquitous and impacts all sunlit surface waters. One application of sunlight inactivation research – disinfection of wastewater in small ponds before use in irrigation (Chapter 6) – was investigated as part of this dissertation, and a few others – differential fates of indicator organisms in the environment (Chapter 5), and virus inactivation in recreational waters (Chapter 2) and in water from an open-water treatment wetland (Chapter 3) – were discussed. The findings of this research, and sunlight inactivation in general, have many other implications and applications; the following list includes a few:

- Bacteriophages play an important role in microbial ecology. As an example, bacteriophages are the most abundant organisms in the ocean (Wommack and Colwell 2000) and are involved in the control of bacteria and phytoplankton communities in marine waters (Fuhrman 1999). As a consequence, viruses influence carbon and nutrient cycling and play a role in bacteria gene transfer and evolution (Fuhrman 1999). Sunlight has been found to be an important factor in marine bacteriophage decay (Fuhrman 1999 and ref. within), and therefore impacts biogeochemical cycles involving microorganisms.

- Fecal indicator organisms are used in all sectors of health-related water microbiology to indicate fecal pollution, with the assumption that there is a connection to health risk. When interpreting water quality data, it is important to know how detection of indicator organisms in the environment reflects the presence of infectious agents. The most commonly used fecal indicator organisms are bacteria, but given that viruses are more resistant to sunlight, infectious viruses could be present even if indicator bacteria are not detected. As presented in this dissertation, even a virus like MS2, which has been suggested as a conservative process indicator of UV and sunlight disinfection, could over-predict the inactivation rate of human viruses (e.g., PV3) in surface waters containing natural photosensitizers (Chapter 3). More research should be conducted to relate the fate of fecal indicator organisms in the environment to that of organisms of public health concern.

- A similar example involves microbial source tracking (MST), which is an approach used to identify the host or environment responsible for microbial contamination. To effectively utilize MST in contexts that include sunlit waters, the effect of sunlight on the detection and viability of MST markers must be better understood.

- Quantitative microbial risk assessment (QMRA) is another field of active research by health-related microbiologists, and is recommended by the World Health Organization for use as a tool when developing regulations for water and wastewater treatment, and water reuse. Some QMRA applications require knowledge of current microbial concentrations in a water source. However, even when utilizing state-of-the-art detection technologies, it is prohibitively expensive to analyze a sample for concentrations of all organisms that are potential risks. Additionally, scientists in some parts of the world, including places facing significant water quality issues, do not have resources to perform analyses other than culture-based assays for fecal indicator bacteria. As discussed in Chapter 5, many researchers use assumed ratios between indicator organisms and pathogens in QMRA models when they are unable to measure pathogen concentrations directly. In Chapter 5 we observed that these relationships may not hold for all organisms after sunlight exposure. Further research into how measurements from different detection methods – such as quantitative PCR (qPCR) – relate to infectivity, how environmental exposure degrades qPCR signals, and the relative rates of degradation for indicators and targets of interest would help improve QMRA modeling.

- Natural treatment systems present a good option for wastewater treatment, such as in low-resource settings and in water-scarce places where effluent water is used for irrigation (Chapter 6). Sunlight is an important factor in disinfection in these systems; through research into sunlight inactivation of pathogens and use of the models developed in Chapter 3, we hope to better design natural treatment systems to maximize disinfection.

- Many viruses are not culturable, making them difficult to study in general, let alone their inactivation rates. Further research to better understand factors that dictate differences in sunlight inactivation rates could help in predicting inactivation rates of non-culturable viruses. These studies should include investigation into protein and nucleic acid degradation that occur with exposure to sunlight, and how this damage affects virus life processes.

In addition to the general research needs stated above, some specific research priorities were discussed in this dissertation, with the goal to better design and manage natural treatment systems – including open-water wetlands, waste stabilization ponds, and on-farm pond systems – to maximize disinfection. To expand sunlight inactivation models to an environmental scale with natural sunlight, we need to develop them to take into account solar zenith angle, annual and diurnal variation in irradiance, and surface water hydrology. To build sunlight inactivation models for additional human viruses, and bacteriophage found in wastewater (e.g., F+ and somatic coliphage), more research is needed to determine the susceptibility of these viruses to endogenous and exogenous inactivation, how the importance of each mechanism changes with

depth in light-attenuating waters, and which reactive oxygen species are most responsible for exogenous inactivation. A starting point should be to further study, and build inactivation rate models for, human adenovirus – due to its prevalence in wastewater, its limited susceptibility to endogenous inactivation, its susceptibility to exogenous inactivation, and the lack of correlation between $[^1O_2]_{ss,bulk}$ and exogenous inactivation rates – and F+ and somatic coliphage isolates from the environment or wastewater. For viruses susceptible to the exogenous mechanism, more research is needed to determine how water quality and natural organic matter (NOM) characteristics affect exogenous inactivation rates and association between the virus and photosensitizers; a first task is to look at how NOM size and divalent cation concentration affect MS2 exogenous inactivation rates.

It is unlikely that we will be able to generate experimental data to build inactivation models for all waterborne bacteriophage and human viruses. Additionally, different serotypes of the same virus (e.g., poliovirus types 1, 2, and 3), different strains of the same serotype (e.g., poliovirus type 1 strains Mahoney and Brunhilde), and different virus species in the same family (e.g., rotaviruses), can have different susceptibilities to disinfectants, including sunlight. For example, human rotavirus Wa and porcine rotavirus OSU had different rates of inactivation when exposed to simulated sunlight in waters containing model photosensitizers (Romero et al. 2013), and poliovirus type 1 Mahony was found to be twice as susceptible to chlorine as poliovirus type 1 Brunhilde despite nearly identical capsid protein sequences and similarly sized genomes (Wigginton and Kohn 2012, and ref. within). While these differences present a challenge in predicting inactivation rates, they also provide an opportunity to help determine how virus composition and structure affect rates and mechanisms of inactivation (Wigginton and Kohn 2012). As part of future research, endogenous and exogenous sunlight inactivation rates of viruses with subtle differences in composition and structure [such as adenovirus and poliovirus serotypes and strains, and additional viruses in MS2's *Leviviridae* family (e.g., fr and GA; Sigstam et al. 2013)] should be compared to better understand what governs susceptibility. This research must also identify protein and nucleic acid modifications that accompany inactivation, and determine whether these modifications lead to inhibition of virus 'life' processes.

References

Amoah, P., Drechsel, P. & Abaidoo, R.C. (2005) Irrigated urban vegetable production in Ghana: sources of pathogen contamination and health risk elimination. *Irrig. Drain.* **54**, S49-S61.

Amoah, P., Keraita, B., Akple, M., Drechsel, P., Abaidoo R.C. & Konradsen, F. (2011) *Low cost options for health risk reduction where crops are irrigated with polluted water in West Africa*. IWMI Research Report Series 141, Colombo.

Armah, G.E., Gallimore, C.I., Binka, F.N., Asmah, R.H., Green, J., Ugoji, U., Anto, F., Brown, D.W.G. & Gray, J.J. (2006) Characterisation of norovirus strains in rural Ghanaian children with acute diarrhoea. *J. Med. Virol.* **78**, 1480-1485.

Awuah, E., Oppong-Peprah, M., Lubberding, H.J. & Gijzen, H.J. (2004) Comparative performance studies of water lettuce, duckweed, and algal-based stabilization ponds using low-strength sewage. *J. Toxicol. Environ. Health* **67,** 1727-1739.

Ayers, R.S. & Westcot, D.W. (1985) *Water quality for Agriculture*. Irrigation and Drainage paper No. 29. Food and Agriculture Organization of the United Nations, Rome, Italy.

Badireddy, A.R., Budarz, J.F., Chellam, S. & Wiesner, M.R. (2012) Bacteriophage inactivation by UV-A illuminated fullerenes: role of nanoparticle-virus association and biological targets. *Environ. Sci. Technol.* **46**, 5963–5970.

Belnap, D.M., McDermott, B.M., Jr, Filman, D.J., Cheng, N., Trus, B.L., Zuccola, H.J., Racaniello, V.R., Hogle, J.M. & Steven, A.C. (2000) Three-dimensional structure of poliovirus receptor bound to poliovirus. *Proc. Natl. Acad. Sci.* **97**, 73–78.

Blough, N.V. & Zepp, R.G. (1995) Reactive oxygen species in natural waters. In: *Active Oxygen in Chemistry* (C.S. Foote, ed.). Chapman & Hall, Glasgow, pp. 342.

Blumenthal, U.J. & Peasey, A. (2002) *Critical review of epidemiological evidence of the health effects of wastewater and excreta use in agriculture*. Report for the World Health Organization, Geneva.

Blumenthal, U.J., Cifuentes, E., Bennett, S., Quigley, M. & Ruiz-Palacios, G. (2001) The risk of enteric infections associated with wastewater reuse: the effect of season and degree of storage of wastewater. *Trans. R. Soc. Trop. Med. Hyg*. **95**, 131-137.

Blumenthal, U.J., Mara, D.D., Peasey, A., Ruiz-Palacios, G. & Stott, R. (2000) Guidelines for the microbiological quality of treated wastewater used in agriculture: recommendations for revising WHO guidelines. *B. World Health Organ.* **78**, 1104-1116.

Boehm, A.B., Yamahara, K.M., Love, D.C., Peterson, B.M., McNeill, K. & Nelson, K.L. (2009) Covariation and photoinactivation of traditional and novel indicator organisms and human viruses at a sewage-impacted marine beach. *Environ. Sci. Technol.* **43**, 8046–8052.

Boreen, A.L., Edhlund, B.L., Cotner, J.B. & McNeill, K. (2008) Indirect photodegradation of dissolved free amino acids: the contribution of singlet oxygen and the differential reactivity of DOM from various sources. *Environ. Sci. Technol.* **42**, 5492–5498.

Brandenburg, B., Lee, L.Y., Lakadamyali, M., Rust, M.J., Zhuang, X. & Hogle, J.M. (2007) Imaging poliovirus entry in live cells. *PLoS Biol.* **5**, 1543-1555.

Cabaniss, S.E., Zhou, Q., Maurice, P.A., Chin, Y.-P. & Aiken, G.R. (2000) A log-normal distribution model for the molecular weight of aquatic fulvic acids. *Environ. Sci. Technol.* **34**, 1103-1109.

Carter, M.J. (2005) Enterically infecting viruses: pathogenicity, transmission and significance for food and waterborne infection. *J. Appl. Microbiol*. **98**, 1354-1380.

Cofie, O.O., Keraita, B. & Drechsel, P. (2010) *Options for simple on-farm water treatment in developing countries*. WHO-FAO-IDRC-IWMI.

Cooper, W.J., Zika, R.G., Petasne, R.G. & Fischer, A.M. (1989) Sunlight-induced photochemistry of humic substances in natural waters: major reactive species. In: *Aquatic Humic Substances: Influence on Fate and Treatment of Pollutants* (I.H. Suffet & P. MacCarthy, eds.). American Chemical Society, Washington, DC, pp. 864.

Curry, S., Chow, M. & Hogle, J.M. (1996) The poliovirus 135S particle is infectious. *J. Virol.* **70**, 7125–7131.

Curtis, T.P., Mara, D.D. & Silva, S.A. (1992) Influence of pH, oxygen, and humic substances on ability of sunlight to damage fecal coliforms in waste stabilization pond water. *Appl. Environ. Microbiol.* **58**, 1335-1343.

Davies, M.J. (2003) Singlet oxygen-mediated damage to proteins and its consequences. *Biochem. Biophys. Res. Commun.* **305**, 761–770.

Davies, M.J. & Truscott, R.J.W. (2001) Photo-oxidation of proteins and its role in cataractogenesis. *J. Photochem. Photobiol. B: Biol.* **63**, 114–125.

Davies-Colley, R.J. (2005) Pond Disinfection. In: *Pond treatment technology* (A. Shilton, ed.). IWA Publishing, London, pp 496.

Davies-Colley, R., Donnison, A. & Speed, D. (2000) Towards a mechanistic understanding of pond disinfection. *Wat. Sci. Technol*. **42**, 149-158.

Davies-Colley, R., Donnison, A., Speed, D., Ross, C. & Nagels, J. (1999) Inactivation of faecal indicator microorganisms in waste stabilisation ponds: interactions of environmental factors with sunlight. *Wat. Res.* **33**, 1220-1230.

DeLeon, R., Shieh, Y.S.C., Daric, R.S. & Sobsey, M. (1990) Detection of enteroviruses and hepatitis A virus in environmental samples by gene probes and polymerase chain reaction: advances in water analysis and treatment. In: *Advances in water analysis and treatment, Proceedings of the Water Quality Technology Conference, San Diego, Calif.* American Water Works Association, Denver, p. 833–853.

Dewilde, A., Pellieux, C., Hajjam, S., Wattré, P., Pierlot, C., Hober, D. & Aubry, J.-M. (1996) Virucidal activity of pure singlet oxygen generated by thermolysis of a water-soluble naphthalene endoperoxide. *J. Photochem. Photobiol. B: Biol.* **36**, 23–29.

Dor, I., Schechter, H. & Bromley, H.J. (1987) Limnology of a hypertrophic reservoir storing wastewater effluent for agriculture at Kibbutz Na'an, Israel. *Hydrobiologia*. **150,** 225-241.

Drechsel, P., Graefe, S., Sonou, M. & Cofie, O.O. (2006) *Informal Irrigation in Urban West Africa: An Overview.* Research Report 102. IWMI, Colombo.

Eischeid, A.C. & Linden, K.G. (2011) Molecular indications of protein damage in adenoviruses after UV disinfection. *Appl. Environ. Microbiol.* **77***,* 1145–1147.

Eischeid, A.C., Meyer, J.N. & Linden, K.G. (2009) UV disinfection of adenoviruses: molecular indications of DNA damage efficiency. *Appl. Environ. Microbiol.* **75**, 23–28.

Ensink, J.H.J., van der Hoek, W. & Amerasinghe, F.P. (2006) *Giardia duodenalis* infection and wastewater irrigation in Pakistan. *T. Roy. Soc. Trop. Med. H.* **100**, 538-542.

Ensink, J.H., van der Hoek, W., Muktar, M., Tahir, Z. & Amerasinghe, F.P. (2005) High risk of hookworm infection among wastewater farmers in Pakistan. *Trans. R. Soc. Trop. Med. Hyg*. **99**, 809-818.

Fauquet, C. (2005) *Virus taxonomy: classification and nomenclature of viruses: eighth report of the international committee on taxonomy of viruses*. Elsevier Academic Press, Hong Kong, pp. 1259.

Field, K.G. & Samadpour, M. (2007) Fecal source tracking, the indicator paradigm, and managing water quality. *Wat. Res.* **41**, 3517-3528.

Fisher, M.B., Love, D.C., Schuech, R. & Nelson, K.L. (2011) Simulated sunlight action spectra for inactivation of MS2 and PRD1 bacteriophages in clear water. *Environ. Sci. Technol.* **45**, 9249–9255.

Fisher, M.B., Keenan, C.R., Nelson, K.L. & Voelker, B.M. (2008) Speeding up solar disinfection (SODIS): effects of hydrogen peroxide, temperature, pH, and copper plus ascorbate on the photoinactivation of *E. coli*. *J. Water Health* **6**, 35–51.

Flint, J.S., Enquist, L.W., Racaniello, V.R. & Skalka, A.M. (2004) *Principles of Virology: Molecular Biology, Pathogenesis, and Control*. ASM Press, Washington, DC.

Flynn-Dapaah, K. (2002) *Land Negotiations and Tenure Relationships: Accessing Land for Urban and Peri-Urban Agriculture in Sub-Saharan Africa*, IDRC Cities Feeding People Series, Report 36, IDRC, Ottawa, Canada.

Fuhrman, J.A. (1999) Marine viruses and their biogeochemical and ecological effects. *Nature* **399**, 541-548.

Gerba, C.P. (1984) Applied and theoretical aspects of virus adsorption to surfaces. *Adv. Appl. Microbiol.* **30**, 133-168.

Grandbois, M., Latch, D.E. & McNeill, K. (2008) Microheterogeneous concentrations of singlet oxygen in natural organic matter isolate solutions. *Environ. Sci. Technol.* **42**, 9184–9190.

Grebel, J.E., Pignatello, J.J. & Mitch, W.A. (2012) Impact of halide ions on natural organic matter-sensitized photolysis of 17β-Estradiol in saline waters. *Environ. Sci. Technol.* **46**, 7128-7134.

Gregory, J.B., Litaker, R.W. & Noble, R.T. (2006) Rapid one-step quantitative reverse transcriptase PCR assay with competitive internal positive control for detection of enteroviruses in environmental samples. *Appl. Environ. Microbiol.* **72**, 3960–3967.

Gueymard, C.A. (2005) Interdisciplinary applications of a versatile spectral solar irradiance model: A review. *Energy*. **30**, 1551–1576.

Haag, W.R. & Hoigné, J. (1986) Singlet oxygen in surface waters. 3. Photochemical formation and steady-state concentrations in various types of waters. *Environ. Sci. Technol.* **20**, 341–348.

Haag, W.R., Hoigné, J., Gassman, E. & Braun, A. (1984a) Singlet oxygen in surface waters – Part I: Furfuryl alcohol as a trapping agent. *Chemosphere* **13**, 631–640.

Haag, W.R., Hoigné, J., Gassman, E. & Braun, A. (1984b) Singlet oxygen in surface waters – Part II: Quantum yields of its production by some natural humic materials as a function of wavelength. *Chemosphere* **13**, 641–650.

Havelaar, A.H., Van Olphen, M. & Drost, Y.C. (1993) F-specific RNA bacteriophages are adequate model organisms for enteric viruses in fresh water. *Appl. Environ. Microbiol.* **59**, 2956–2962.

Heaselgrave, W., Patel, N., Kilvington, S., Kehoe, S.C. & McGuigan, K.G. (2006) Solar disinfection of poliovirus and Acanthamoeba polyphaga cysts in water-a laboratory study using simulated sunlight. *Lett. Appl. Microbiol.* **43**, 125–130.

Hijnen, W.A.M., Beerendonk, E.F. & Medema, G.J. (2006) Inactivation credit of radiation for viruses, bacteria and protozoan (oo)cysts in water: A review. *Water Res*. **40**, 3-22.

Hogle, J.M. (2002) Poliovirus cell entry: common structural themes in viral cell entry pathways. *Ann. Rev. Microbiol*. **56**, 677-702.

Hogle, J.M., Chow, M. & Filman, D.J. (1985) Three-dimensional structure of poliovirus at 2.9 A resolution. *Science* **229**, 1358–1365.

Hooker, J. M., Kovacs, E. W. & Francis, M. B. (2004) Interior surface modification of bacteriophage MS2. *J. Am. Chem. Soc.* **126**, 3718-3719.

Huang, Y., Hogle, J.M. & Chow, M. (2000) Is the 135S poliovirus particle an intermediate during cell entry? *J. Virol.* **74**, 8757–8761.

Jagger, J. (1985) *Solar-UV actions on living cells*. Praeger Publishers, New York.

Jenkins, M.W., Tiwari, S., Lorente, M., Gichaba, C.M. & Wuertz, S. (2009) Identifying human and livestock sources of fecal contamination in Kenya with host-specific *Bacteroidales* assays. *Wat. Res.* **43**, 4956-4966.

Jiang, S., Noble, R. & Chu, W. (2001) Human adenoviruses and coliphages in urban runoff-impacted coastal waters of Southern California. *Appl. Environ. Microbiol.* **67**, 179–184.

Jiménez, B. (2006) Irrigation in developing countries using wastewater. *Int. Rev. Environ. Strat.* **6**, 229-250.

Jothikumar, N., Cromeans, T.L., Hill, V.R., Lu, X., Sobsey, M.D. & Erdman, D.D. (2005) Quantitative real-time PCR assays for detection of human adenoviruses and identification of serotypes 40 and 41. *Appl. Environ. Microbiol.* **71**, 3131-3136.

Juanico, M. (1996) The performance of batch stabilization reservoirs for wastewater treatment, storage and reuse in Israel. *Wat. Sci. Technol*. **33,** 149-159.

Juanico, M. & Shelef, G. (1994) Design, operation and performance of stabilization reservoirs for wastewater irrigation in Israel. *Wat. Res.* **28,** 175-186.

Kadir, K. & Nelson K.L. (2013) Sunlight mediated inactivation of *Enterococcus faecalis* and *Escherichia coli* in waste stabilization pond water. *Wat. Res.* In press.

Kageyama, T., Kojima, S., Shinohara, M., Uchida, K., Fukushi, S., Hoshino, F.B., Takeda, N. & Katayama, K. (2003) Broadly reactive and highly sensitive assay for norwalk-like viruses based on real-time guantitative reverse transcription-PCR. *J. Clin. Microbiol.* **41**, 1548-1557.

Keraita, B., Drechsel, P. & Konradsen, F. (2008a) Using on-farm sedimentation ponds to improve microbial quality of irrigation water in urban vegetable farming in Ghana. *Wat. Sci. Technol*. **57,** 519-525.

Keraita, B., Drechsel, P. & Konradsen, F. (2008b) Perceptions of farmers on health risks and risk reduction measures in wastewater-irrigated urban vegetable farming in Ghana. *J. Risk. Res.* **11**, 1047–1061.

Keraita, B., Drechsel, P. & Amoah, P. (2003) Influence of urban wastewater on stream water quality and agriculture in and around Kumasi, Ghana. *Environ. Urban.* **15**, 171-178.

Kildare, B.J., Leutenegger, C.M., McSwain, B.S., Bambic, D.G., Rajal, V.B., Wuertz, S. (2007) 16S rRNA-based assays for quantitative detection of universal, human-, cow-, and dog-specific fecal *Bacteroidales*: A Bayesian approach. *Wat. Res.* **41**, 3701-3715.

Knight, R.L., Walton, W.E., O'Meara, G.F., Reisen, W.K. & Wass, R. (2003) Strategies for effective mosquito control in constructed treatment wetlands. *Eco. Eng.* **21,** 211-232.

Kohn, T., Grandbois, M., McNeill, K. & Nelson, K.L. (2007) Association with natural organic matter enhances the sunlight-mediated inactivation of MS2 coliphage by singlet oxygen. *Environ. Sci. Technol.* **41**, 4626–4632.

Kohn, T. & Nelson, K.L. (2007) Sunlight-mediated inactivation of MS2 coliphage via exogenous singlet oxygen produced by sensitizers in natural waters. *Environ. Sci. Technol.* **41**, 192–197.

Kördel, W., Dassenakis, M., Lintelmann, J. & Padberg, S. (1997) The importance of natural organic material for environmental processes in waters and soils. *Pure & Appl. Chem.* **69**, 1571-1600.

Kovacs, E.W., Hooker, J.M., Romanini, D.W., Holder, P.G., Berry, K.E. & Francis, M.B. (2007) Dual-surface-modified bacteriophage MS2 as an ideal scaffold for a viral capsid-based drug delivery system. *Bioconjugate Chem.* **18**, 1140−1147.

Kowalski, W.J., Bahnfleth, W.P. & Hernandez, M.T. (2009) A genomic model for predicting the ultraviolet susceptibility of viruses. *UVA News* **11**, 15-28.

Kreader, C.A. (1995) Design and evaluation of *Bacteroides* DNA probes for the specific detection of human fecal pollution. *Appl. Environ. Microbiol*. **61**, 1171-1179.

Kuzmanovic, D.A., Elashvili, I., Wick, C., O'Connell, C. & Krueger, S. (2006) The MS2 coat protein shell is likely assembled under tension: a novel role for the MS2 bacteriophage A protein as revealed by small-angle neutron scattering. *J. Mol. Biol*. **355**, 1095–1111.

Langlais, B., Reckhow, D.A. & Brink, D.R. (1991) *Ozone in Water Treatment, Applications and Engineering.* Lewis Publishers, Inc., Chelsea, MI.

Latch, D.E. & McNeill, K. (2006) Microheterogeneity of singlet oxygen distributions in irradiated humic acid solutions. *Science* **311**, 1743-1747.

Liran, A., Juanico, M. & Shelef, G. (1994) Coliform removal in a stabilization reservoir for wastewater irrigation in Israel. *Wat. Res.* **28,** 1305-1314.

Lloyd, B. (2005) Operation, maintenance and monitoring. In: *Pond Treatment Technology* (Shilton, A., ed). IWA Publishing, London, pp. 250-281.

Loisy, F., Atmar, R.L., Guillon, P., Le Cann, P., Pommepuy, M., & Le Guyader, F.S. (2005) Real-time RT-PCR for norovirus screening in shellfish. *J. Virol. Methods* **123**, 1-7.

Love, D.C., Casteel, M.J., Meschke, J.S. & Sobsey, M.D. (2008) Methods for recovery of hepatitis A virus (HAV) and other viruses from processed foods and detection of HAV by nested RT-PCR and TaqMan RT-PCR. *Int. J. Food Microbiol.* **126**, 221-226.

Love, D.C., Silverman, A. & Nelson, K.L. (2010) Human virus and bacteriophage inactivation in clear water by simulated sunlight compared to bacteriophage inactivation at a Southern California beach. *Environ. Sci. Technol.* **44**, 6965–6970.

Lukasik, J., Scott, T.M., Andryshak, D. & Farrah,S.R. (2000) Influence of salts on virus adsorption to microporous filters. *Appl. Environ. Microbiol*. **66**, 2914-2920.

Lydecker, M. & Drechsel, P. (2010) Urban agriculture and sanitation services in Accra, Ghana: the overlooked contribution. *Int. J. Agr. Sustain.* **8**, 94-103.

Lytle, C.D. & Sagripanti, J.-L. (2005) Predicted inactivation of viruses of relevance to biodefense by solar radiation. *J. Virol.* **79**, 14244-14252.

Mara, D.D., Hamilton, A., Sleigh, A. & Karavarsamis, N. (2010) *Discussion paper: options for updating the 2006 WHO Guidelines.* WHO-FAO-IDRC-IWMI.

Mara, D.D. & Sleigh, A. (2010) Estimation of norovirus infection risks to consumers of wastewater-irrigated food crops eaten raw. *J. Wat. Health* **8**, 39-43.

Mara, D.D., Sleigh, P.A., Blumenthal, U.J. & Carr, R.M. (2007) Health risks in wastewater irrigation: Comparing estimates from quantitative microbial risk analyses and epidemiological studies. *J. Wat. Health* **5**, 39-50.

Mara, D.D. (2004) *Domestic wastewater treatment in developing countries*. Earthscan, London.

Mattle, J.M. & Kohn, T. (2012) Inactivation and tailing during UV_{254} disinfection of viruses: Contributions of viral aggregation, light shielding within viral aggregates, and recombination. *Environ. Sci. Technol.* **46**, 10022–10030.

Mattle, J.M., Crouzy, B., Brennecke, M., Wigginton, K.R., Perona, P. & Kohn, T. (2012) Impact of virus aggregation on inactivation by peracetic acid and implications for other disinfectants. *Environ. Sci. Technol.* **45**, 7710-7717.

Mayo, A.W. (1995) Modeling coliform mortality in waste stabilization ponds. *J. Environ. Eng.* **121**, 140-152.

Mayo, A.W. (1989) Effect of pond depth on bacterial mortality rate. *J. Environ. Eng.* **115**, 964-977.

Mendelsohn, C.L., Wimmer, E. & Racaniello, V.R. (1989) Cellular receptor for poliovirus: molecular cloning, nucleotide sequence, and expression of a new member of the immunoglobulin superfamily. *Cell* **56**, 855–865.

Mensah, E., Amoah, P., Drechsel, P. & Abaidoo, R.C. (2001) Environmental concerns of urban and peri-urban agriculture: case studies from Accra and Kumasi. In: *Waste Composting for Urban and Peri-urban Agriculture: Closing the Rural–Urban Nutrient Cycle in Sub-Saharan Africa* (Drechsel, P. & Kunze, D., eds). IWMI-FAO-CABI, Wallingford, UK, pp. 55-68.

Michen, B. & Graule, T (2010) Isoelectric points of viruses. *J. Appl. Microbiol*. **109**, 388–397.

Miller, G.C. & Zepp, R.G. (1979) Effects of suspended sediments on photolysis rates of dissolved pollutants. *Wat. Res.* **13**, 453-459.

Murray, A. & Drechsel, P. (2011) Why do some wastewater treatment facilities work when the majority fail? Case study from the sanitation sector in Ghana. *Waterlines* **30**, 135-149.

Nelson, K.L., Jimenez, B., Tchobanoglous, G. & Darby, J.L. (2004) Sludge accumulation, characteristics, and pathogen inactivation in four primary waste stabilization ponds in central Mexico. *Wat. Res.* **38,** 111-127.

Nelson, K.L. (2003) Concentrations and inactivation of *Ascaris* eggs and pathogen indicator organisms in wastewater stabilization pond sludge. *Wat. Sci. Technol.* **48**, 89-95.

Nguyen, M.T., Silverman, A.I. & Nelson, K.L. (In review) Modeling sunlight inactivation of MS2 in the absence of photosensitizers using a photoaction spectrum: Progress and challenges.

Noble, R.T., Griffith, J.F., Blackwood, A.D., Fuhrman, J.A., Gregory, J.B., Hernandez, X., Liang, X., Bera, A.A. & Schiff, K. (2006) Multitiered approach using quantitative PCR to track sources of fecal pollution affecting Santa Monica Bay, California. *Appl. Environ. Microbiol.* **72**, 1604–1612.

Obuobie, E., Keraita, B., Danso, G., Amoah, P., Cofie, O.O., Raschid-Sally, L. & Drechsel, P. (2006) *Irrigated Urban Vegetable Production in Ghana: Characteristics, Benefits and Risks.* IWMI-RUAF-CPWF, Accra, Ghana.

Oguma, K., Katayama, H., Mitani, H., Morita, S., Hirata, T. & Ohgaki, S. (2001) Determination of pyrimidine dimers in *Escherichia coli* and *Cryptosporidium parvum* during UV light inactivation, photoreactivation, and dark repair. *Appl. Environ. Microbiol.* **67**, 4630–4637.

Oragui, J.I., Curtis, T.P., Silva, S.A. & Mara, D.D. (1986) The Removal of excreted bacteria and viruses in deep waste stabilization ponds in northeast Brazil. *Wat. Sci. Technol.* **18**, 31-35.

Paul, A., Hackbarth, S., Vogt, R.D., Röder, B., Burnison, K.B. & Steinberg, C.E.W. (2004) Photogeneration of singlet oxygen by humic substances: comparison of humic substances of aquatic and terrestrial origin. *Photochem. Photobiol. Sci.* **3**, 273–280.

Pearson, H.W., Mara, D.D. & Arridge, H.A. (1995) The influence of pond geometry and configuration on facultative and maturation waste stabilization pond performance and efficiency. *Wat. Sci. Technol.* **31**, 129-139.

Pearson, H.W. (2005) Microbiology of waste stabilization ponds. In: *Pond Treatment Technology* (Shilton, A., ed). IWA Publishing, London, pp. 14-48.

Pecson, B.M., Ackermann, M. & Kohn, T. (2011) Framework for using quantitative PCR as a nonculture based method to estimate virus infectivity. *Environ. Sci. Technol*. **45**, 2257–2263.

Pellieux, C., Dewilde, A., Pierlot, C. & Aubry, J.-M. (2000) Bactericidal and virucidal activities of singlet oxygen generated by thermolysis of naphthalene endoperoxides. *Meth. Enzymol.* **319**, 197–207.

Peterson, B.M., McNally, A.M., Cory, R.M., Thoemke, J.D., Cotner, J.B. & McNeill, K. (2012) Spatial and temporal distribution of singlet oxygen in Lake Superior. *Environ. Sci. Technol.* **46**, 7222-7229.

Quaranta, M.L., Mendes, M.D., & MacKay, A.A. (2012) Similarities in effluent organic matter characteristics from Connecticut wastewater treatment plants. *Wat. Res*. **46**, 284-294.

Raschid-Sally, L. & Jayakody, P. (2008) *Drivers and characteristics of wastewater agriculture in developing countries: results from a global assessment* (IWMI Research Report No. 127). IWMI, Colombo, Sri Lanka.

Reed, R.H. (2004) The inactivation of microbes by sunlight: solar disinfection as a water treatment process. *Adv. Appl. Microbiol.* **54**, 333–365.

Reither, K., Ignatius, R., Weitzel, T., Seidu-Korkor, A., Anyidoho, L., Saad, E., Djie-Maletz, A., Ziniel, P., Amoo-Sakyi, F., Danikuu, F., Danour, S., Otchwemah, R.N., Schreier, E., Bienzle, U., Stark, K. & Mockenhaupt, F.P. (2007) Acute childhood diarrhoea in northern Ghana: epidemiological, clinical and microbiological characteristics. *BMC Infect. Dis.* **7**, 104-111.

Reymond, P., Cofie, O.O., Raschid, L. & Kone, D. (2009) *Design considerations and constraints in applying on-farm wastewater treatment for urban agriculture*. 4th SWITCH Scientific Meeting, Delft, The Netherlands. 4-7 Oct 2009.

Romero, O.C., Sadik, N.J., Rosado-Lausell, S.L., Pugh, C.R., Niu, X-.Z., Crour, J-.P. & Nguyen, T.H (2013) Sunlight-induced inactivation of human Wa and porcine OSU rotaviruses in the presence of exogenous photosensitizers. *Environ. Sci. Technol.* **47**, 11004-11012.

Romero, O.C., Straub, A.P., Kohn, T. & Nguyen, T.H. (2011) Role of temperature and suwannee river natural organic matter on inactivation kinetics of rotavirus and bacteriophage MS2 by solar irradiation. *Environ. Sci. Technol.* **45**, 10385–10393.

Saqqar, M.M. & Pescod, M.B. (1991) Microbiological performance of multi-stage stabilization ponds for effluent use in agriculture. *Wat. Sci. Technol.* **23**, 1517-1524.

Sarikaya, H.Z., Saatci, A.M. & Abdulfattah, A.F. (1987) Effect of pond depth on bacterial die-off. *J. Environ. Eng.* **113**, 1350-1362.

Sassoubre, L.M., Love, D.C., Silverman, A.I., Nelson, K.L. & Boehm, A. B. (2012) Comparison of enterovirus and adenovirus concentration and enumeration methods in seawater from Southern California, USA and Baja Malibu, Mexico. *J. Water Health*. **10**, 419–430.

Schwartzbrod, L. (1995) *Effect of human viruses on public health associated with the use of wastewater and sewage sludge in agriculture and aquaculture*. Report of the World Health Organization, Geneva.

Scott, C., Faruqui, N.I. & Raschid, L. (2004) Wastewater use in irrigated agriculture: management challenges in developing countries. In: *Wastewater Use in Irrigated Agriculture: Confronting the Livelihood and Environmental Realities* (C. Scott, N.I. Faruqui & L. Raschid, eds.). CABI-IWMI-IRDC, pp. 1-10.

Sedmak, G., Bina, D., MacDonald, J. & Couillard, L. (2005) Nine-year study of the occurrence of culturable viruses in source water for two drinking water treatment plants and the influent and effluent of a wastewater treatment plant in Milwaukee, Wisconsin (August 1994 through July 2003). *Appl. Environ. Microbiol.* **71**, 1042–1050.

Seidu, R., Heistad, A., Amoah, P., Drechsel, P., Jenssen, P.D. & Stenström, T.-A. (2008) Quantification of the health risk associated with wastewater reuse in Accra, Ghana: a contribution toward local guidelines. *J. Wat. Health* **6**, 461-471.

Shilton, A., ed. (2005) *Pond Treatment Technology*. IWA Publishing, London.

Shilton, A. & Walmsley, N. (2005) Introduction to pond treatment technology. In: *Pond Treatment Technology* (Shilton, A., ed). IWA Publishing, London, pp. 1-13.

Shuval, H., Lampert, Y. & Fattal, B. (1997) Development of a risk assessment approach for evaluating wastewater reuse standards for agriculture. *Wat. Sci. Technol.* **35**, 15-20.

Siebenga, J.J., Vennema, H., Zheng, D.-P., Vinjé, J., Lee, B.E., Pang, X.-L., Ho, E.C.M., Lim, W., Choudekar, A., Broor, S., Halperin, T., Rasool, N.B.G., Hewitt, J., Greening, G.E., Jin, M., Duan, Z.-J., Lucero, Y., O'Ryan, M., Hoehne, M., Schreier, E., Ratcliff, R.M., White, P.A., Iritani, N., Reuter, G. & Koopmans, M. (2009) Norovirus illness is a global problem: Emergence and spread of Norovirus GII.4 variants, 2001-2007. *J. Infect. Dis.* **200**, 802-812.

Sigstam, T., Gannon, G., Cascella, M., Pecson, B.M., Wigginton, K.R. & Kohn, T. (2013) Subtle differences in virus composition affect disinfection kinetics and mechanisms. *Appl. Environ. Microbiol.* **79**, 3455-3467.

Silkie, S.S. & Nelson, K.L. (2009) Concentrations of host-specific and generic fecal markers measured by quantitative PCR in raw sewage and fresh animal feces. *Wat. Res.* **43**, 4860-4871.

Silva, P.A., Stark, K., Mockenhaupt, F.P., Reither, K., Weitzel, T., Ignatius, R., Saad, E., Seidu-Korkor, A., Bienzle, U. & Schreier, E. (2008) Molecular characterization of enteric viral agents from children in northern region of Ghana. *J. Med. Virol.* **80**, 1790-1798.

Silverman, A.I., Peterson, B.M., Boehm, A.B., McNeill, K. & Nelson, K.L. (2013a) Sunlight inactivation of human viruses and bacteriophages in coastal waters containing natural photosensitizers. *Environ. Sci. Technol.* **47**, 1870-1878.

Silverman, A.I., Akrong, M.O., Amoah, P., Drechsel, P. & Nelson, K.L. (2013b) Quantification of human norovirus GII, human adenovirus, and fecal indicator organisms in wastewater used for irrigation in Accra, Ghana. *J. Wat. Health.* **11**, 473-488.

Simonet, J. & Gantzer, C. (2006) Inactivation of poliovirus 1 and F-specific RNA phages and degradation of their genomes by UV irradiation at 254 nanometers. *Appl. Environ. Microbiol.* **72**, 7671–7677.

Sinton, L.W., Hall, C.H., Lynch, P.A. & Davies-Colley, R.J. (2002) Sunlight inactivation of fecal indicator bacteria and bacteriophages from waste stabilization pond effluent in fresh and saline waters. *Appl. Environ. Microbiol.* **68**, 1122-1131.

Sinton, L.W., Finlay, R.K. & Lynch, P. A. (1999) Sunlight inactivation of fecal bacteriophages and bacteria in sewage-polluted seawater. *Appl. Environ. Microbiol.* **65**, 3605–3613.

Sutherland, B.M. & Shih, A.G. (1983) Quantitation of pyrimidine dimer contents of nonradioactive deoxyribonucleic acid by electrophoresis in alkaline agarose gels. *Biochemistry* **22**, 745–749.

Taylor, H.D., Bastos, R.K.X., Pearson, H.W. & Mara, D.D. (1995) Drip irrigation with waste stabilization pond effluents: solving the problem of emitter fouling. *Wat. Sci. Technol.* **31**, 417-424.

Templeton, M.R., Andrews, R.C. & Hofmann, R. (2008) Particle-associated viruses in water: impacts on disinfection processes. *Crit. Rev. Environ. Sci. Technol.* **38**, 137–164.

Teunis, P.F.M., Moe, C.L., Liu, P., E. Miller, S., Lindesmith, L., Baric, R.S., Le Pendu, J. & Calderon, R.L. (2008) Norwalk virus: how infectious is it? *J. Med. Virol.* **80**, 1468-1476.

US EPA. (2004) *Guidelines for Water Reuse.* Report of the United States Environmental Protection Agency (EPA/625/R-04/108), Washington D.C.

Van De Werfhorst, L.C., Sercu, B. & Holden, P.A. (2011) Comparison of the host specificities of two *Bacteroidales* quantitative PCR assays used for tracking human fecal contamination. *Appl. Environ. Microbiol.* **77**, 6258-6260.

Viau, E.J., Lee, D. & Boehm, A.B. (2011) Swimmer risk of gastrointestinal illness from exposure to tropical coastal waters impacted by terrestrial dry-weather runoff. *Environ. Sci. Technol.* **45**, 7158-7165.

von Sperling, M. (2005) Modeling of coliform removal in 186 facultative and maturation ponds around the world. *Wat. Res.* **39**, 5261-5273.

von Sperling, M. (1999) Performance evaluation and mathematical modeling of coliform die-off in tropical and subtropical waste stabilization ponds. *Wat. Res.* **33**, 1435-1448.

Walters, S.P. & Field, K.G. (2009) Survival and persistence of human and ruminant-specific faecal *Bacteroidales* in freshwater microcosms. *Environ. Microbiol.* **11**, 1410-1421.

Walters, S.P., Yamahara, K.M. & Boehm, A.B. (2009) Persistence of nucleic acid markers of health-relevant organisms in seawater microcosms: implications for their use in assessing risk in recreational waters. *Wat. Res.* **43**, 4929–4939.

Wershaw, R.L. (2004) *Evaluation of Conceptual Models of Natural Organic Matter (Humus) From a Consideration of the Chemical and Biochemical Processes of Humification*; 2004-5121. United States Geological Survey, Reston, Virginia, pubs.usgs.gov/sir/2004/5121/.

White, G.C. (1999) *Handbook of Chlorination and Alternative Disinfectants*. John Wiley & Sons, Inc., New York.

Widdowson, M.-A., Sulka, A., Bulens, S.N., Beard, R.S., Chaves, S.S., Hammond, R., Salehi, E.D.P., Swanson, E., Totaro, J., Woron, R., Mead, P.S., Bresee, J.S., Monroe, S.S. & Glass, R.I. (2005) Norovirus and foodborne disease, United States, 1991–2000. *Emerg. Infect. Dis.* **11**, 95-102.

Wigginton, K.R. & Kohn, T. (2012) Virus disinfection mechanisms: the role of virus composition, structure, and function. *Curr. Opin. Virol.* **2**, 84–89.

Wigginton, K.R., Pecson, B.M., Sigstam, T., Bosshard, F. & Kohn, T. (2012) Virus inactivation mechanisms: Impact of disinfectants on virus function and structural integrity. *Environ. Sci. Technol.* **46**, 12069-12078.

Wigginton, K.R., Menin, L., Montoya, J.P. & Kohn, T. (2010) Oxidation of virus proteins during UV254 and singlet oxygen mediated inactivation. *Environ. Sci. Technol.* **44**, 5437–5443.

Williams, G.J. (2009) *The effect of loading rate on tertiary wastewater filtration*. PhD Dissertation, University of California, Berkeley.

Wommack, K.E. & Colwell, R.R. (2000) Virioplankton: viruses in aquatic ecosystems. *Microbiol. Molecul. Biol. Rev*. **64**, 69-114.

Wong, K., Mukherjee, B., Kahler, A.M., Zepp, R. & Molina, M (2012) Influence of inorganic ions on aggregation and adsorption behaviors of human adenovirus. *Environ. Sci. Technol.* **46**, 11145−11153.

World Health Organization (2006) *Guidelines for the Safe Use of Wastewater, Excreta and Greywater in Agriculture. Volume II: Wastewater Use in Agriculture.* World Health Organization, Geneva.

World Health Organization (2003) *Guidelines for safe recreational water environments. Volume 1: Coastal and fresh waters.* World Health Organization, Geneva.

World Health Organization (1989) *Health Guidelines for the Use of Wastewater in Agriculture and Aquaculture.* Technical Report Series 778. World Health Organization, Geneva.

Yafal, A.G., Kaplan, G., Racaniello, V.R. & Hogle, J.M. (1993) Characterization of poliovirus conformational alteration mediated by soluble cell receptors. *Virology* **197**, 501–505.

Zepp, R.G. (1988) Environmental photoprocesses involving natural organic matter. In: *Humic Substances and Their Role in the Environment* (F.H. Frimmel & R.F. Christman, eds.). Wiley, pp. 271.

Zepp, R., Schlotzhauer, P. & Sink, R. (1985) Photosensitized transformations involving electronic-energy transfer in natural waters – Role of humic substances. *Environ. Sci. Technol.* **19**, 74−81.

Zepp, R. & Cline, D. (1977) Rates of direct photolysis in aquatic environment. *Environ. Sci. Technol.* **11**, 359−366.

Zhang, P., Mueller, S., Morais, M.C., Bator, C.M., Bowman, V.D., Hafenstein, S., Wimmer, E. & Rossmann, M.G. (2008) Crystal structure of CD155 and electron microscopic studies of its complexes with polioviruses. *Proc. Natl. Acad. Sci.* **105**, 18284–18289.